Fiber/Fabric-Based Piezoelectric and Triboelectric Nanogenerators for Flexible/Stretchable and Wearable Electronics and Artificial Intelligence

Kai Dong, Xiao Peng, and Zhong Lin Wang*

Integration of advanced nanogenerator technology with conventional textile processes fosters the emergence of textile-based nanogenerators (NGs), which will inevitably promote the rapid development and widespread applications of next-generation wearable electronics and multifaceted artificial intelligence systems. NGs endow smart textiles with mechanical energy harvesting and multifunctional self-powered sensing capabilities, while textiles provide a versatile flexible design carrier and extensive wearable application platform for their development. However, due to the lack of an effective interactive platform and communication channel between researchers specializing in NGs and those good at textiles, it is rather difficult to achieve fiber/fabric-based NGs with both excellent electrical output properties and outstanding textile-related performances. To this end, a critical review is presented on the current state of the arts of wearable fiber/fabric-based piezoelectric nanogenerators and triboelectric nanogenerators with respect to basic classifications, material selections, fabrication techniques, structural designs, and working principles, as well as potential applications. Furthermore, the potential difficulties and tough challenges that can impede their large-scale commercial applications are summarized and discussed. It is hoped that this review will not only deepen the ties between smart textiles and wearable NGs, but also push forward further research and applications of future wearable fiber/fabric-based NGs.

1. Introduction

As marks of our era, modern mobile electronic devices and wireless communication networks are marching into every corner of modern society and changing every aspect of our daily life. With the advance toward the fourth industrial revolution, a wave of emerging industries and advanced multidisciplinary fields is breaking out, such as the Internet of Things (IoTs), big data, humanoid robotics, and artificial intelligence (AI). Nowadays, the rapid advancement of these functional electronic devices is transforming the way people communicate with each other and with their surroundings, which has integrated our world into an intelligent information network. Owing to that no electronics works without electricity, the processes of human informatization and intelligence depend on broad energy supplies and powerful power supports. In other words, electric power can be regarded as the flowing blood that keeps every components of the current society running normally and healthily. However, with the rapid consumption of conventional fossil fuels as well as the growing voice of environmental protection, the current energy structure and its supply status are facing unprecedented challenges. On the one hand, the overwhelming energy crisis and ecological deterioration have become huge bottlenecks restricting socioeconomic development.[1] Some serious situations may even worsen to the root of interstate interest conflicts or the disaster that threatens the survival of mankind. In this case, the transform of energy structure from scarce, pollution-prone, and irreproducible mineral resources to abundant, environmentally friendly, and renewable green energies is desperately required. On the other hand, the traditional centralized, immobile, and ordered energy supply patterns based on power plants are incompatible with the present development of functional electronics associated with individual person, which follows a general trend of miniaturization, portability, and low power. As the information age is coming, billions of things must be connected with sensors for various measurements, perceptions, controls, and data transmissions.[2] These mobile, human-oriented, randomly and massively distributed sensing networks also require the corresponding matched power supply system. Therefore, it turns out that the unreasonable energy structures as well as the mismatched supply pattern lead to the current development dilemma.

Portable power supplies and self-powered systems are the most promising solutions for the above straits. For wearable power sources, one of the compromises is to choose small-size

Dr. K. Dong, X. Peng, Prof. Z. L. Wang
Beijing Institute of Nanoenergy and Nanosystems
Chinese Academy of Sciences
Beijing 100083, P. R. China
E-mail: zhong.wang@mse.gatech.edu
Prof. Z. L. Wang
School of Material Science and Engineering
Georgia Institute of Technology
Atlanta, GA 30332-0245, USA

The ORCID identification number(s) for the author(s) of this article can be found under https://doi.org/10.1002/adma.201902549.

and rechargeable energy storage devices, which mainly include conventional rigid battery, electrochemical capacitor, and lithium-ion battery. However, the storage electricity of these devices still draws from conventional energy structures. Furthermore, with the inherent shortcomings of limited electric capacitance, frequent charging times, calculable life cycles, potential safety risks, expensive deposal cost, and serious environmental hazards, they are also not the fundamental solution for future wearable electronics. From a long-term, economic, and environmental perspective, power acquisition directly from our environments is the ideal choice for future wearable electronics. As the world we live is absolutely conserved, pervasively connected, and cyclic reversible, it is possible for us to gain useful resources from our surroundings in a sustainable, renewable, eco-friendly, low-cost, and self-powered manner. To this end, several forms of green and renewable energies have emerged, such as magnetic, solar, thermal, mechanical, and microbial chemical energies. Electromagnetic generator is the backbone of today's power generator, which has contributed to the Second Industrial Revolution and advancing human civilization ever since.[3] But it may not be suitable for wearable applications, due to its heavy weight, rigid texture, and large space occupied. The recent decades have also witnessed the emergence and growth of solar cells,[4,5] thermoelectric generators,[6,7] and biofuel cells.[8,9] Although all of them have the ability to generate electricity, they depend too much on external factors, such as sunlight, temperature, and auxiliary catalyst, making them difficult to be effectively utilized on a large scale. Particularly, as one of the most abundant energies in our living environment, mechanical energy possesses the features of continuity, independence, easy access, and widespread existence. However, it is usually ignored and wasted, due to its dispersed form, small energy density, low frequency and utilization rate. Thanks to the advance of nanotechnology, a kind of mechanical energy harvester, i.e., nanogenerators (NGs) makes it possible to expediently and effectively recycle mechanical energies. The theoretical origin of the NG has been found, which makes it not only a practical technology, but also a research discipline. The second term in the Maxwell's displacement current equations is directly related to the output electric current of the NGs.[10] NGs are relatively simple in device design, do no need high frequency mechanical input, and are capable of high-efficiency energy conversion of low-frequency mechanical triggering, which have promising applications in wearable power supplying and multifunctional self-powered sensing. According to material composition, structural characteristics, and working mechanisms, the NGs can be mainly divided into piezoelectric nanogenerator (PENG, originating in 2006),[11] triboelectrical nanogenerator (TENG, starting from 2012)[12] and pyroelectric nanogenerator.[13] PENG utilizes piezoelectric effect to convert the stress inside the material into electricity, while TENG can effectively harness various types of mechanical energies based on a coupling effect of contact electrification (CE) and electrostatic induction. Pyroelectric nanogenerator can convert periodically fluctuating thermal energy into electricity using pyroelectric effect.[14] Owing to the abilities of light weight, low cost, environmental friendliness, and universal availability, NGs have received considerable research interests and have been regarded as effective tool to harvest mechanical energy that

Kai Dong received his M.S. and Ph.D. degrees in textile science and engineering from Donghua University in 2015 and 2018, respectively. He joined Donghua University from November 2018 to June 2019 as a faculty member. Currently, he is an associate professor at the Beijing Institute of Nanoenergy and Nanosystems, CAS. His research interests include smart/electronic textiles, fiber/fabric-based piezoelectric and triboelectric nanogenerators, and self-powered wearable sensors.

Xiao Peng received her B.S. degree in textile commerce and her M.S. degree in textile biomaterial from Donghua University in 2013 and 2016, respectively. After graduation, she worked as Seat Design Engineer at Yanfeng Adient Company from 2016 to 2019. Currently, she is pursuing her Ph.D. degree at the Beijing Institute of Nanoenergy and Nanosystems, CAS. Her research interests focus on textile-based triboelectric nanogenerators, wearable functional electronics, and self-powered smart device design.

Zhong Lin Wang is the Hightower Chair in Materials Science and Engineering and Regents' Professor at Georgia Tech, and Founding Director and Chief Scientist at Beijing Institute of Nanoenergy and Nanosystems, Chinese Academy of Sciences. He pioneered nanogenerators from fundamental principles to technological applications. He coined and pioneered the fields of piezotronics and piezo-phototronics for third-generation semiconductors. His research on self-powered nanosystems has inspired the worldwide effort within academia and industry to study energy for micro–nano-systems, which is now a distinct discipline in energy research and future sensor networks.

is ubiquitous but usually wasted in our everyday life, which have broad application prospects in wearable power technology, motion tracking, physiological monitoring, intelligent humanoid robot, and human-interactive interfaces.

**ADVANCED
SCIENCE NEWS**
www.advancedsciencenews.com

**ADVANCED
MATERIALS**
www.advmat.de

The rapid developments and widespread applications of NGs require corresponding operation carriers and broad service platforms. Since human itself is not only a rich source of mechanical energy, but also the application terminal of wearable electronics, it is possible for us to realize the energy acquisition and utilization in a self-sufficient way. Therefore, the key issue lies in achieving the seamless combination of NGs and human motions. Endowing NGs with wearability is considered to be one of the most promising and practical solutions at present. A larger number of human-oriented wearable NGs have been attached on or carried by human body to harvest human motion energies. However, most of them present rigid planar construction or occupy large space area, which makes the overall aesthetic loss and meanwhile restricts the normal movements of human body. The desired wearable NGs should be designed as a comfortable platform to minimize the additional burden or physical effect on the human body during motion while maintaining power conversion efficiency of as high as possible.

It is well known that food, clothing, shelter, and transportation are the basic necessities of human life. Among them, clothing, i.e., textiles and fibers are regarded as the second human skin and have been widely used by humans for thousands of years, due to its unique features and excellent performances. First, textiles can withstand versatile complex mechanical deformations, e.g., stretching, twisting, bending, and tearing, which exhibit outstanding ability of structural retention and fatigue resistance during wearing and washing.[15] Second, due to high porosity and large specific surface area, much still airs are trapped inside fabrics making them possess good air permeability and warmth retention. Third, it is easy to endow textiles with varied fabric styles, multiple color combinations, and different pattern designs.[16,17] Last but not the least, textiles are soft, flexible, comfortable, and wearable, having the most desired features of human-friendliness thus are ideal to be used for the interface platform between human and machines.[15] As we enter into the information age, textiles are no longer limited to safety protecting, warm keeping, and aesthetic usages. Functionality, intelligence, and informatization should be incorporated so as to echo the requirement of the times and enrich our living environment. Conversely, textiles with versatile designability and excellent performance represent an attractive interactive medium for human-oriented electronic integration. Electrical functionality can be seamlessly integrated into textile architectures with add-on or built-in technology, which will impose no additional burdens on normal human behaviors. The combination of electronic components and traditional textiles gives birth to a revolutionary product, i.e., smart textiles or electronic textiles (e-textiles).[18,19] Delivery of electronic functionality to the human body using e-textiles that are able to collect, process, store, transmit, and display information is important for realizing the future of wearable electronics.[20] Moreover, e-textiles can be a useful tool to generate and store energy, sense and respond to environmental stimuli, and even communicate with users, which will attract considerable research interest and enrich a wide range of application areas ranging from wearable power sources, multifunctional sensors, and healthcare monitoring to humanoid robotics and human–machine interfaces.[21–25]

Integration of advanced mechanical energy harvesting technologies into traditional textile architectures contributes to the emergence of a new kind of smart textile, i.e., textile-based NGs, which make full use of their respective merits while make up for their demerits. On the one hand, NGs can be easily designed as or integrated into textile structures, such as fiber, yarn, and fabric, endowing them with mechanical energy harvesting and self-powered signal sensing capabilities. On the other hand, textile is especially promising and suitable for NGs, because it is wearable, breathable, comfortable, structural flexible, mechanically robust, fit for low-cost implementation and large-scale production. Since human body is an inexhaustible and cost-free power source, and clothes are an indispensable necessity in people's life, textile-based NGs will become a highly attractive platform for unobtrusively harvesting human motion energy. With the help of textile-based NGs, an individual in motion can not only be regarded as a source of biomechanical energies but also an emitter of various signals. The collected electricity can not only be used to power up a variety of miniature wearable electronics, but also act as the interactive signals between human and external environment. Since the whole process of electricity supply and demand is conducted on human body, a complete wearable smart system can be established. Without additional energy supplies and deliberate external working conditions, the systems can operate normally and continuously without interruption. **Figure 1** demonstrates several kinds of human-oriented wearable textile-based NGs as well as their multifunctional applications. It can be found that human motion energy harvesting and versatile active sensing are their two main applications. As a mechanical energy harvester, it is often attached on or embedded in the parts with a larger range of motion, e.g., ankle, knee, elbow, armpit, etc. As a self-powered sensor, it is usually used for action identifying and motion tracking, healthcare monitoring and safe guarding, pressure detecting and tactile sensing, electronic skin and humanoid robotic, and more powerful human–machine interacting. Based on the motion or signal features of body parts that need to be harvested or detected, appropriated material selections and optimized structure designs of textile-based NGs are required. In the near future, it can be believed that the wearable textile-based NGs will bring new vitality and more possibilities for next-generation wearable functional electronics, and lead the way of people's life toward a more functional, informative, humane, and intelligent developing direction.

Although textile-based NGs have been largely fabricated and extensively reported, several fundamental issues, such as development history, material selection system, general fabrication methods, basic working mechanisms, potential performance enhancement methods, broad evaluation criterions, promising application occasions, etc., are still not comprehensively and systematically overviewed. For textile-based NGs, the basic knowledge of textiles and the approaches to incorporate the energy harvesting units into traditional textile structures are also not roundly and comparatively summarized. In addition, it is still not clear about the standardizations and figure of merits of textile-based NGs. These urgent issues have seriously hindered the process of commercialization and industrialization of textile-based NGs in future. Although advances are continuing and more prototypes are becoming available, there remains a
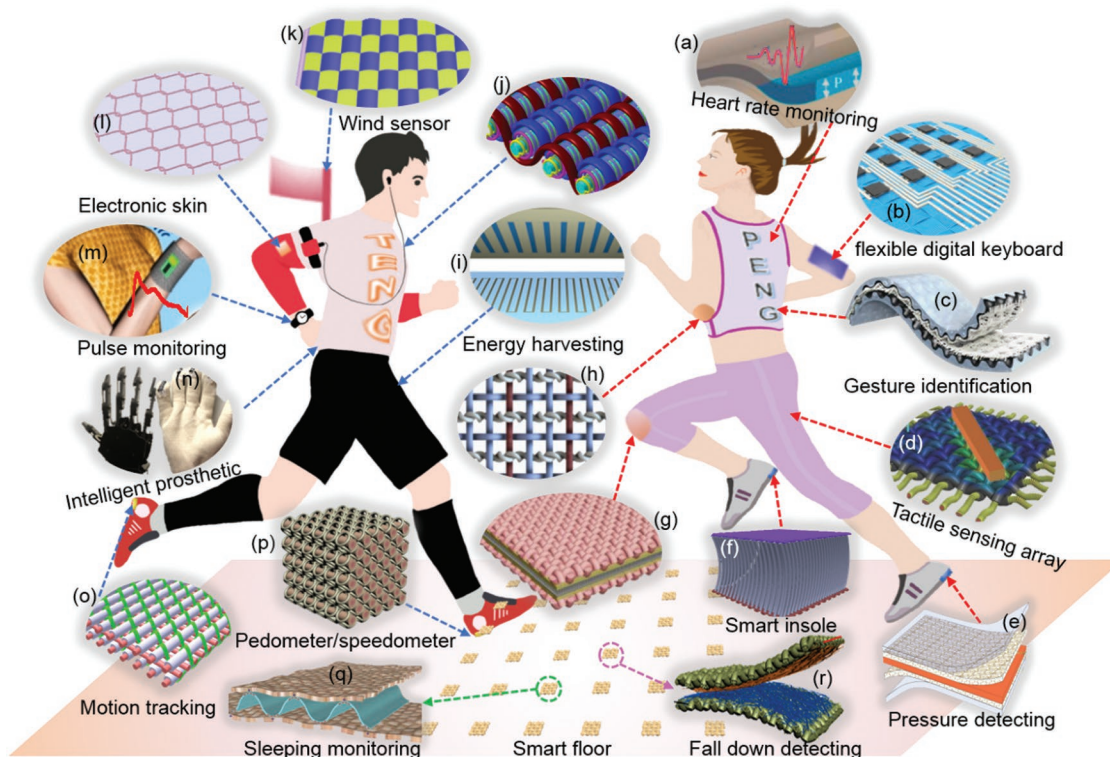
Figure 1. Schematic illustrations and application demonstrations of human-oriented wearable textile-based nanogenerators. a–h) Applications of textile-based piezoelectric nanogenerators. a) Reproduced with permission.[26] Copyright 2018, Elsevier. b) Reproduced with permission.[23] Copyright 2017, Wiley-VCH. c) Reproduced with permission.[27] Copyright 2018, Wiley-VCH. d) Reproduced with permission.[24] Copyright 2016, Wiley-VCH. e) Reproduced with permission.[28] Copyright 2013, Royal Society of Chemistry. f) Adapted with permission.[29] Copyright 2014, Royal Society of Chemistry. g) Reproduced with permission.[30] Copyright 2019, Elsevier. h) Reproduced with permission.[31] Copyright 2015, American Chemical Society. i–r) Applications of textile-based triboelectric nanogenerators. i) Reproduced with permission.[32] Copyright 2016, Wiley-VCH. j) Reproduced with permission.[33] Copyright 2018, Wiley-VCH. k) Reproduced with permission.[34] Copyright 2016, American Chemical Society. l) Reproduced with permission.[35] Copyright 2018, Wiley-VCH. m) Reproduced with permission.[36] Copyright 2014, American Chemical Society. n) Adapted with permission.[25] Copyright 2018, Elsevier. o) Adapted with permission.[37] Copyright 2018, Wiley-VCH. p) Reproduced with permission.[38] Copyright 2018, Elsevier. q) Reproduced with permission.[39] Copyright 2018, Wiley-VCH. r) Reproduced with permission.[40] Copyright 2018, Elsevier.

large gap between the best current textile-type electronics and real applications.

Herein, we cover the recent progress of textile-based NGs for both biomechanical energy harvesting and self-powered sensing. We also point out the challenges and future research directions in the field. We expect this review article to greatly benefit the related scientific research community. Our motivation is not just a summary of what has been achieved, but more importantly is to provide a guideline for future development.

2. Smart Textiles

2.1. Classification of Textiles

Textiles can be broadly categorized based on constitute raw materials, dimensional characteristics, and manufacturing techniques. The characteristics and properties of each textile type determine its suitability for a particular application. Reasonable design and effective utilization of textile-based NGs rely on all-round understandings and comprehensive comparisons of different textile types. Herein, a rough

classification of textiles is made according to its structural dimensions and manufacturing techniques. As illustrated in **Figure 2**, from the perspective of fiber orientation and architecture dimensions, textiles are mainly divided into 0D or dimensionless, 1D, 2D, and more complex 3D structures. While from the viewpoint of manufacturing techniques, textiles can be fabricated by weaving, knitting, braiding, and nonwoven methods. Fiber is the fundamental building block as well as the smallest visible unit of the textile world, just as mankind is the basic component of human society. Considering its diameter much shorter than its length, fiber that mainly includes staple fiber and filament is artificially defined as 0D or dimensionless material. By assembling/interlocking thousands of fibers with various techniques (e.g., twisting, twining, or blending) along their axial directions, 1D yarn or thread can be formed. 1D yarns can be further integrated into 2D or 3D fabrics by means of weaving, knitting, stitching, braiding, and felting methods. Among them, the 2D woven structure is the most widely used in the textile industry. Woven fabrics are produced by interlacing two sets of yarns, i.e., warp and weft yarns, both of which are mutually positioned under the angle of 90°. According to the interlacing law between warp and weft yarns,
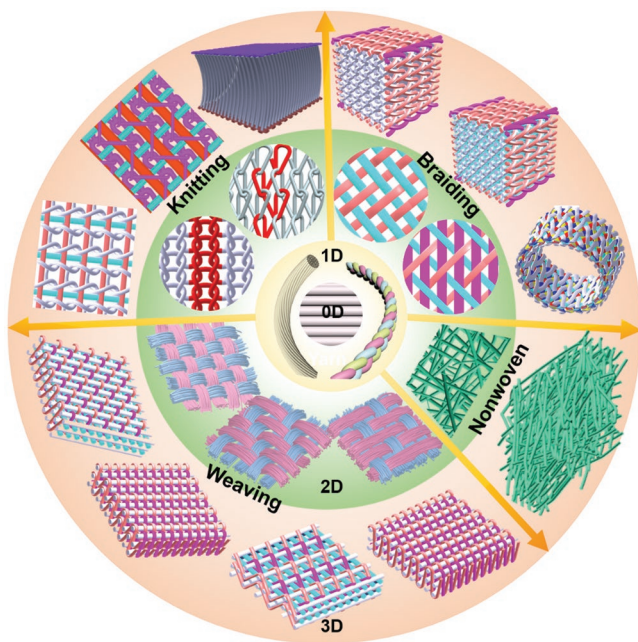
**ADVANCED
SCIENCE NEWS**

www.advancedsciencenews.com

**ADVANCED
MATERIALS**

www.advmat.de

Figure 2. Classification of textiles from the perspective of structural dimensions and manufacturing techniques. Based on the formation processes, textiles are mainly divided into weaving, knitting, braiding, and nonwoven. According to the internal geometries and dimensional characteristics, textiles are generally categorized as 0D fibers, 1D yarns, 2D fabrics, and 3D fabrics. 0D staple fibers or filaments are usually obtained from various spinning methods, such as melt spinning, wet spinning, dry spinning, etc. Multiple bundles of 0D fibers can be directly processed into 1D yarns by means of twisting, winding, and compounding techniques. 1D yarns can be woven, knitted, braided, and felted into 2D or 3D fabrics. Compared with conventional 2D woven fabrics, mainly include plain, twill, and satin, 3D woven fabrics, such as 3D orthogonal woven, 3D layer-to-layer angle-interlock woven, and 3D through-thickness angle-interlock woven, increase the number of layers in the thickness direction. 3D warp and weft knitting fabrics can be obtained by stacking straight yarns into 2D weft and warp knitting systems, respectively. Biaxial and triaxial interlacing forms are the main representatives of 2D braided structures, while four directional and five directional structures are the basic types of 3D braided fabrics. The 3D nonwoven mats are usually formed by stacking multilayer 2D nonwoven webs along the thickness direction.

2D woven structures can be further classified into plain, twill, and satin pattern. Unlike the yarns in weaving that are always straight and run parallel, the yarn in knitted fabrics follows a meandering path, which forms symmetric loop structures. The knitted stitch arranges horizontally (course) while interlocks longitudinally (wale). Based on the interloping directions, there are two major varieties of knitting, i.e., weft knitting (the wales are perpendicular to the course) and warp knitting (the wales and courses run roughly parallel). One remarkable feature of knitting fabric is that the meandering and suspended loops can be easily stretched in different directions endowing it with much more elasticity than other types of fabrics.[41,42] Braiding is traditionally a social art, starting from the elders making simple knots and plaits for younger children. As the simplest braiding structure, 2D biaxial braid is intertwined by two braider yarns with each other in biased oriented direction. If another system of yarns oriented longitudinally is inserted

into the biaxial braiding structure, a triaxial braid is obtained. Braid is a flexible product and can be manufactured into various shapes, such as planar, rectangle, tubular, etc. Nonwoven is a fabric-like material produced by entangling discontinuous staple fibers or filaments in a randomly oriented way. 2D nonwoven fabrics with sheet or web structures are bonded together by employing various techniques, such as mechanical, chemical, thermal or solvent treatment.[43] Nonwoven fabrics provide a variety of specific functions, such as absorbency, liquid repellence, resilience, softness, flame retardancy, thermal insulation, acoustic insulation, and so on.[44] The most common methods for nonwoven production are needle punching, stitch loading, thermal welding, chemical bonding, laminating, and electrospinning.

Almost all of the 2D fabrics mentioned above can be further evolved into 3D fabrics by adding additional oriented yarns. Compared to conventional 2D structures, 3D fibrous structures are used in various industrial applications since they have distinct properties, such as structure integrity, dimensional stability, high protection, and warmth retention. 3D woven structures have substantial dimension in the third (thickness) direction formed by layers of yarns. In other words, yarns are intertwined, interlaced, or intermeshed in the X (longitudinal), Y (transverse), and Z (thickness) directions.[45] In 3D woven fabrics, 3D orthogonal woven (3DOW)[46] and 3D angle-interlock woven (3DAW)[47] architectures are the most widely used weave structures. Particularly, the 3DAW can be further divided into two groups, i.e., 3D layer-to-layer angle-interlock woven (3DLAW)[48] and 3D through-the-thickness angle-interlock woven (3DTAW),[49] based on whether the interlaced yarns run through the thickness direction.[50] In 3DOW, there are three sets yarns that are perpendicular to each other. Z-binding yarns interconnect all individual warp and weft yarns and thus solidify the fabric. In 3DTAW, warp yarn travels from one surface of the fabric to the other holding all the layers together, whereas warp yarn travels from one layer to the adjacent layer and back in 3DLAW. A set of warp weaves together hold all of the layers of the weave structure. Knitting technology can also be used to produce complex 3D shapes. Particularly, 3D warp-knitted spacer fabric (3DWKS) consists of two separate outer fabric layers (top and bottom) connected by intermediary yarns or knitted layers that can either fix both directly or space them apart.[51] With the properties of excellent resilience, structure lighter, heat and moisture permeability, the 3DWKS is widely used in insole, mattress, automobile seat, and pressure sensors.[52] 3D braided fabric composed of mutual yarns intertwining can be obtained by introducing longitudinal (axial)-oriented yarns into its structure.[53,54] Based on the number of oriented braider yarns, 3D braided fabric can be classified into four directional and five directional structures. Through adjusting the arrangement or motion trajectory of braider yarns, the shape of 3D braided fabrics can be changed to rectangle, tubular, T-beam, I-beam, etc. 3D nonwoven fabrics can be obtained by stacking or stitching multiple layers of 2D nonwoven flat webs together in the thickness direction.[55] It is worth noting that 2D or 3D nonwoven fabrics can also be directly manufactured from 0D fibers. In practice, fibers in 3D nonwoven fabrics are aligned in all spatial directions.

**ADVANCED
SCIENCE NEWS**
_____
www.advancedsciencenews.com

**ADVANCED
MATERIALS**
www.advmat.de

Table 1. Comparison of structure characteristics between different textile dimensions.

Dimensions	Classifications	Main representatives	Structural characteristics	Merits
0D	Fiber	Staple fiber, filament	Basic unit, smallest visible part	Micro/nanoscale size
1D	Yarn/thread	Yarn/thread	Thousands of fibers twisting/twining	High strength and flexibility
2D	Weave	Plain, twill, satin	Warp and weft yarns making a series of interlacements with one another based on a weave pattern	Most common, dimensional stability
	Knit	Weft/warp knitting	Yarn loops interlacing to each other and to the neighboring rows and columns	High stretchability
	Braid	Biaxial, triaxial	Braiders intertwining with each other around the axial yarns in a cross path	Structure integrity
	Nonwoven	Web, sheet, mat, net	Holding short fibers together	Large specific surface area, light weight
3D	Weave	Orthogonal, angle interlock	Warp and weft yarns placed in multilayers	Dimension stability
	Knit	Weft/warp/spacer knitting	Binding by yarns in thickness direction	High air permeability
	Braid	Four/five directional	Braider yarns intertwining with each other and traveling through the thickness	Conformability, torsion stability
	Nonwoven	Felt, membrane	Stacking and stitching multiple 2D nonwoven layers	Large specific surface area

The classifications and comparisons of different textile structures are further summarized in **Table 1**. It is necessary to point out that all of the above textile forming technologies have widely existed in the present textile field, which are suitable for large-scalable industrial production. Each manufacturing technique has its own advantages and disadvantages in terms of the selection can be made based on the end use. It is hoped that these relatively detailed and comprehensive textile-related knowledge will provide method guidance and design inspirations for future research and applications of textile-based NGs.

2.2. Conductive Textiles

Smart textiles not only inherit all of the characteristics of normal textiles, but also have their own properties. Electrical conductivity is one of the most prominent capabilities that they possess. It can be said without exaggeration that good electrical conductivity of smart textiles is equivalent to the stable blood circulation of human beings. In addition, seamlessly integrating excellent electronic functionalities into traditional textiles is also an intriguing avenue to endow them with the abilities of communicating or interacting with ourselves and environment. In order to impose good electrical conductivity to textile-based NGs, it is extremely necessary to make overall understandings and detailed analyses about the current conductive materials for textiles as well as their corresponding fabrication methods. Thus, this review also makes a briefly summary and targeted comparison about the frequently adopted conductive mediums and imposing techniques for textile-based NGs, as shown in **Figure 3**.

2.2.1. Conductive Materials

One important consideration for textile-based NGs is the choice of conductive materials with good overall electrical performance, desired mechanical properties, reliable safety, and environmental stability. No matter what kinds of conductive materials
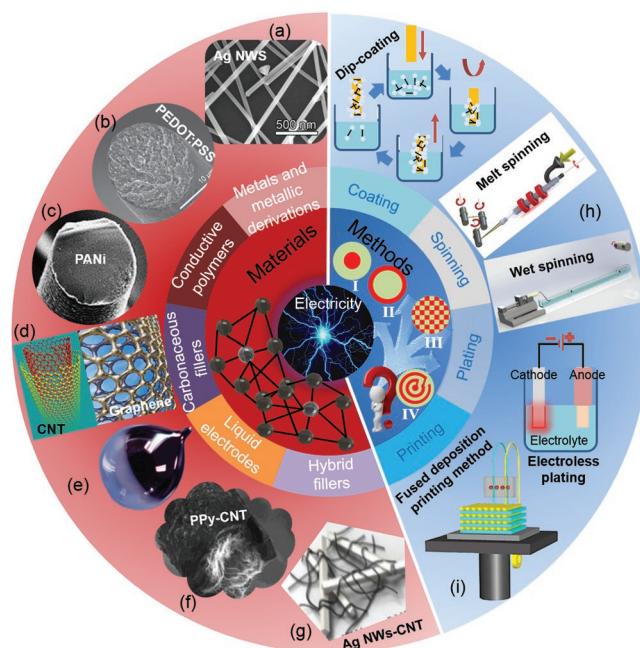

Figure 3. Commonly adopted conductive material systems and fabrication methods of electronic textiles. The frequently used conductive materials for textiles are broadly divided into five categories, i.e., metals and metallic derivations, conductive polymers, carbonaceous fillers, liquid electrodes, and their hybrid fillers. The main preparation methods for conductive textile materials include coating, spinning, plating, and printing. There are mainly four types of compounding structures between conductive materials and other functional materials, i.e., inner embedding (I), outer covering (II), homogenous blending (III), and spiral cladding (IV). a) Reproduced with permission.[56] Copyright 2018, American Chemical Society. b) Reproduced with permission.[57] Copyright 2011, Wiley-VCH. c) Reproduced with permission.[58] Copyright 2006, Elsevier. d) Reproduced with permission.[59] Copyright 2012, Royal Society of Chemistry. e) Reproduced with permission.[31] Copyright 2017, Royal Society of Chemistry. f) Reproduced with permission.[60] Copyright 2012, Royal Society of Chemistry. g) Reproduced with permission.[61] Copyright 2014, Wiley-VCH. h) Reproduced with permission.[62] Copyright 2012, Royal Society of Chemistry. i) Reproduced with permission.[63] Copyright 2018, Elsevier.

Table 2. Summary and comparison of frequently used conductive materials for smart textiles.

Classification	Categories	Advantages	Disadvantages
Metals and its derivatives	Metal, alloy, semiconductor, metallic nanoflakes/nanoparticles/nanowires	High conductivity, high mechanical robustness, good stability, ease of process	Unconformable, low flexibility, easy to rust, easy to oxidize
Conducting polymers	PPy, PEDOT/PEDOT:PSS, PANi, PAc, PTh, PPV, Pfu, PPP	High flexible, solution processable, easily controlled	Relatively high cost, different to prepare, low electrical conductivity, poor stability
Carbonaceous fillers	Carbon black/particle/fiber, CNT, CMF/CNF, carbon aerogel, G/GO/rGO	High aspect ratio, nanoporous architecture, superior mechanical property, environmental stability	Difficult in structure control, poor solution dispersion
Liquid electrodes	Liquid metals (e.g., EGaIn), liquid electrolytes (e.g., NaCl)	Soft, high electrical conductivity, good thermal conductivity, excellent flowability	Heavy, oxidize and leakage, toxicity, expensive
Hybrid fillers	Combination of different conductive materials (e.g., Ag NWs/CNTs)	Synergistic effect	Increased preparation cost and workload

are used, a basic principle is that they have no negative effect on the original performance of textiles. According to element compositions and conductive mechanisms, the present frequently used conductive materials for textiles are broadly categorized into five groups, i.e., metals and metallic derivatives, conductive polymers, carbonaceous fillers, liquid electrodes, and hybrid conductive fillers (Figure 3). The main representatives as well as advantages and disadvantages of these conductive materials are also summarized and compared in **Table 2**.

Metals as well as their alloys are the earth-abundant and most widely employed conductive elements in engineering field, considering their high electrical conductivity, universal existence, strong mechanical stability, and convenient recyclability. However, due to heavy weight, large volume, easy to rust, intrinsic brittle and rigid nature, it is difficult to achieve large-scale applications of block metals. In order to facilitate electric power transmission and practical usages, bulk metals are gradually designed into the shapes of strap or wire. As wearables increase in popularity, the drawback of metal strips or wires gradually emerge, which is not suitable for wearable usages requiring adequate flexibility and deformability. Recently, low-dimensional nanostructural metallic derivatives, such as nanoflakes/nanosheets, nanoparticles (NPs), nanowires (NWs), and nanoclusters, are particularly attractive for flexible and stretchable wearable electronics. The nanoscale-sized structures provide an excellent bonding interface between metallic nanomaterials and textile substrates. Moreover, their high surface to volume ratio can effectively increase surface energy and surface tension. By means of commercial physical depositing, electrodeless plating, or screen-printing methods, metallic nanomaterials are easily adhered on or incorporated in textile systems.[64,65] Among various metallic nanomaterials, metal NWs, such as Cu NWs,[66] Au NWs,[67] and Ag NWs,[24,56,68] have gained a substantial amount of attention due to their versatile properties, such as high electric and thermal conductivity, optical transparency, intrinsic flexibility, and chemical inertness.[69] Metallic NWs have been shown to be compatible with solution-based processing, low cost and large-area deposition techniques. Due to percolating network structure and high aspect ratio, metallic NWs can exhibit electrical performance similar to bulk metals while consuming a substantially low quantity of raw materials. At present, the greatest challenge of metallic nanomaterials for flexible electronic applications is their high cost, low solid content, and electromigration behavior.[65]

Conductive polymers (CPs) are a new class of organic functional materials, which have received a great deal of attention in various fields, such as electronics, supercapacitors, sensors, transistors and memories, due to their light weight, resistance to corrosion, and excellent electrical, mechanical, and optical properties.[70,71] The merits of solution processability, tailorable solubility, and electron affinity endow CPs with printable, easy-controlled, and flexible properties. A large number of CPs have been developed, such as polyacetylene (PAc),[72] polyaniline (PANI),[73] polypyrrole (PPy),[74] polythiophene (PTh),[75] poly[3,4-(ethylenedioxy)thiophene] (PEDOT),[76] and so on. Among them, PEDOT:PSS is one of the most promising CPs. The widespread use of PEDOT:PSS (commercial available) stems from the fact that it has good thermal and environmental stability, high conductivity, good optical transmission, good water solubility, and excellent processability.[57,77,78] A diverse array of strategies has been developed to modify and tune the CPs to integrate and interface them into functional electronics. To realize the advantages and large-scale applications of CPs, it is very essential to increase their processability, environmental and thermal stabilities.[79]

Carbonaceous fillers have also attracted unprecedented attention due to their many fancy merits, such as large surface area, excellent environmental stability, high electrical and thermal conductivity. According to structural dimensions, carbonaceous fillers are mainly divided into 0D carbon black/particle, 1D carbon macro/micro/nanofibers and nanotubes, 2D graphene (G) and its derivatives, i.e., graphene oxide (GO) and reduced graphene oxide (rGO).[59] Among these, CNTs and graphene are the most intensively explored in academic community and evaluated as the electrode materials with great potential in wearable electronics.[80] The major challenge for large-scale application of CNTs and graphene is their poor dispersion in common solvents due to their nonpolar structure.[81] Furthermore, the high aspect ratio and strong van der Waals attraction make CNTs prone to accumulate and even form large bundles. Thus, the development of suitable solvents is critical for fabricating high-performance CNT-based conductive materials. Due to high carrier mobility, excellent Young's modulus, and high conductivity and light transmission, graphene has attracted increasing attention in recent years. Various methods have been developed to fabricate large-area, highly conductive and defect-free graphene for industrial applications. Graphene obtained from mechanical exfoliation and chemical reduction has high electrical

**ADVANCED
SCIENCE NEWS**
www.advancedsciencenews.com

**ADVANCED
MATERIALS**
www.advmat.de

conductivity but cannot be well dispersed in common solvents due to its inherently inert surface.[59] Different from graphene, GO has oxygen containing groups on its surface. Therefore, GO can be well dispersed in polar solvents such as water, ethanol, acetone, and ethylene glycol, making it suitable for solution procession. The relatively poor electrical conductivity of GO can be further enhanced by a series of thermally or chemically reduced process, which leads to the formation of rGO.

Liquid electrode is also an important and promising substitute for flexible and stretchable conductive materials. Liquid electrolyte and liquid metal are the two main representatives of liquid electrodes. The movement of anions and cations in opposite directions within the electrolyte solution amounts to a current. The electrical conductivity of liquid electrolytes (e.g., NaCl and KCl) depends on the free-moving ion concentration in solution. Recently, room temperature Ga-based eutectic alloys, such as Ga–indium (EGaIn),[82] Ga–tin (EGaSn),[83] and Ga–In–Sn (Galinstan),[31,84] are realized to hold huge values in many important fields, owing to their capabilities in simultaneously exhibiting many extraordinary physical properties such as low melting point, excellent liquidity, high electrical conductivity, high surface tension, good thermal stability, low vapor pressure, and low toxicity in comparison to mercury.[85] Liquid metal possessing both metallic and fluidic properties provide unrivaled combination of conductivity and deformability of any known materials. Liquid metals can form circuits that are deformable, stretchable, self-healing, and shape-reconfigurable, which have much more potential to be utilized in the field of stretchable wires and interconnects, reconfigurable antennas, soft sensors, self-healing circuits, and conformal electrodes.[86,87]

As each material has its own strength and weakness, devices with a single material inevitably brings the demerit in use.[61] By combing two or more different materials, hybrid conductive fillers can make full use of their merits and meanwhile compensate for the shortcomings of each material.[88] Hybrid conductive fillers have also been widely reported, such as PPy/CNT,[60,89,90] Ag NWs/CNT,[61,62,91] G/PEDOT:PSS,[92,93] PANI/CNT,[58,94–96] PEDOT:PSS/Ag NWs,[97,98] CNT/G,[99–102] and so on. Hybrid conductive fillers with obvious synergistic effect have been proved as an effective method to enhance the electrical conductivity and mechanical properties that have more potential applications in flexible and wearable electronics.

2.2.2. Fabrication Methods

After making a general understanding of the frequently used conductive materials for smart textiles, the next question is naturally raised that how to impose these conductive elements into textile systems. One of the biggest challenges for large-scale applications of conductive materials is to provide the most convenient and economic approach to realize a good compatibility with existing textile technologies. However, owing to variable curved structures, uneven surface morphologies, and complex material property, it is difficult to achieve good combinations between conductive elements and textile systems. Numerous approaches have been designed and adopted to yield electrically conductive textiles, such as coating, spinning, depositing, and printing (Figure 3). Herein, the commonly adopted fabrication methods for textiles are also summarized and compared in **Table 3**.

Table 3. Summary and comparison of commonly adopted fabrication methods for electrical textiles.

Methods	Categories	Advantages	Disadvantages
Coating	Dip coating	Simple, fast, all size	Time consuming, large solution consumption, poor mechanical stability,
	Casting	Simplest, high efficiency, low cost	Uncontrollable thickness
	Doctor blading	Well-defined thickness, less wasted	Relatively slow speed, not fit for high concentration crystalline solution
	Spin coating	Simple, homogenous, highly reproductive	Only surface coverage, no pattering
Spinning	Wet spinning	High mechanical performance	Poor conductivity, low speed, solvent dissolvable
	Dry spinning	Easily solidification, wide raw material and application scope	Need highly volatile, solvent dissolvable
	Melt spinning	Simple, low cost, high production speed, without solvents, no environment pollution	Need high working temperature, hard to produce fine fiber, require specific machine
	Electrospinning	High aspect ratio, controlled pore size, superior mechanical properties	Need high voltage, small area
Plating	Electroless depositing	High conductivity,	Poor efficiency/stability, time consuming, limited to scaling up
	Thermal depositing	Hard, corrosion resistant, excellent abrasion resistance, durable	Requiring high working environment
	Magnetron sputtering	Fast speed, fit for mass production, better adhesion, uniform	Higher cost, low target utilization rate
Printing	Fused deposition modeling	Low cost, high speed, simplicity	Weak mechanical properties, layer-by-layer appearance, poor surface quality
	Screen printing	Simple, versatile, inexpensive	Limit for high viscous and low volatile solution
	Inkjet printing	Quite high resolution	Limited printing speed
	Roll-to-roll printing	Fit for high-volume and large-scale Manufacture, complex structure and pattern	Required process-dependent contact pressure, slower, higher cost
Injecting	Liquid injecting	Ultraflexible/stretchable	Limited to liquid electrode, easy to leakage

**ADVANCED
SCIENCE NEWS**

www.advancedsciencenews.com

**ADVANCED
MATERIALS**

www.advmat.de

Currently, coating technique are often used in the laboratory to manufacture electronic devices. The common coating methods mainly include dip coating, flow coating, spin coating, roll coating, doctor blading, casting and painting.[5] Casting is probably the simplest film-forming technique available. Dip coating is a useful technique when it is desirable to coat both sides of a part with the same coating. However, the ability of dip coating is sometimes limited by the size, shape, or surface features of the part. Flow or spin coating is a useful application when it is desirable to coat only one side of a part or when it is desirable to coat different sides of a part with different coatings. Spin coating is typically used for parts that are nearly flat and symmetrical in shape. However, both of the two coating methods have some limitations on parts that contain holes, protrusions, or other surface irregularities. The reverse roll coating is widespread adopted in applying various thin films onto a variety of substrates. Although the roll coating has the advantages of high efficiency, good accuracy, and controlled viscosity, it is unsuitable for curved shape and small-scale production.

Spinning is the most primitive process for producing polymer fibers or yarns. Spinning is a specialized form of extrusion that uses a spinneret to form multiple continuous filaments or mono filaments. The commonly used spinning methods mainly include wet spinning, dry spinning, melt spinning, gel spinning, and electrospinning. Both wet spinning and dry spinning require polymer that can be dissolved into solution. If the solvent in spinning solution can be rapidly evaporated or volatilized by hot air flow, dry spinning is the best choice. However, when the solvent is hard to be evaporated but can be removed by chemical means, wet spinning is the preferred embodiment. Melt spinning uses heat to melt the polymer to a viscosity suitable for extrusion. This type of spinning is used for polymers that cannot be decomposed or degraded but be melted easily under a certain temperature condition. Gel spinning, also known as dry–wet spinning, use high concentration polymer or plasticized gel to obtain high strength or other special properties in the fibers. Electrospinning is a versatile process that allows the production of micro or nanoscale fibers from a wide range of polymers.

As a special depositing method, plating is a surface covering in which a metal is deposited on a conductive surface. Multiple plating techniques exist, mainly including electroplating and electroless plating. Based on the principle of electrolysis, the electroplating is a process to accumulate a thin layer of metal on the surface of other metals. The plating metal is on anode, while the material to be plated is on cathode. On the one hand, both the cathode and anode are submerged in and meanwhile connected by an electrolyte solution containing dissolved metal salts or ions. On the other hand, the anode and cathode are also connected to an external power source providing a direct electrical current, which results in the transfer of metal ions to the cathode. Compared with the electroplating, the electroless plating, i.e., chemical plating, requires no additional electric field. According to the principle of redox reaction, metal ions in the chemical bath are reduced to metal by strong reductant and then deposited on the surface of materials with any geometry or intricate shape.

As a cutting-edge and reproductive technique, printing provides a promising solution to the large-scale fabrication and reducing high shape complexity. Various printing techniques have been developed, such as fused deposition modeling, inkjet printing, gravure printing, screen printing, flexographic printing, and offset printing.[5,63] In addition, printing can achieve extremely high throughput with low raw material consumption that brings a significant reduction in cost. Printing technology enables cost-effective manufacturing of different devices into large-area electronics systems that has been employed to fabricate various electronic devices, including flexible circuits, supercapacitors, batteries, solar cells, and nanogenerators.[103,104]

As for the compounding structures between conductive materials and other functional materials, there are mainly four types, i.e., inner embedding (Figure 3I), outer covering (Figure 3II), homogeneous blending (Figure 3III), and spiral cladding (Figure 3IV).

3. Piezoelectric Nanogenerators

Piezoelectricity means stress-induced electricity, which is based on piezoelectric effect.[105,106] Piezoelectric effect is the ability of certain materials to generate an electric charge in response to applied mechanical stress. One of unique characteristics of the piezoelectric effect is that it is reversible, meaning that it can convert the stress inside the material into electricity and vice versa. When piezoelectric materials are subjected to an external force, spatially separated electrical charges with opposite sign will be generated. The accumulation of electrical charges at two ends of the material body allows the formation of an electric dipole. The relative displacement of the cations with respect to the anions results in the formation of a piezoelectric potential, or piezopotential. A PENG is an energy harvesting device capable of converting nanoscale mechanical energy into electrical energy by means of piezoelectric effect.[107,108]

3.1. Piezoelectric Materials

A huge number of piezoelectric materials have been demonstrated since the discovery of piezoelectricity. Representative piezoelectric materials can be categorized into piezoceramics and piezopolymers. Piezoceramics, or inorganic piezoelectric materials, mainly include semiconducting nanomaterials (e.g., ZnO, GaN, CdS, InN, and ZnS), lead based (e.g., PZT, $PbTiO_3$, and $PbZrO_3$) and lead-free ceramics (e.g., $BaTiO_3$, KNN, $KNbO_3$, $LiNbO_3$, $LiTaO_3$, and Na_2WO_3). Piezoceramics are mechanically strong, hard, chemically inert, and immune to humidity, exhibiting high level of inherent piezoelectric characteristics. Piezopolymers means piezoelectric class of organic polymers, such as polyamide 11 (PA-11),[109] polypropylene (PP),[110] poly(vinylidene fluoride) (PVDF)[111] and its copolymer poly(vinylidene fluoride-co-tri-fluoroethylene) (PVDF–TrFE).[112,113] Among these piezopolymers, PVDF is a semicrystalline polymer with up to five different crystal phases, i.e., α, β, γ, δ, and ε. Between these electrically active polar phases, the β phase is of greater importance due to exhibition of large polarization and high piezoelectric sensitivity.[114] For PVDF to be used as a piezoelectric material, it must be processed in such a way that it crystallizes in its β-phase. Various

Table 4. Classification and discussion of common piezoelectric materials.

Classifications	Main types	Merits	Demerits
Piezoceramics	ZnO, PZT, BaTiO$_3$, PbTiO$_3$, KNbO$_3$, LiNbO$_3$, LiTaO$_3$, Na$_2$WO$_3$, GaN, CdS, InN, PbZrO$_3$, ZnS	Superior energy conversion efficiency, high strength	Mechanically brittle, heavy weight, poisonous, low durability
Piezopolymers	PVDF and its polymer PVDF–TrFE, PA-11, PP	Inherently flexible, easy for processing, adequate mechanically strong, strong sensitivity	Weak electromechanical coupling, low energy conversion efficiency

strategies have been employed for obtaining a higher percentage of β phase in PVDF, such as in situ poling,[115] thermally drawing, and high electric field.[116] Due to its high piezoelectric activity and availability as flexible nanofiber structures, PVDF promises potential applicability in diverse fields of technology. PVDF–TrFE has another advantage over PVDF owing to its ferroelectricity with definite Curie transition temperature and adequately large electromechanical coupling coefficient.[112,117,118] PVDF and PVDF–TrFE are the most widely used in piezoelectric textiles because of their advantageous properties in terms of structural flexibility, ease of processing, good chemical resistance, excellent biocompatibility, and mechanical strength.[119] However, since the piezoelectric charge constants of piezopolymers are much smaller compared to those of piezoceramics, the practical application of piezopolymers in energy harvesting is greatly restricted. A notable disadvantage of them is that achieving good performance requires electrical poling in which mechanical stretching processes need to align the dipole of the polarization structures.

The comparison and discussion between piezoceramics and piezopolymers are analyzed in **Table 4**. Piezoceramics have high piezoelectric coefficient and electromechanical conversion efficiency, but their intrinsic rigid nature restricts their applications in flexible devices. On the contrary, piezopolymers have smaller electromechanical coupling constants and lower piezoelectric coefficients but much higher flexibility than piezoceramics. Piezopolymers are attractive for wearable usages due to their flexibility and conformability over piezoceramics. Some researchers have also demonstrated that incorporating piezoceramics into piezopolymers to create a hybrid material can achieve higher piezoelectric constant and excellent electromechanical coupling factor. For example, ZnO has been incorporated into or grown on PVDF to fabricate hybrid PENGs.[120–124] In addition, both of piezoceramics and piezopolymers can be further optimized with nanostructures,[125] such as nanowire, nanofiber, nanotube, and nanosheet. The merits of nanostructures include enhanced piezoelectric effect, superior mechanical properties, higher flexibility, and high sensitivity to small forces.

3.2. Piezoelectric Mechanism

Conventionally, metal–insulator–metal structure, consisting of an insulating piezoelectric layer sandwiched between two metal
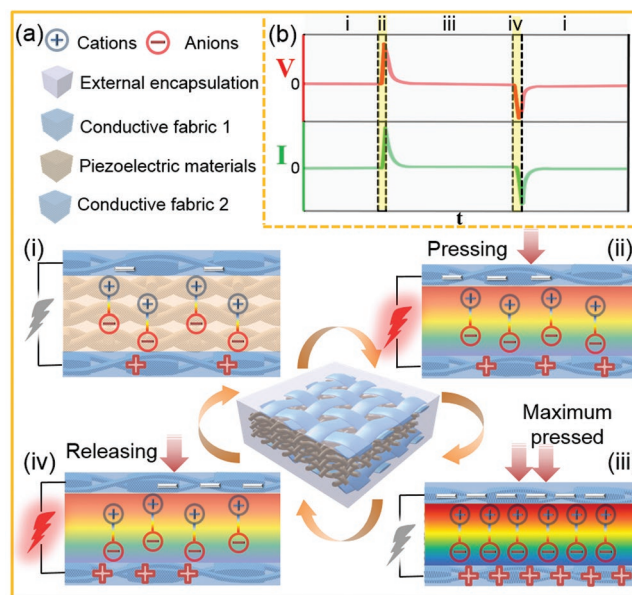

Figure 4. Working mechanisms of textile-based PENGs (as a fabric-based PENG for example). a) Schematic illustration of piezoelectric charge generation process. b) Typical open-circuit voltage (V_{oc}) and short-circuit current (I_{sc}) versus time curves, in which four parts corresponded to the four movement processes in (a).

electrodes was considered as a readily developed technique for PENGs.[85] **Figure 4** demonstrates a complete electrical generation process and corresponding electrical output characteristics of a piezofabric during one pressing and releasing movement. At the beginning and undisturbed state, the charge centers of the cations and anions coincide with one another. No polarization can be observed inside the piezoelectric material (Figure 4ai). When the pressing force is applied, deform of the piezofabric produces a negative strain and decreased volume. The charge centers separate to form electrical dipoles and electric dipole moments change, which will result in the formation of a piezopotential between the electrodes. If the electrodes are connected with an external load, the piezopotential will drive electrons to flow through the external circuit in order to partially screen the piezopotential and achieve a new equilibrium state (Figure 4ii). As a result, mechanical energy is converted into the electricity. As the fully contact between the two conductive fabric electrodes is made, the maximized pressed state is achieved with the highest polarization density (Figure 4iii). When the external force is released, electrons flow back to rebalance the charge induced by the strain releasing in the short-circuit condition (Figure 4iv). A steady stream of pulse current will flow through the external circuit if the piezopotential is continuously changed by applying a reciprocating straining phenomenon. One remarkable feature of PENGs is that the output voltage and current reverse their signals when the measurement system is reversely connected.

3.3. Piezoelectric Textiles

It is found that the material selections, structure designs, and potential performance are the most important aspects

**ADVANCED
SCIENCE NEWS**

www.advancedsciencenews.com

**ADVANCED
MATERIALS**

www.advmat.de

for PENGs. In addition, the flexibility and wearability are also necessary for the textile-based PENGs. Nowadays, many attempts have been made to design piezoelectric textiles with the purpose of enhancing electromechanical conversion efficiency, improving wearable functionality, and expanding application scopes. According to the structural characteristics and fabrication methods, the present textile-based PENGs are mainly divided into three groups, i.e., single fiber-based PENGs, fabric-based PENGs with textile forming structures, and fabric-based PENGs with multilayer stacking structures. In the following, the related research works of these three types are introduced, respectively.

3.3.1. Single Fiber-Based PENGs

Since fiber is the smallest structure unit of textile materials, it is of great strategic significance to make it into PENGs. Nowadays, with the great demands of wearable power supplying and active sensing devices, a large number of single fiber-based PENGs have been developed. At the beginning, flexible piezoelectric materials were simply wrapped around fiber substrates with high strength and high modulus. The first fiber-based PENG was fabricated by entangling a Kevlar fiber covered by ZnO NWs and the fiber that further coated with Au electrode together (**Figure 5**a).[126] However, its power generation depends on the specific relative brushing between the two fibers, which is inconvenient for daily wearable usage. Later researchers attempt to design fiber-based PENGs within a single fiber. The most common method is to sandwich piezoelectric materials between the inner and outer electrodes. For example, ZnO thin film was sandwiched between an inner carbon fiber and an outer silver paste (Figure 5b).[127] Alternatively, ZnO NWs grown on carbon fibers was further covered by an indium tin oxide (ITO) electrode layer (Figure 5c).[128] However, a potential issue of these fiber-based PENGs is that piezoelectrical materials and external covered electrodes are vulnerable to be destroyed under complex mechanical stimuli, which will lead to reducing their energy harvesting capability or even making their useless. In order to improve their long-term working stability, several approaches have been adopted, such as fixing positions with polymer, wrapping with outer protective layer, fabricating with hybrid materials, and adopting with melt-spun method. In term of fixing positions with polymer, the roots of ZnO NWs were bonded by PDMS to meet safety requirements and simultaneously guarantee high flexibility (Figure 5d).[129] The protection of ZnO NWs grown on fibers can also be obtained by further wrapping an outer encapsulating layer. For instance, a carbon fiber grown with ZnO NWs was further wrapped by an outer folded Au-coated ZnO NWs paper tube (Figure 5e).[130] The established core–shell nanostructure provides more polarization possibilities between inner and outer ZnO NWs. If there are more than two piezoelectric materials existing in one PENG, the hybrid PENGs can be obtained which can improve the mechanical endurance as well as piezoelectric output performance. Generally speaking, membrane-like piezopolymers are coated on the surface of nanostructural piezoelectric materials.[122,131] As shown in Figure 5f, PVDF film was conformally applied on the surface of electrospinning PVDF nanofibers to fabricate a

high-performance fiber-based PENG.[132] In this hybrid structure, PVDF nanofibers function as piezoelectric material and porous scaffolds to absorb PVDF polymer. A similar example that PVDF polymer is infiltrated into ZnO NW forests is displayed in Figure 5g.[133] The ZnO NW arrays not only serve as the piezoelectric material, but also assist the formation of PVDF polymer on the outermost surface of the device. Although the above three approaches can improve the working stability of fiber-based PENGs to some extent, there still remains the possibilities of damage. In addition, multiple processing steps are also required for the above fiber-based PENGs, which is contrary to their future large-scale industrial applications. With the advantages of one-time forming, high forming quality, and fast production speed, melt spinning has been widely used to prepare fiber-shaped piezoelectric polymers.[110,134–137] As shown in Figure 5h, a simple melt-spun piezoelectric fiber was developed by wrapping a fiber core electrode around β-phase PVDF microfibers.[136] With the prepared piezoelectric fiber, a fiber-based PENG is fabricated by further spirally winding an outer fiber electrode around it, which can effectively harvest human motion energies and even in rainy days. Instead of twining the outer fiber electrode, other directly deposited the outer electrode on the surface of melt spinning piezoelectric fiber. As a case, a fiber-based PENG is obtained by depositing Au on the surface of the melt spinning PTFE–TrFE/Cu coaxial filament via vacuum deposition method.[113] The entire structure of fiber-based PENG can be accomplished through one-time thermal drawing in a straightforward manner. As shown in Figure 5i, a multimaterial fiber-based PENG containing PVDF–TrFE piezoelectric shell sandwiched by the inner and outer CPC/indium electrodes was fabricated through one-time thermal-drawing processes.[134] In order to enhance the piezoelectric response of fiber-based PENGs, piezoceramics are usually incorporated into piezopolymers during their thermal drawing processes. For example, BaTiO₃, PZT, or CNT enhanced PVDF acted as piezoelectric layers is alternatively wrapped around carbon-loaded polycarbonate (CPC) to fabricate an all-polymer flexible piezoelectric fiber with a spiral multilayer cladding structure (Figure 5j).[116] The designed spiral multilayer cladding structure can greatly increase the active area of piezoelectric composites resulting in higher power generation efficiency. Since stretchability is also a desirable property for wearable electronics, some studies attempt to endow fiber-based PENGs with high stretchability. As illustrated in Figure 5k, a highly flexible and stretchable fiber-based PENG was fabricated by a simple rolling and coating method.[138] The PVDF–TrFE electrospinning mats were manually wrapped around Ag-coated nylon multifilament yarn and then covered by highly conductive CNTs. The prepared fiber-based PENG was finally dip-coated in an elastomeric styrene–ethylene–butylene–styrene (SEBS) to provide mechanical protection and electrical insulation. In addition to fabricating with all inherent stretchable materials, high stretchability of PENGs can also be obtained from structural design. As exhibited in Figure 5l, a PVDF piezoelectric strap and a fabric band were helically twined around an elastic core in counter directions.[139] The helix could produce an alternating potential during continuous stretching and contraction motions. The stretchability of piezoelectric fibers can also be directly achieved by twisting electrospun PVDF–TrFE nanofibers into stretchable
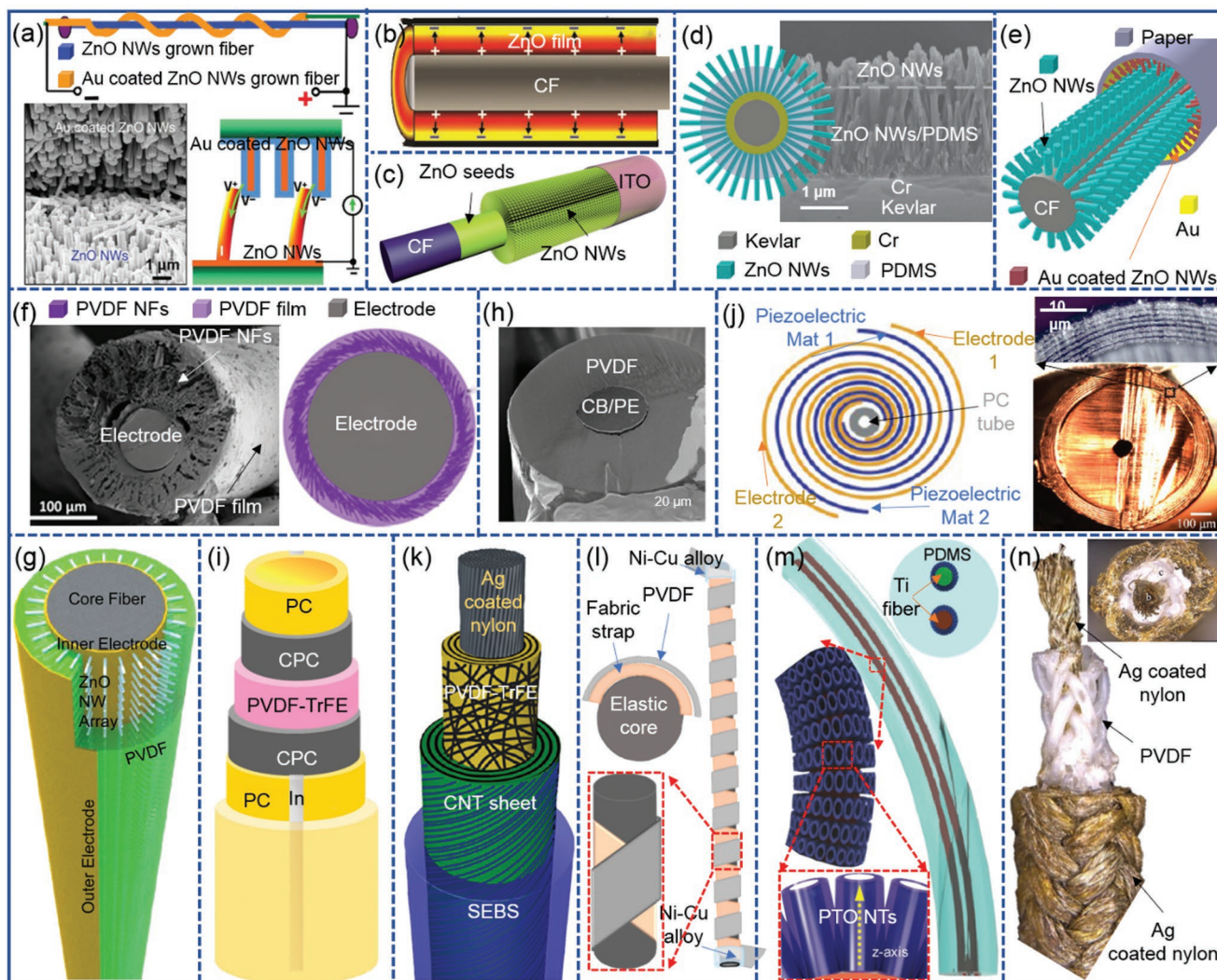
**ADVANCED
SCIENCE NEWS**

www.advancedsciencenews.com

**ADVANCED
MATERIALS**

www.advmat.de

Figure 5. Typical single fiber-based PENGs. a) The first fiber-based PENG developed by entangling a Kevlar fiber covered by ZnO NWs and the fiber that further coated with Au together. Reproduced with permission.[126] Copyright 2008, Springer Nature. b) An air/liquid-pressure and heartbeat-driven flexible fiber-based PENG designed by covering textured ZnO thin film on the surface of cylindrically carbon fibers. Reproduced with permission.[127] Copyright 2011, Wiley-VCH. c) A fiber-based PENG composed of carbon fibers and ZnO NWs based on an insulating interface barrier. Reproduced with permission.[128] Copyright 2017, Royal Society of Chemistry. d) A high-reliability Kevlar microfiber–ZnO NW hybrid PENG. Adapted with permission.[129] Copyright 2015, Wiley-VCH. e) A flexible fiber-based PENG consisting of ZnO NWs on carbon fibers and foldable Au-coated ZnO NWs on paper. Adapted with permission.[130] Copyright 2014, Tsinghua University Press and Springer-Verlag GmbH Germany, part of Springer Nature. f) A flexible piezoelectric yarn consisting of a layer of electrospun PVDF nanofibers integrated with PVDF film around a Ag-deposited nylon filament. Reproduced with permission.[132] Copyright 2018, IOP Publishing. g) A hybrid-fiber PENG with ZnO NWs and a PVDF infiltrating polymer as the hybrid piezoelectric layer. Reproduced with permission.[133] Copyright 2012, Wiley-VCH. h) A melt-spun piezoelectric microfiber consisting of a conducting core surrounded by β-phase PVDF. Reproduced under the terms of the CC-BY Creative Commons Attribution 4.0 International License (http://creativecommons.org/licenses/by/4.0/).[136] Copyright 2018, The Authors, Published by Springer Nature. i) A multimaterial piezoelectric fiber comprising middle melt-pressed PVDF–TrFE shell and carbon-loaded polycarbonate with indium filaments and a polycarbonate cladding. Reproduced with permission.[134] Copyright 2010, Springer Nature. j) An all-polymer flexible piezoelectric fiber featuring a soft hollow polycarbonate core surrounded by a spiral multilayer cladding consisting of alternating layers of piezoelectric nanocomposites and conductive polymer. Reproduced with permission.[116] Copyright 2017, American Chemical Society. k) A highly flexible piezoelectric fiber fabricated by sandwiching electrospun PVDF–TrFE mat between inner Ag-coated nylon fiber and outer CNT sheet. The whole system is covered by elastomeric styrene–ethylene–butylene–styrene. Reproduced with permission.[138] Copyright 2017, Wiley-VCH. l) A helical structural fiber-based PENG composed of an elastic core and a polymer piezoelectric strap twining the core. Reproduced under the terms of the CC-BY 4.0 Creative Commons Attribution license (https://creativecommons.org/licenses/by/4.0/).[139] Copyright 2017, The Authors, Published by MDPI. m) A fiber-type PENG based on perovskite PbTiO$_3$ nanotubes synthesized by anodic oxidation and hydrothermal method using TiO$_2$ NT as a positive template. Reproduced with permission.[141] Copyright 2017, Wiley-VCH. n) A triaxial braided PVDF yarn harvester developed by braiding melt-spun PVDF piezoelectric and conductive Ag-coated nylon yarns. Reproduced with permission.[142] Copyright 2019, Royal Society of Chemistry.

ribbons.[140] Recently, some new piezoelectric materials and fabrication techniques have been adopted to fabricate fiber-based PENGs. As illustrated in Figure 5m, a flexible fiber-type PENG

based on perovskite PbTiO$_3$ nanotube arrays (PTO NTs) was fabricated by embedding two PTO NTs/Ti core–shell fibers in PDMS.[141] The PTO NTs were grown by using hydrothermal

method with anodized TiO_2 NT as a positive template. The perovskite-based fiber-type PENG allowed arbitrary-direction bending and continuous harvesting mechanical energy from our natural environment. In term of fabrication techniques, a novel triaxial braided structure has been developed to design fiber-based PEGNs based on melt-spun PVDF fibers and Ag-coated nylon yarns.[142] As shown in Figure 5n, melt-spun PVDF filaments were first braided around Ag-coated nylon yarns (inner electrode) and then the whole structure was braided a second time with Ag-coated nylon yarns (outer electrode). The developed triaxial braided fiber-based PENG exhibited improved mechanical and piezoelectric properties.

Whatever the materials and structures are selected, one common feature of single fiber-based PENGs is that all of them present coaxial and core–shell structure. Flexible piezoelectric materials are usually existed between the inner and outer fiber electrodes.

3.3.2. Fabric-Based PENGs with Textile Forming Structures

The piezoelectric outputs of single fiber-based PENGs are relatively low, due to limited number and small active area. In order to improve the overall piezoelectric outputs, one promising strategy is to combine multiple piezoelectric fibers into 2D or 3D fabrics by using various textile forming techniques. Therefore, a variety of fabric-based PENGs with optimized fabric structures have been reported. The simplest 2D fabric-based PENGs are directly woven from one type of piezoelectric fibers. For instance, a wearable and self-powered fabric-based PENG as a highly pressure-sensitive electronic skin was woven from PEDOT-coated PVDF electrospun yarns (**Figure 6**a).[143] The high sensitivity of the fabric-based electronic skin was attributed the accumulation of PEDOT nanoparticle doped PVDF nanofibers which increased the contact joints and the total contact area under subtle stress. Although the fabric-based PENGs made from one kind of fiber system is relatively simple and easy to prepare, the power outputs are unsatisfactory. Therefore, a majority of fabric-based PENGs with optimized structures are fabricated from two or three types of fibers. For example, a 2D woven PENG was fabricated from two kinds of fibers, i.e., one grown with ZnO NWs and the other covered with ZnO NWs coated with palladium (Pd).[144] As exhibited in Figure 6b, continuous piezoelectric charges could be generated through periodically sliding back and forth as well as squeezing with each other between the two kinds of fibers. Although the plain-patterned woven structure can improve piezoelectric output to some degree, short circuit often occurs due to the damage of surface nanostructures or other encapsulating layers. In order to effectively prevent short circuit between adjacent fiber electrodes, nonconductive fibers and piezoelectric fibers are usually arranged in a staggered manner. As shown in Figure 6c, a 2D fabric-like PENG was developed based on three kinds of fibers including $BaTiO_3$ NWs/PVC hybrid piezoelectric fibers, conventional cotton fibers, and Cu wires.[145] The Cu wires served as electrodes, while the cotton fibers were employed as spacer to avoid the shorting of electrodes as well as to enhance the durability of the whole device. Another kind of 2D woven PENG with the similar structure while different

materials is also presented in Figure 6d.[31] PVDF–TrFE yarn employed as piezoelectric component was twisted from aligned electrospinning nanofiber mats. To prevent electrically shorting the collected charges, conventional cotton fibers were used between each conductive fiber as separators. Comparing with the above complicated fiber-shaped piezoelectric components, it seems more convenient and faster to prepare 2D fabric-based PENGs directly from fabric or film straps. For example, a scalable woven fabric-based PENG was designed by interlacing piezoelectric film straps with yarn strings in an orthogonal direction (Figure 6e).[146] The piezoelectric straps were made of PVDF films with metal electrodes on both surfaces. The fabric-based PENG with piezoelectric film straps can further be optimized into tactile sensor arrays. As shown in Figure 6f, a 2D woven power-generating tactile sensor array with high stretchability was composed of elastic tubes and piezoelectric film straps with metal films deposited on both sides.[147] The piezoelectric straps were stitched to each other in a diagonal direction across the woven mesh structure of the elastic hollow tubes. The abilities of energy harvesting and tactile sensing could be simultaneously possessed within the proposed structure. Although the electricity outputs of 2D fabric-based PENGs have been greatly improved compared with single fiber-based PENGs, further enhancement the energy harvesting capability of fabric-based PENGs are still required. 3D fabric structures with more piezoelectric components incorporated are desirable for high-performance fabric-based PENGs. As displayed in Figure 6g, a 3D interlock woven fabric-based PENG was developed based on 100% melt-spun piezoelectric PVDF fibers.[148] By comparing the electrical outputs of a 2D plain woven PENG, it was found that the energy harvesting ability of the 3D interlock woven structure was greatly improved. Another 3D fabric structure that has been designed into fabric-based PENG is 3D spacer knitted structure. As exhibited in Figure 6h, a 3D spacer knitted PENG consists of high β-phase ($\approx$80%) piezoelectric PVDF monofilaments as the spacer yarn interconnected between Ag-coated polyamide (PI) yarn layers acting as the top and bottom electrodes.[29] The 3D spacer knitted structure provides a progressive compression process of PVDF yarns, leading to enhanced performance. In general, due to the increased number of piezoelectric fibers per unit area, 3D fabric structures possess significantly higher energy harvesting efficiencies than the existing 2D textile structures.

3.3.3. Fabric-Based PENGs with Multilayer Stacking Structures

Fabric-based PENGs can not only be fabricated by traditional textile forming processes, but also obtained from planar fabric substrates or nanofiber webs through multilayer stacking method. As for multilayer fabric stacking structures, piezoelectric materials can be directly grown or covered on the surface of fabric substrates. For example, ZnO NW, nanorod or nanoflower arrays have been successfully grown on conductive fabric substrates by traditional hydrothermal method.[30,149–153] As shown in **Figure 7**a, a fabric-based PENG with hybrid energy generation mechanism of electrostatic and piezoelectric effects was proposed by growing ZnO NWs on a Au-coated fabric.[149] An insulating film was placed between the bottom ZnO NWs
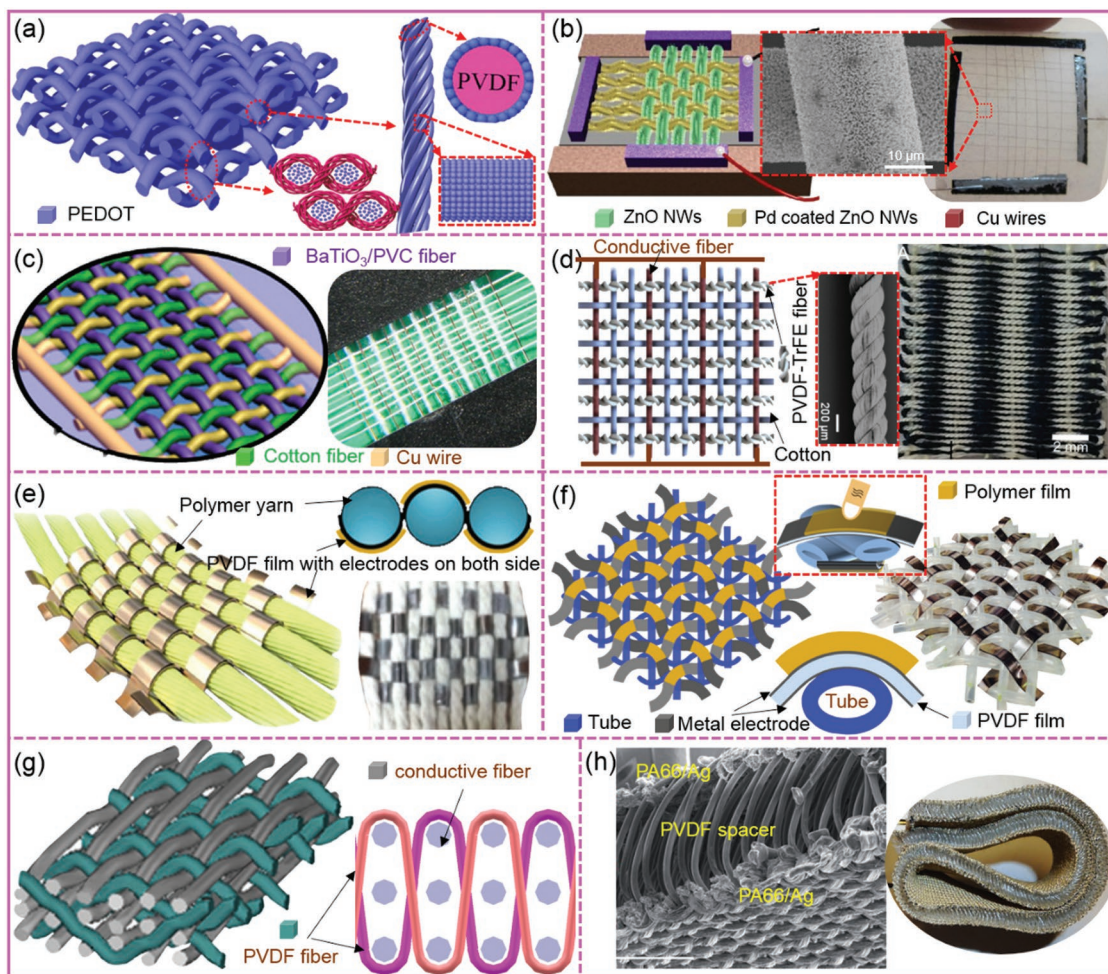
ADVANCED
SCIENCE NEWS
www.advancedsciencenews.com

ADVANCED
MATERIALS
www.advmat.de

Figure 6. Fabric-based PENGs with fiber weaving structures. a) A pressure-sensitive nanofiber woven fabric sensor fabricated by weaving PVDF electrospun yarns of nanofibers coated with PEDOT. Reproduced under the terms of the Creative Commons Attribution 4.0 International License (http://creativecommons.org/licenses/by/4.0/).[143] Copyright 2017, The Authors, published by Springer Nature. b) A 2D woven PENG composed of two kinds of fibers crossing with each other, one kind of fibers grown with ZnO NWs and the other kind of fibers covered with ZnO NWs coated with palladium (Pd) on their surface. Reproduced with permission.[144] Copyright 2013, Elsevier. c) A 2D fabric PENG consisting of BaTiO$_3$ nanowire-PVC piezoelectric fibers integrated with conducting wires electrodes and insulating spacer cotton yarns. Reproduced with permission.[145] Copyright 2015, Elsevier. d) A nanofibrous smart piezofabric woven twisted PVDF–TrFE piezoyarns with conductive threads and conventional PET yarns. Reproduced with permission.[31] Copyright 2015, American Chemical Society. e) A scalable woven PENG composed of warp and weft threads made of yarn strings and piezoelectric film straps. Reproduced with permission.[146] Copyright 2015, IOP Publishing. f) A power-generating tactile sensor array consisting of rows and columns of piezoelectric straps woven on a mesh structure of elastic hollow tubes. Reproduced with permission.[147] Copyright 2015, IOP Publishing. g) A 3D diagonal interlock woven structure PENG developed by fabricating PVDF fibers and conductive fibers. Reproduced with permission.[148] Copyright 2018, IOP Publishing. h) An all-fiber piezoelectric fabric with 3D spacer knitted structure consisting of high β-phase piezoelectric PVDF monofilaments as the spacer yarn interconnected between Ag-coated PA multifilament yarn layers as the top and bottom electrodes. Reproduced with permission.[29] Copyright 2014, Royal Society of Chemistry.

covered conductive fabric and top conductive fabric to enhance electrostatic effect and improve power output. A similar work that vertically arranged ZnO nanorods were sandwiched between two symmetrical Ag-coated fabrics had also been reported (Figure 7b).[30] When external force was applied, the upper and lower ZnO nanorods were in contact and squeezed with each other, leading to the generation of electricity. Unlike piezoceramics such as ZnO usually attached on fabric substrates, piezopolymers such as PVDF and PVDF–TrFE are directly used as nanofiber webs or nets which are fabricated with electrospinning and nonwoven techniques.[26,111,154,155] As shown in Figure 7g, a highly durable all-fiber based PENG was

fabricated by sandwiching a PVDF–NaNbO$_3$ piezoelectric nonwoven fabric as an active piezoelectric component between two elastic knitted fabric electrodes.[28] The whole device was further packaged with PDMS to enhance mechanical robustness and protect it from dust and water. In order to achieve high stretchability of nanofiber-based PENGs, both stretchable conductive and piezoelectric materials should be employed. As exhibited in Figure 7h, an omnidirectional stretchable hybrid nanofiber-based PENG was developed based on a stretchable graphite electrode and a stacked mat of piezoelectric nanofibers.[27] The stacked nanofiber mat was alternatively composed of nanocomposite nanofibers of BaTiO$_3$ nanoparticles

ADVANCED
SCIENCE NEWS
www.advancedsciencenews.com

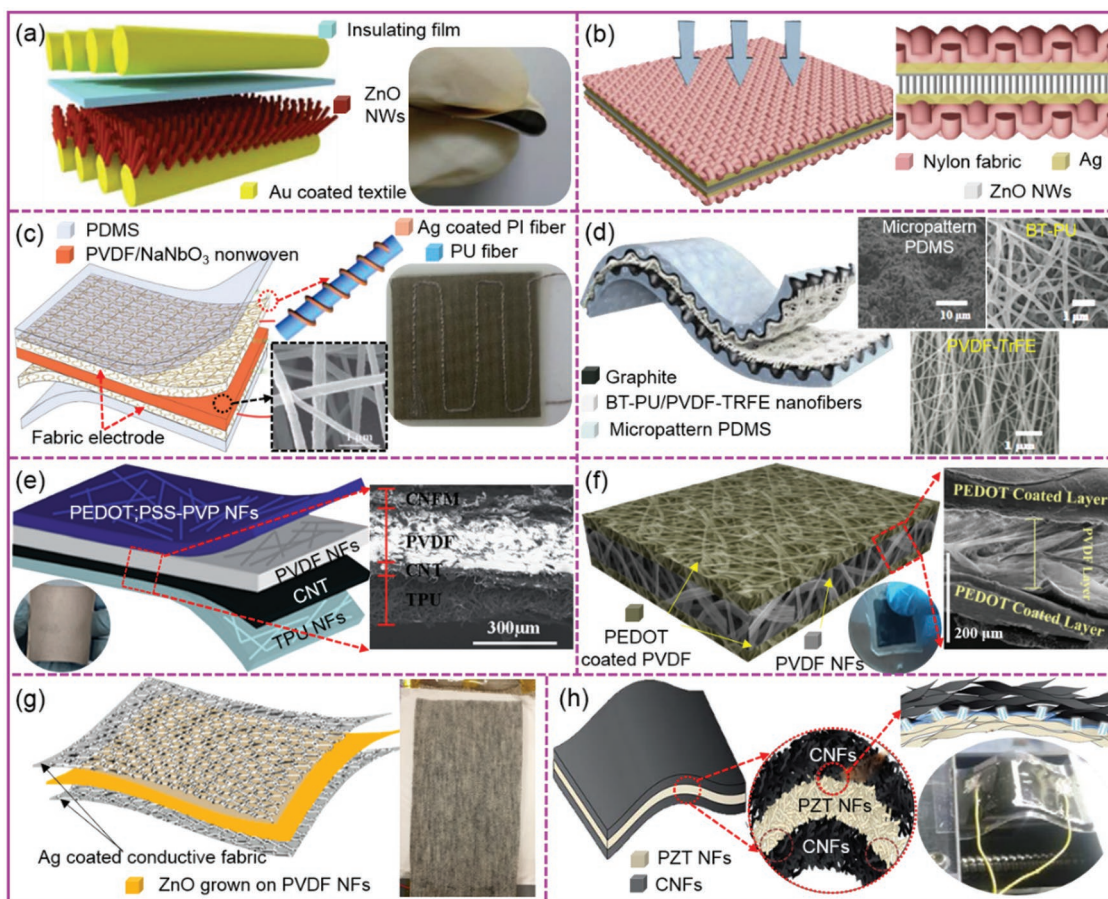ADVANCED
MATERIALS
www.advmat.de

Figure 7. Fabric-based PENGs with multilayer stacking structures. a) A fully textile PENG demonstrated by integrating a charged dielectric layer and piezoelectric ZnO NWs between textile substrates. Reproduced with permission.[149] Copyright 2012, Royal Society of Chemistry. b) A ZnO nanorods pattern textile PENG that consists of vertically arranged ZnO nanorod arrays sandwiched between two symmetrically layers of Ag-coated fabrics. Reproduced with permission.[30] Copyright 2019, Elsevier. c) An all-fiber wearable PENG consisting of a PVDF–NaNbO$_3$ nonwoven fabric as an active piezoelectric component and an elastic conducting knitted fabric as the top and bottom electrodes. Reproduced with permission.[28] Copyright 2013, Royal Society of Chemistry. d) An omnidirectionally stretchable PENG based on a stretchable graphite electrode on a 3D micropatterned substrate and a stacked mat of piezoelectric nanofibers. Reproduced with permission.[27] Copyright 2018, Wiley-VCH. e) A self-powered nonwoven nanofiber based PENG obtained by using an electrospun TPU NFs as a substrate and a conductive PEDOT:PSS-PVP NFs and a CNT layer as electrodes. Reproduced with permission.[156] Copyright 2018, The Royal Society of Chemistry. f) An all-organic PENG with multilayer assembled nanofiber mats assembled by sandwiching neat PVDF NFs as active component between two PEDOT-coated PVDF NFs as electrodes. Reproduced with permission.[157] Copyright 2018, American Chemical Society. g) A breathable and flexible piezoelectric membrane developed by growing ZnO nanorods on the surface of electrospun PVDF nanofibers. Reproduced under the terms of the CC-BY 4.0 Creative Commons Attribution license (https://creativecommons.org/licenses/by/4.0/).[120] Copyright 2018, The Authors, Published by MDPI. h) A PZT nanofiber-based PENG fabricated by sandwiching the PZT nanofibers between the top and bottom CNF NFs webs. Reproduced with permission.[162] Copyright 2016, Royal Society of Chemistry.

embedded in PU and PVDF nanofibers. This nanofiber stacked PENG exhibited a high stretchability of 40% and high mechanical durability up to 9000 stretching cycles at 30% strain, which were attributed to the stress-relieving nature of the 3D micropattern on the substrate and the freestanding stacked hybrid nanofiber. Instead of employing common fabrics or polymer membranes as substrates, nanofiber-based PENGs can also be fabricated with all-nanofiber structures. A potential advantage of all-nanofibers based PENGs is that they can provide more contact probabilities between piezoelectric components and conductive materials than membranous-like structures. For example, a flexible all-nonwoven PENG was developed by using electrospinning PVDF nanofibers as piezoelectric components, electrospinning TPU as substrates, PEDOT:PSS/PVP

nanofibers and CNTs as electrodes (Figure 7e).[156] The structure of nanofiber-based PENG can be further simplified by directly depositing electrodes on the surface of piezoelectric nanofibers. As displayed in Figure 7f, an all-organic PENG was designed based on multilayer assembled electrospun PVDF nanofiber mats.[157] Vapor-phase polymerized PEDOT-coated PVDF NFs were assembled as the electrodes at both ends, while neat PVDF NFs were utilized as an active piezoelectric component. The multilayer networked structure integrated with compatible electrodes enhanced power outputs. Hybrid piezoelectric materials are also employed in nanofiber-based PENGs to improve piezoelectric outputs. Particularly, ZnO NWs can be directly grown on the surface of piezopolymer NFs to enhance piezoelectric effect.[120,158] For instance, a breathable and flexible piezoelectric

**ADVANCED
SCIENCE NEWS**
www.advancedsciencenews.com

**ADVANCED
MATERIALS**
www.advmat.de

fabric was developed by growing ZnO nanorods on the surface of electrospinning PVDF nanofibers (Figure 7g).[120] The hybrid ZnO/PVDF piezoelectric web was further sandwiched between two conductive knitted fabric as flexible electrodes. In addition to PVDF and PVDF–TrFE, other piezoelectric materials can also be fabricated into nanofibers. PZT NFs[159,160] or BaTiO$_3$ NFs[161] based PENGs have also been successfully proposed via electrospinning processes. As shown in Figure 7h, an all-nanofiber PENG were fabricated by sandwiching PZT nanofibers between two CNF electrodes at both sides.[162] By comparing with conventional ITO electrodes with CNTs, the nanofiber-based PENG showed improved electrical outputs, due to the improved contact between PZT and CNT fibers.

Throughout the above studies on textile-based PENGs, it can be found ZnO and PVDF are the most widely employed piezoelectric materials for fiber/fabric-based PENGs. ZnO in the form of NWs often grows on textile substrates, while PVDF is usually fabricated into filaments or nanofiber nets by means of melt spinning or electrospinning, respectively. Surface nanostructures and hybrid piezoelectric materials are the most adopted strategies to improve total piezoelectric outputs. Effective surface protection, such as polymer encapsulation, is also necessary to improve mechanical properties and long-term stability of PENGs with nanostructures. Due to the varied selected materials, imposing conditions and geometric sizes, such as force, frequency, and contact area, it is difficult to compare electrical outputs among different textile-based PENGs. However, it can provide a basic research orientation, design framework, and tradeoff platform for future fiber/fabric-based PENGs. Herein, a roughly summary of the structures and performances of the present textile-based PENGs is presented in **Table 5**.

4. Triboelectric Nanogenerators

Triboelectrification is a universal and ubiquitous phenomenon in our daily life, which has been known for thousands of years. However, due to lack of reasonable cognition and utilization technology, it is usually regarded as a negative effect and avoided if at all possible. As a versatile mechanical energy harvesting technology, the newly developed TENG can convert abandoned mechanical energy into precious electricity based on a coupled effect of contact electrification and electrostatic induction.[163–166] Due to its high efficiency, light weight, low cost, environmentally friendly, and universal availability, it has promising applications in scavenging both small mechanical energy and large-scale energy generation. The TENG has been demonstrated to harvest various kinds of mechanical energies that are omnipresent but otherwise wasted in our daily life, such as human motion,[37,167–169] mechanical trigging,[170–172] vibration,[173–175] wind,[176–178] flowing water,[179–181] and more. The power outputs of TENGs can not only be used for wearable power supplying, but also adopted as active self-powered sensors.

4.1. Triboelectric Materials

It is well known that triboelectric effect exists between any two kinds of materials and even the same materials.

Therefore, all types of materials can be candidates for fabricating TENGs, so that the materials choices for TENGs are huge. The triboelectric polarities of materials have a significant impact on the final electrical output performance of TENGs. Triboelectric series of materials is the main principles of material selections for TENGs. The position of a material in the triboelectric series determines how effectively the charges will be exchanged. Moreover, selection of appropriate paired tribomaterials with opposite triboelectric polarities from the triboelectric series is crucial to achieve an enhanced electrical output TENG. The further away two materials are from each other on the series, the greater the charge transferred. The first triboelectric series including ten kinds of common materials were drawn up in the order of polarity.[182] Subsequently, some scholars have also made contributions to further supplement the triboelectric series.[183,184] Recently, a more comprehensive triboelectric series for TENGs has been summarized based on previous studies.[163] More recently, Zou et al.[185] have made a further measurement of triboelectric series of materials that are widely used to design TENGs. In order to conduct a standard measurement, they qualitatively ranked the triboelectric series from a wide range of polymers with regards to their triboelectric polarization in a well-controlled environment. Shape-adaptive liquid metal of mercury was utilized as the other triboelectrification material to maximize the contact area with measured solid surfaces. The quantitative triboelectric series they updated might serve as a textbook standard for the design of TENGs. Since textiles are highly porous and deformable materials with a structural hierarchy, the triboelectric series measured from planar membranous structures may not be very accurate for textile materials. Therefore, an extended textile-related triboelectric series including 21 types of commercial and new fibers has also been reported.[186,187] Effective charge density of textiles can be reliably measured when the triboelectrification process reach its saturation under the fabric densification pressure.[186] It turns out that there is no significant difference of the triboelectric series measured from planar membranous structure and hierarchical fiber-shaped structure. Therefore, the triboelectric series obtained from film materials can also be used for textile materials. Since the triboelectric series of materials can be obtained from previous literatures, this review will no longer specifically list and compare them again.

4.2. Working Modes of Textile-Based TENGs

Based on the circuit connection methods and load applying directions, TENGs can be categorized into four different operation modes, i.e., single-electrode (SE) mode, lateral-sliding (LS) mode, vertical contact–separation (CS) mode, and freestanding triboelectric-layer (FT) mode. **Figure 8** exhibits the four operating modes of textile-based TENGs which presents in the form of fabric structure. Each working mode has its own structural characteristics, application occasions, merits and demerits, which is summarized and compared in **Table 6**. The SE mode takes the ground as the reference electrode and is versatile in harvesting energy from a freely moving object without attaching

Table 5. Summary and comparison of current textile-based PENGs.

Ref.	Electrode	Active materials	Structure	Electric outputs	Stretchability/durability	Main applications
[126]	Au	ZnO NWs	Spiral twining	1 mV, 5 pA, 20 mW m^2	30 min	Energy scavenging
[116]	Carbon-filled PE	BTO/PZT/CNT-PVDF	Spiral multilayer	6 V, 4 nA	26 000 cycles	Stand-off sound detector
[127]	Carbon fiber (inner), Ag (outer)	ZnO film	Coaxial	3.2 V, 0.15 µW cm^{-2}	NF	Heart-pulse driven
[129]	Cr-coated Kevlar	ZnO NWs	Coaxial	1.8 mV, 4.8 pA	NF	UV detector
[128]	Carbon fiber (inner), ITO (outer)	ZnO NWs	Core–sheath	2 mV, 0.2 nA	NF	Energy harvesting
[130]	CF (inner), Au (outer)	ZnO	Core–sheath	17 mV, 0.09 µA cm^{-2}	NF	Energy harvesting
[139]	Ni/Cu alloy	PVDF film	Spiral winding	20 V, 1.42 mW, (3 MΩ, 1 Hz)	158%	Energy harvesting
[143]	PEDOT	PVDF fiber	Coaxial	1 V, 0.15 mA	7500 cycles	Pressure sensor
[133]	Au (inner and outer)	ZnO-PVDF	Coaxial	0.1 V, 10 nA cm^{-2}, 16 µW cm^{-3}	NF	Energy harvesting
[132]	Ag-coated nylon yarn	PVDF NFs and film	Coaxial	0.52 V, 18.76 nA (0.02 MPa)	50 000 cycles	Energy harvesting
[138]	Ag-coated nylon (inner), CNT sheet (outer)	PVDF–TrFE mats	Coaxial (rolling)	2.6 V	50%/40 000 stretching cycles	Human motion sensors
[134]	Carbon (inner), indium (outer)	PVDF–TrFE	Coaxial	1 V	NF	Acoustic measurement
[136]	Ag-coated PI/stainless steel	Melt-spun PVDF	Woven	3.5 V, 130 nW	0.25%	Shoulder strap
[137]	Carbon black on PE	Poled PVDF	Coaxial	4 V (0.05 N)	NF	Heartbeat /respiration
[113]	Cu wire (inner)/Au (outer)	Melt-spinning PVDF–TrFE	Coaxial	–	–	Stress sensor
[140]	Aluminum foils	PVDF–TrFE	Twisted	20 mV	740%	Energy harvesting
[142]	Ag-plated PA yarns	PVDF fibers	Coaxial (Braided)	380 mV, 29.62 µW cm^{-3}	50%/thousands of cycles	Energy harvesting
[149]	Au-coated fabric	ZnO NWs	Sandwich	8 V, 2.5 µA (100 dB, 100 Hz)	–	Energy harvesting
[150]	Ag-coated cotton fabric	ZnO nanorods	Sandwich	9.5 mV	–	Power generation
[30]	Ag-coated fabric	ZnO nanorods	Sandwich	4 V, 20 nA	–	Energy harvesting
[144]	Cu wires	ZnO/Pd-coated ZnO NWs	Woven	3 mV, 17 pA	–	UV sensor
[145]	Cu wires	BaTiO$_3$	Woven	1.9 V, 24 nA, 10 nW (80 MΩ)	–	Energy harvesting
[31]	Stainless steel	PVDF–TrFE	Woven	16.2 mV	–	
[147]	Ni/Cu alloy	PVDF film	2D woven	51 V, 850 µW	–	Tactile sensor
[148]	Cu wires	Melt-spinning PVDF fibers	3D interlock	2.3 V	–	Energy harvesting
[29]	Ag-coated PI yarn	Melt-spinning PVDF fibers	3D spacer knitted	5.1 µW cm^{-2} (0.1 MPa)	150 cycles	Energy harvesting
[154]	Cu foil	Electrospinning PVDF NFs	Sandwich	76 mV, 39 nA (0.05%, 7 Hz)	–	Energy harvesting
[28]	Ag-coated PI yarns	PVDF–NaNbO$_3$ NFs	Sandwich	3.4 V, 4.4 µA (1 Hz, 0.2 MPa)	10^6 cycles	Energy harvesting
[120]	Ag conductive fabric	ZnO NWs grown on PVDF NFs	Sandwich	6.36 V, 0.17 µA	–	Energy harvesting
[162]	CNF (inner and outer)	PZT NFs	Sandwich	2 V, 50 nA	200 bending cycles	Energy harvesting
[157]	PEDOT	PVDF NFs	Sandwich	48 V, 6 µA (8.3 kPa)	6 months	Weight measurement
[160]	Ag	PZT NWs	Sandwich	6 V, 45 nA	–	UV sensor
[146]	Ni/Cu wires	PVDF	Woven	42.5 V, 125 µW cm^{-2} (6 Hz, 6.6 MΩ)	–	Energy harvesting
[26]	Cu–Ni-plated PET fabric	Pt-PVDF NFs	Sandwich	30 V, 6 mA cm^{-2}, 22 µW cm^{-2}	–	Tactile sensor
[156]	PEDOT:PSS (top) CNTs (bottom)	Nonwoven PVDF NFs	Sandwich	3 V, 15 nA (1.2 Hz)	–	Motion recognition

an electric conductor. The vertical CS mode depends on relative motion between two triboelectric layers perpendicular to the interface, while the LS mode relies on the relative displacement in the direction parallel to the interface. The FT mode consists of a triboelectric layer with grating segments and two stationary electrodes with interdigital patterns. The LS and FT modes can also be implemented in a compact package via rotation-induced movements.
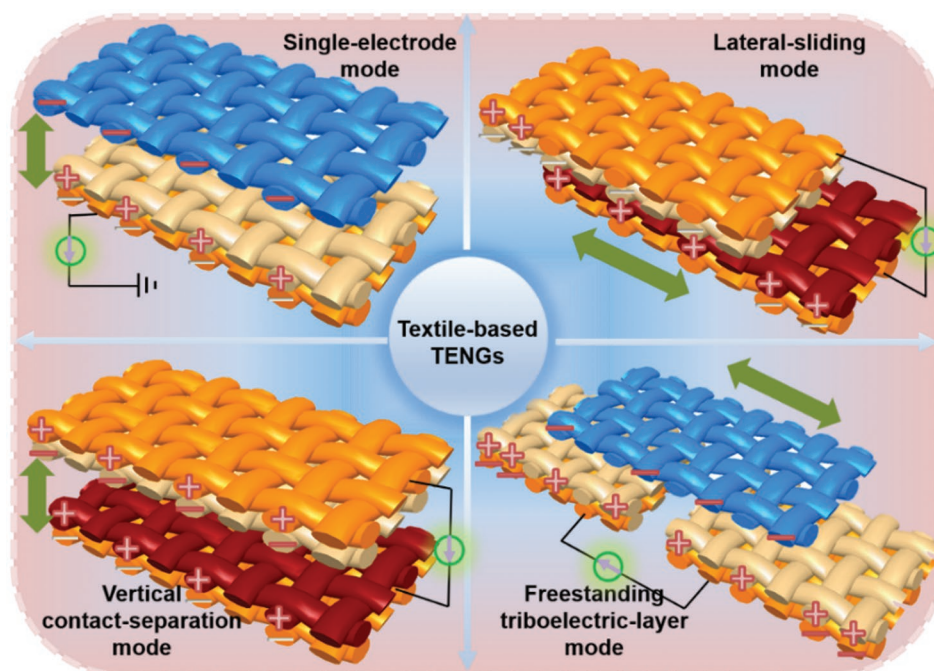
ADVANCED
SCIENCE NEWS
www.advancedsciencenews.com

ADVANCED
MATERIALS
www.advmat.de

Figure 8. Four basic operation modes of textile-based TENGs, which take the fabric-based TENGs as examples. The yellow models refer to conductive fabrics, while the gray, crimson, and blue models represent dielectric fabrics.

4.3. Triboelectric Mechanisms

Triboelectric effect is the phenomenon that a material becomes electrically charged after it contacts with a different material through friction.[165] Although it is one of the most frequently experienced effects in our daily life, the nature of the charge carriers and their transfer mechanisms behind triboelectrification or contact electrification are still puzzled or more precisely under debate. Recently, Xu and co-workers[188–190] and Lin et al.[191] have conducted some theoretical studies in order to deeply explore the triboelectrification behaviors. It is found that the electron transfer instead of ion transport is the dominant process of triboelectrification. The charge retention characteristic of materials after the process of CE is attributed to the existed potential barrier. The surface states model originating from the band structure theory of semiconductors can only explain the CE mechanism of metal–insulator systems or two different insulators.[188] Inspired by the atomic or molecular orbits model, the electron cloud-potential well model is proposed based on electron cloud interaction, which can explain the CE mechanism for all types of materials.[189] Temperature plays an important role on the behavior of CE and there is a limit temperature that TENGs can still work. Electron thermionic emission is the dominant deterring factor of CE at high temperatures and its role becomes more significant with the increase of temperatures. When two materials with different temperatures come into contact, hotter solid tends to be positively charged, while cooler solid prefers to be negatively charged. Due to the thermionic emission effect, electrons are thermally excited and transferred from a hotter part to a cooler one. The CE behaviors between identical materials have also been investigated.[190] Charge transfer between similar

Table 6. Comparison of the four operational modes of TENGs.

| Modes	Structural characteristics	Advantages/disadvantages	Application occasions	Key parameters
SE	Only one electrode, another electrode is ground	(A) Simple, versatile in harvesting energy, easy for integration and to carry (D) Relatively low output and signal instability	Sliding/typing/touching screen	Electrode gap distance, area size
LS	Horizontal/rotational movement, almost without gap	(A) High frequency, continuous and high electricity output (D) Easy damage of friction surface, poor long-term stability	Rotational and air/water flow energy harvesting	Sliding distance and velocity
CS	Vertical movement, a large gap existed	(A) High output voltage (D) Pulse output	Pressing, impacting, bending, sharking, vibration	Separation distance, average velocity, dielectric thickness
FT	Multiple forms of movements, symmetric electrodes, asymmetric charge distribution	(A) High energy conversion efficiency (D) Inconvenient to move due to fixed electrodes, complex for integration	Rotational and vibration energy harvesting	Freestanding height, electrode gap
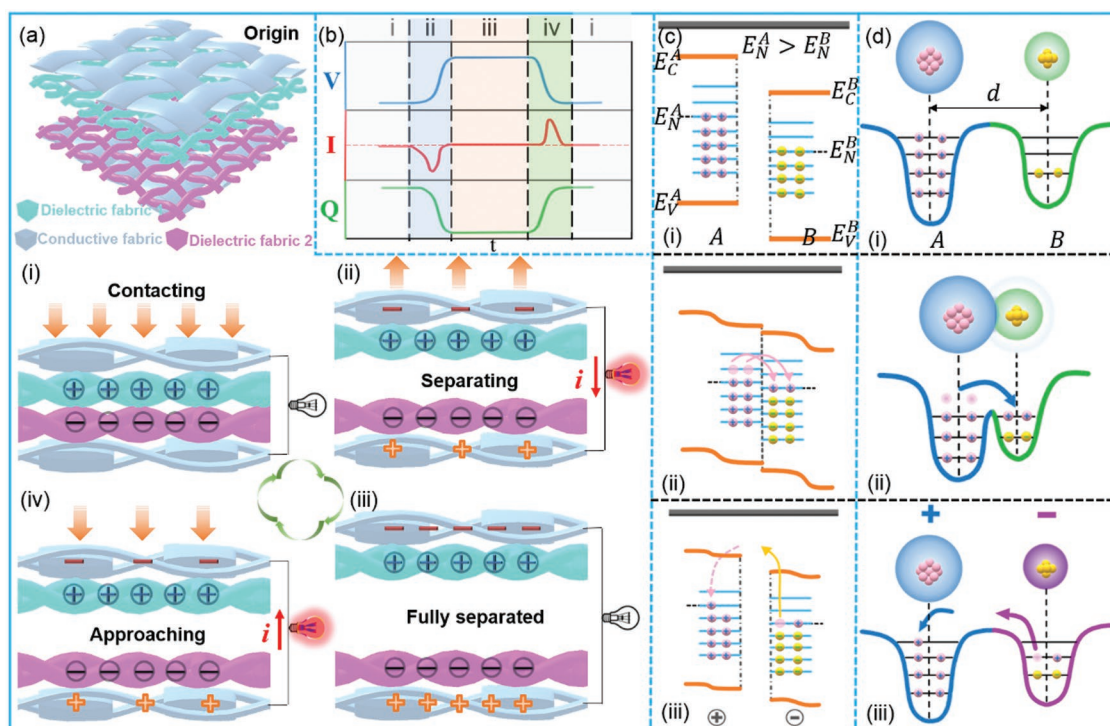
Figure 9. Charge generation and transfer mechanisms of TENGs. Taking the fabric-based TENG based on vertical contact–separation mode as an example. a) Basic working models, including: i) original state, ii) separating from each other, iii) fully separated, and iv) approaching to each other. The charges with circle represent the triboelectric charges, and those without circle refer to the electrostatic induced charges. b) Electrical output characteristics (i.e., V_{oc}, I_{sc}, and Q_{sc}) in a complete contact–separation process. c) Surface states models between two different dielectric materials, including: i) charge transfer before contact, ii) in contact, and iii) after contact. Superscript A and B represent two different dielectric materials. E_C, E_N, and E_V refer to conductive band, neutral level of surface states, and valence band, respectively. In this case, $E_N^A > E_N^B$. d) Electron cloud-potential well models between any two solid materials, including: i) electron clouds before colliding, ii) electron clouds in colliding, and iii) electron clouds after colliding.

materials can be observed from curved surfaces rather than flat structures. The curvature-dependent charge transfer model is established based on curvature-induced energy shifts of the surface states, which can reveal the charge transfer mechanisms between similar materials. When two materials with irregular surfaces come into contact, the convex surfaces are prone to be negatively charged, while the concave surfaces are inclined to be positively charges. These innovative achievements further lay the theoretical foundation for TENG, making it more scientific and systematic. Herein, in order to further illustrate the charge generation and transfer mechanisms of TENGs, relevant theoretical models from multiple levels are also established, such as basic working model (**Figure 9**a), surface states model (Figure 9c), and electron cloud-potential well model (Figure 9d).

The working mechanisms of the four operational modes of TENGs are similar, all of which are based on the combination of electrification effect and electrostatic induction. Therefore, a comprehensive analysis of one working mode is enough. As shown in Figure 9a, the charge generation and transfer process of a typical CS-mode fabric-based TENG is investigated. One cycle of electrical generation corresponds to a contact–separation movement occurring between the upper and lower fabric layers, both of which include a conductive and a dielectric fabric. Originally, due to no electrical potential difference existed, no charge is generated or induced. Once the upper and lower fabric layers contact with each other,

electrification occurs at their interfaces, generating the same amount of charges with the opposite polarities on their surfaces (Figure 9ai). The polarities of both sides depend on their ability to gain and lose charges. Since the opposite triboelectric charges coincide at almost the same plane, there is practically no electrical potential difference between the two fabric layers. When they are separating and gradually moving away, positive and negative charges are induced on the bottom and top fabric electrodes, respectively, due to the electrostatic induction effect (Figure 9aii). The accumulated electrical potential difference between them prompts electrons to flow, generating an instantaneous current. When the two fabric layers are completely separated, the positive and negative triboelectric charges are fully equilibrated by the electrostatic induced charges (Figure 9aiii). Under this circumstance, electrical signal is absent between the two fabric layers, reflecting the neutralization of charges in this period. It is noteworthy that the accumulated charges will not be entirely annihilated. On the contrary, due to the innate features of insulator, they will be maintained for a sufficiently long time. In the reverse case, if the two fabric layers are approaching back to each other, the accumulated induced charges will flow back through the external load to compensate for electrical potential differences (Figure 9aiv). After the whole system returns to the initial state (Figure 9ai), the positive and negative triboelectric charges are fully offset again. As a result, a contact–separation process between the

**ADVANCED
SCIENCE NEWS**
www.advancedsciencenews.com

**ADVANCED
MATERIALS**
www.advmat.de

upper and lower fabric layers will generate an instantaneous alternating potential and current through the external load. The characteristics of electrical output signals of TENGs, i.e., open-circuit voltage (V_{oc}), short-circuit current (I_{sc}), and short-circuit charge transfer (Q_{sc}) in the corresponding movement processes are shown in Figure 9b.

The CE behaviors of the vertical contact–separation mode TENG between the two fabric layers can also be illustrated based on surface states model (Figure 9c). The energy band before the mutual contact between the two dielectric fabrics is shown in Figure 9ci. In this model, it is assumed that the neutral level of surface state of dielectric fabric A (E_N^A) is higher than that of dielectric fabric B (E_N^B). When they contact with each other, the electron located at high energy states in dielectric fabric A will transit to the low energy states of dielectric fabric B (Figure 9cii). After the two dielectric fabrics are separated, the transferred electrons in dielectric fabric B escape from its surface because of thermionic emission (Figure 9ciii). Meanwhile, since it currently has more positive charges, dielectric fabric A is likely to capture electrons from the environment. Ultimately, dielectric fabric A is positively charged, while dielectric fabric B is negative charged.

The CE mechanism of TENGs can also be reflected on the atomic or molecular scale. As exhibited in Figure 9d, Electron cloud-potential well model is established to describe the CE mechanism between any two solid materials. Prior to contact between the two fabric layers, their respective electron clouds remain separated without overlap, due to that potential wells bind the electrons and prevent them from freely escaping (Figure 9di). When they get to close and contact with each other, the electron clouds collide with each other to form ionic or covalent bonds (Figure 9dii). The initial balanced potential well is broken to asymmetric double-well potential, leading to electrons hopping from one with higher energy to its counterpart. After separated, the transferred electrons remain but the thermionic emission of triboelectric charges occurs, resulting in partial release of the electrons from dielectric fabric B (Figure 9diii). Meanwhile, electrons from the environment will be replenished by dielectric fabric A, leading to it positively charged.

4.4. Triboelectric Textiles

Integration of TENG technology with conventional textiles brings new vitality and more possibilities for smart textiles. Textile-based TENGs are highly desirable for next-generation wearable energy harvesters and human-oriented self-powered sensors that are expected to be lightweight, long-lasting, breathable, deformable, and washable. This new class of wearable electronics can conform to complex, nonplanar shapes while maintain satisfactory performance, reliability, and integration. Herein, based on operational modes, structural characteristics, and fabrication methods, textile-based TENGs are divided into four main categories, i.e., single fiber-based TENGs, fabric-based TENGs with textile forming structures, fabric-based TENGs with multilayer fabric stacking structures, fabric-based TENGs working with lateral sliding mode, and fabric-based TENGs with nanofiber reticular or textile-involved membranous structures.

4.4.1. Single Fiber-Based TENGs

As mentioned above of textile-based PENGs, single fiber/yarn is also the smallest design unit for textile-based TENGs. Coaxial or core–shell configuration is the commonly adopted design structure for single fiber-based TENGs. According to the working modes, single fiber-based TENGs can be further classified into single-electrode mode and vertical contact–separation mode. The SE mode single fiber-based TENGs usually consist of an inner fiber electrode and an outer encapsulated layer, in which the outer cladding layer acts as the dielectric layer as well as the protective layer. In general, the CS mode single fiber-based TENGs are usually designed as core–sheath structure and there is a gap between inner core column and outer sheath tube. In this section, we will introduce the relevant studies on the SE mode and CS mode single fiber-based TENGs, respectively.

With the merits of simple structure, good performance, and versatile applications, the SE model single fiber-based TENGs have been widely designed and reported. The simplest structure of SE mode single fiber-based TENGs is that dielectric polymers are directly wrapped around core fiber electrodes. As shown in **Figure 10**I, single energy harvesting fiber was fabricated by coating PDMS or silicone rubber on the surface of conductive fiber.[42,170,192,193] The obtained energy harvesting fiber can be crookedly sewn on a cloth (Figure 10a),[192] or directly woven (Figure 10b)[193] or knitted (Figure 10c)[42] into 2D fabric. However, the surface-coated polymers will not only increase the overall diameter of fibers, but also cause itching of human skin. Therefore, artificial commercial fibers are gradually used to replace polymers. As exhibited in Figure 10II, a coaxial energy harvesting fiber was developed by tightly twining artificial fibers around a conductive core fiber, which could be further woven or knitted into fabrics (Figure 10d).[194] Due to low cost, high efficiency, and mature technology, it is very possible to realize the large-scale production of this energy harvesting fiber. Printing as one of effective methods for mass production has also been adopted to prepare a SE-mode single fiber-based TENG by using CNTs as a conductive core and silk fibroin as a dielectric sheath.[195] Unfortunately, stretchability is absent in the above SE mode single fiber-based TENGs due to the existence of straight core fiber. Stretchability can be obtained by either selecting stretchable materials or applying stretchable structure. As shown in Figure 10III, stretchability can be achieved by twining fiber electrodes on the surface of stretchable fibers. After further coating with the outer dielectric layer, the energy harvesting fiber is obtained which can also be woven into fabrics (Figure 10e).[196–198] Another example of achieving stretchability is that conductive fiber with built-in helical structure is inserted into elastic silicone rubber tubes, as illustrated in Figure 10IV.[199,200] In addition, energy harvesting fibers made up of stretchable components are also certainly stretchable.[84,201] For example, a superstretchable SE mode single fiber-based TENG was obtained by injecting nontoxic liquid metals, e.g., Galinstan and EGaIn into stretchable silicone rubber tube (Figure 10f).[84] In theory, the stretchability of the fiber fabricated with inherent stretchable materials is higher than that designed with stretchable structures.
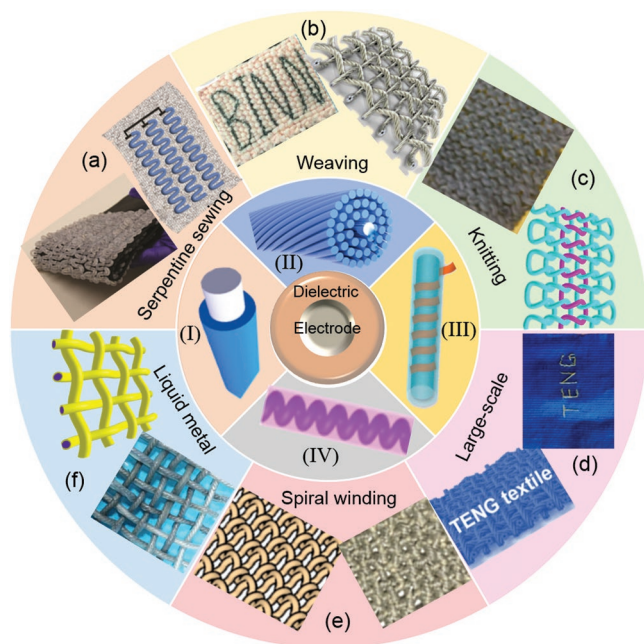
ADVANCED
SCIENCE NEWS

www.advancedsciencenews.com

ADVANCED
MATERIALS

www.advmat.de

Figure 10. Typical SE mode single fiber-based TENGs, which own one fiber electrode. a) A highly stretchable and scalable TENG textile realized by sewing the energy-harvesting fiber that composed of silicone rubber coated stainless-steel fiber into a serpentine shape on an elastic textile. Reproduced with permission.[192] Copyright 2017, Wiley-VCH. b) A yarn-shaped TENG obtained by coating conductive Cu-coated yarn electrode with a layer of PDMS as electrification layer. Reproduced with permission.[193] Copyright 2019, Wiley-VCH. c) A stretchable and washable TENG fabric knitted with a single energy-harvesting yarn that is obtained by coating silicone rubber on the surface of three-ply twisted stainless-steel/PET blended yarn. Reproduced with permission.[42] Copyright 2017, American Chemical Society. d) A core–shell-yarn-based TENG applied by twining artificial polymer fibers tightly around core conductive fibers. Reproduced with permission.[194] Copyright 2017, American Chemical Society. e) A single-strand fiber-based woven-structured TENG proposed by spirally winding Au-coated Cu threads on a silicone rubber column. Reproduced with permission.[198] Copyright 2018, AIP Publishing Group. f) A liquid-metal fiber-based TENG developed by injecting Galinstan as the electrode into a silicone rubber tube as the triboelectric and encapsulation layer. Reproduced with permission.[84] Copyright 2018, American Chemical Society.

Although the SE mode single fiber-based TENG is easy to prepare and convenient for usage, low and unstable outputs restrict its wide application. In order to improve power outputs and working stability of single fiber-based TENGs, SE mode is usually optimized to CS mode. CS mode single fiber-based TENGs can be simply obtained by twisting a SE mode energy harvesting fiber and a conductive fiber together.[36,202,203] However, the twisted structure is not only inconvenient to implement, but also easy to cause abrasion between fibers. In most cases, CS mode single fiber-based TENGs are designed with the core–shell structure, in which a gap exists between the inner core column and the outer shell tube. According to its structures, the CS mode single fiber-based TENGs can be classified into four main types, i.e., dielectric layer wrapped around inner electrode as the core and only outer electrode as the shell (type I, **Figure 11**I), dielectric layer wrapped around inner electrode as the core and the same configuration as the

shell (type II, Figure 11II), inner electrode wound on dielectric fiber as the core and the same configuration as the shell (type III, Figure 11III), and the outer surface of the type III further covered by dielectric or encapsulation layer (type IV, Figure 11IV). No matter what type is selected, one of the basic design principles is that materials with different triboelectric polarities are chosen for the outer side of the inner core column and the inner side of the outer shell tube. Type I is the simplest structural type of the CS mode single fiber-based TENGs. As presented in Figure 11a, a fiber-based TENG was designed with CNTs wrapped by silicone rubber as the core and Cu wire as the shell.[204] Its high stretchability was achieved by convolving Cu wire onto the inner core column. In order to avoid charge leakage from the bare outer electrode, the outmost layer of type I is further covered by another dielectric layer. In this case, type I is transformed to type II. There are some studies based on type II that have been reported. For example, a core–shell triboelectric fiber was developed with nylon fiber wound on conductive fiber as the core and Ag NWs coated bamboo fibers sandwiched between silicone rubber tube and PDMS encapsulated film as the shell (Figure 11b).[205] Another similar fiber-based TENG was prepared with PTFE coated PU/Ag NWs as the core and AgNWs/PDMS as the shell, as shown in Figure 11c.[206] If both the inner core column and the outer shell tube are reversely constructed comparing with the type II, the third type of CE mode single fiber-based TENG is proposed. Based on the type III, a nanostructured fiber-based TENG was developed by inserting Au coated ZnO NWs grown on Al wires into Al foil wrapped nanostructured PDMS tube (Figure 11d).[207] Another example is a triboelectric fiber with multilayered wrinkled structure, which was designed with PU fiber wrapped by Ag-coated nylon fiber as the core and CNTs coated PVDF–TrFE as the shell (Figure 11e).[208] In most cases, the outmost of type III is further covered by another dielectric layer to prevent charge leakage just as type I is optimized to type II. The obtained type IV is the most commonly used structure for the CS mode single fiber-based TENGs, which has been widely reported. As shown in Figure 11f, a coaxial triboelectric fiber was developed with CNT coated PDMS as the core and CNT sandwiched between two PDMS layers as the shell.[209] PMMA microspheres were deposited on the inner CNT electrode in order to increase effective contact between the core and shell. With the similar structure, a triboelectric fiber was fabricated with silicone rubber tube covered by Ni-coated PET fabric as the core and CNTs layer sandwiched between two silicone rubber layer as the shell (Figure 11g).[210] In addition, a superflexible tube-like TENG with a high surface charge density of 250 μC m^{-2} was designed by inserting a helix conductive belt into the shell tube consisting of carbon black/CNTs layer sandwiched between two silicone rubber layers (Figure 11h).[211] As for type IV, conductive fibers are usually wound around dielectric fibers in order to provide stretchability. As shown in Figure 11i, a varnished wire consisting of conductive Cu and insulation varnish at both ends acted as the shell was spirally wound around a core fiber, which was fabricated with CNT/PANI-coated silicone rubber.[212] The winding structure can also be achieved on the inner core column,[213] or even on both the inner and outer fibers.[33] For instance, a versatile triboelectric fiber was developed with a spring-like spiral winding structure
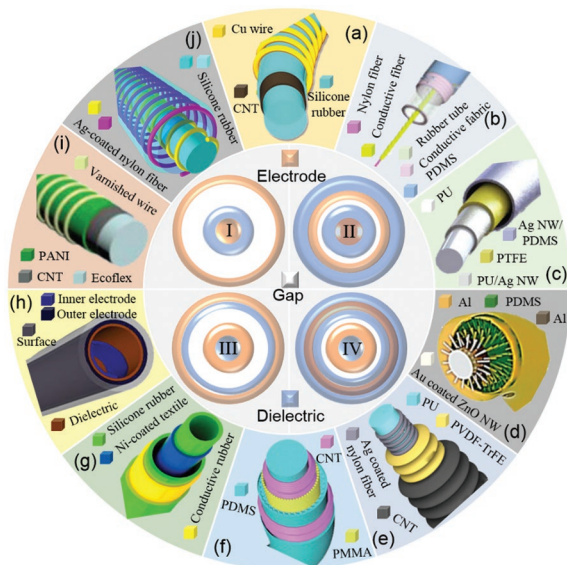
**ADVANCED
SCIENCE NEWS**

www.advancedsciencenews.com

**ADVANCED
MATERIALS**

www.advmat.de

Figure 11. CS mode single fiber-based TENGs working with representative core–shell structure. Based on the structure composition and electrode position, the CS mode single fiber-based TENGs can be divided into four types, i.e., dielectric layer wrapped around inner electrode as the core and only outer electrode as the shell (I), dielectric layer wrapped around inner electrode as the core and the same configuration as the shell (II), inner electrode twining on inner dielectric fiber as the core and outer electrode covered on outer dielectric tube as the shell (III), the structure of (III) further covered by outmost dielectric or encapsulation layer (IV). a) A highly stretchable fiber-based TENG fabricated by convolving Cu microwire onto a stretchable CNT/silicone rubber fiber. Reproduced with permission.[204] Copyright 2017, Wiley-VCH. b) A fibroid core–sheath structural triboelectric kinematic sensor containing conductive metal fiber wrapped by nylon fiber as the core and Ag NW-coated bamboo fiber twining on silicone rubber tube as the shell. Reproduced with permission.[205] Copyright 2017, Elsevier. c) A stretchable fiber-based TENG with a core–sheath fiber configuration assembled from a core fiber comprising Ag NW and PTFE coatings on a bare PU fiber, and a sheath electrode of PDMS–Ag NW film. Reproduced with permission.[206] Copyright 2017, Elsevier. d) A core–shell and fully sealed energy-harvesting fiber containing a Au-coated ZnO NWs grown on Al wire in the core and a nanostructured PDMS tube in the shell. Reproduced with permission.[207] Copyright 2015, American Chemical Society. e) A stretchable triboelectric fiber with multilayered core–shell and wrinkle structures designed with Ag-coated nylon fiber twining around PU fiber as the core and wrinkled PVDF–TrFE/CNT layer as the shell. Reproduced under the terms of the CC-BY Creative Commons Attribution 4.0 International License (http://creativecommons.org/licenses/by/4.0/).[208] Copyright 2016, The Authors, Published by Springer Nature. f) A coaxial triboelectric fiber developed by using aligned CNT sheets as inner and outer electrodes and designing porous structures in triboelectric polymers of PDMS and PMMA. Reproduced with permission.[209] Copyright 2017, Royal Society of Chemistry. g) A core–shell coaxially structured fiber-based TENG designed with conductive textile wrapped silicone rubber tube as the core and CNT sandwiched between two silicone rubber layers as the shell. Reproduced with permission.[210] Copyright 2018, Royal Society of Chemistry. h) A high-output tube-like TENG proposed by attaching a belt-like inner electrode to the interior surface of a silicone rubber tube, which is further covered by outer electrode and outmost encapsulation layer. Reproduced under the terms of the Creative Commons Attribution 4.0 International License (http://creativecommons.org/licenses/by/4.0/).[211] Copyright 2016, The Authors, published by Springer Nature. i) A self-powered wearable sensing fiber presented by coating multiwall CNT and PANI derivatives on silicone rubber fiber, and further twining with varnished wires. Reproduced with permission.[212] Copyright 2018, IOP Publishing. j) A highly stretchable yarn-based TENG designed with coaxial core–sheath and built-in spring-like spiral winding structures. Reproduced with permission.[33] Copyright 2018, Wiley-VCH.

for both the inner core and the outer shell. As exhibited in Figure 11j, the inner core was made of Ag-coated nylon fiber wound silicone rubber fiber, while the outer shell was formed by winding Ag-coated nylon fiber on silicone rubber tube, which was further coated by silicone rubber.[33]

The structures and performance of single fiber-based TENGs are also summarized and compared in **Table 7**. Generally speaking, CS mode single fiber-based TENGs have higher electrical outputs and better strechability than those with SE mode.

4.4.2. Fabric-Based TENGs with 2D Textile Forming Structures

In order to improve electrical outputs as well as promote its wide applications, textile-based TENGs usually present in the form of fabrics. Through various textile forming techniques, it is possible to process conductive or dielectric fibers into fabrics. For facilitating fabrication and increasing the effective contact area, fabric-based TENGs are originally prepared from narrow thin film tapes or cloth strips. So far, several kinds of fabric band-based TENGs have been reported and studied. For example, a micro-cable structured power textile was woven by interlacing Cu-coated PTFE strips with Cu wires in a staggered way on an industrial weaving machine via a shuttle-flying process (**Figure 12**a).[214] It is also found that among the three basic weaving patterns, plain weave has the highest electrical output while twill weave exhibits the lowest, due to variation of the effective contact area. A similar fabric-based TENG was also woven by PTFE strip covered Cu foil bands. As shown in Figure 12b, the PTFE-wrapped Cu strips were woven from both the warp and weft directions into a plain-weave mode.[215] In addition, an energy harvesting flag was also fabricated with the similar techniques by interlacing Ni coated PET strips and Kapton-wrapped Cu foils to harvest high-altitude wind energy from arbitrary directions (Figure 12c).[34] A gap at the interlacing point between the two strips allowed their contact and separation motion driven by wind fluttering. Due to low flexibility of thin films and metal foils, common cloth strips are gradually used to prepare fabric band-based TENGs. For instance, a woven structured TENG was fabricated by interlacing PET fabric wrapped Ag-coated cloth strips and nylon fabric wrapped Ag-coated cloth strips into a plain pattern (Figure 12d).[216] In addition, belt-type Ni-coated PET cloth strips and that further coated with parylene film as the building blocks were also woven into fabric-based TENGs (Figure 12e).[217,218] Electrical output properties of this kind of energy harvesting fabric can be further optimized by replacing the surface coated parylene with silicone rubber. As exhibited in Figure 12f, a high-performance fabric band-based TENG was woven by Ni-coated PET fabric bands and that further coated with silicone rubber.[219] With the advantages of simple prepared method, high output performance, and stable mechanical property, it seems that the fabric band-based TENGs satisfy the practical usages. However, they are only suitable for traditional manual weaving while incompatible to other textile forming methods and the present large-scale industrial production, which limits their wide applications to a large extent.

Under normal circumstances, single fiber-based TENGs can be made into energy harvesting fabrics through various textile processing technologies. As illustrated in **Figure 13**a,

**ADVANCED
SCIENCE NEWS**

www.advancedsciencenews.com

**ADVANCED
MATERIALS**

www.advmat.de

Table 7. Summary and comparison of single fiber-based TENGs.

Ref.	Modes	Structures	Components and methods	Outputs	Stretchability	Main applications
[192]	SE	Coaxial	SS fibers wrapped by silicone rubber	15 V, 12 nC, 7 μA	–	Human-interactive sensing
[42]	SE	Coaxial	SS/PET-blended fibers wrapped by silicone rubber	18 V, 6 nC, 0.3 μA	–	Power textiles
[194]	SE	Coaxial	SP fibers twined around core SS fiber	–	–	Power cloths
[84]	SE	Coaxial	Galinstan injected into silicone rubber	–	300%	Energy harvesting
[196]	SE	Coaxial	Ag-coated PET fibers spirally wound on silicone rubber	28 V, 0.56 μA	100%	Smart clothing
[197]	SE	Coaxial	Carbon fiber bundles wound over silicone rubber	42 V, 15 nC, 0.5 μA, (2.5 Hz)	Stretchable	Power fabrics
[201]	SE	Coaxial	Carbon-deposited petal-like PDMS mold inserted into silicone rubber tube	32.2 V, 1.15 μA (2 Hz, 40 N)	Stretchable	Landslide monitoring
[193]	SE	Coaxial	Cu-coated PET fiber wrapped by PDMS	–	–	Power textiles
[199]	SE	Coaxial	Helical-structure SS yarns inserted into silicone rubber tube	4.2 V (30 cm, 100%)	200%	Large-scale self-powered textiles
[52]	CS (iii)	Core–shell	(C) Al wires grown on ZnO NWs, further deposited on Au (S) Nanostructured PDMS tube covered by Al foil	40 V, 10 μA (50 N, 10 Hz)	–	Large-scale power mats
[208]	CS (iii)	Core–shell	(C) Ag-coated nylon fibers wound on PU fibers (S) PVDF–TrFE mats covered by CNT sheets	24 mV, 8 nA, 10 pC	50%	Kinematic sensing
[211]	CS (iv)	Core–shell	(C) Helix belt made up of CB/CNTs mixed with silicone rubber (S) CB/CNT layer sandwiched between two silicone rubber layers	145 V, 250 μC m^{-2}, 5 mA m^{-2} (2 Hz)	620%	Biomechanical energy harvesting
[209]	CS (iv)	Core–shell	(C) PDMS fiber wrapped by CNT sheets, further covered by PMMA microspheres (S) CNT sheets sandwiched by two PDMS films	5 V, 240 nA (25 N)	Stretchable	Energy harvesting and sensing
[204]	CS (i)	Core–shell	(C) CNT films wrapped on silicone rubber fiber, further covered by silicone rubber film (S) Cu wires	140 V, 0.18 μA m^{-1}, 6.1 nC m^{-1} (5 Hz)	70%	Power generation
[205]	CS (ii)	Core–shell	(C) Nylon fibers wrapped around conductive fiber (S) Ag NWs covered on silicone rubber tube, and further wrapped by PDMS	3.22 V, 1.3 mW m^{-2} (100%)	100%	Kinematic sensor
[212]	CS (iv)	Core–shell	(C) CNT/PANI covered on silicone rubber fiber (S) Varnished wire containing insulation varnish	0.2 V, 12.5 nA	250%	Self-powered wearable electronics
[206]	CS (ii)	Core–shell	(C) Ag NWs wrapped on PU fiber, further covered by PTFE (S) PDMS–Ag NW film	2.25 nW cm^{-2}	50%	Personal healthcare monitoring
[33]	CS (iv)	Core–shell	(C) Ag-coated nylon fibers spirally wound around silicone rubber fiber (S) Ag-coated nylon fibers spirally wound on silicone rubber tube, further covered by silicone rubber film	19 V, 6.5 nC, 0.43 μA (5 Hz)	200%	Human-interactive sensing
[213]	CS (iv)	Core–shell	(C) Cu/Ag PET fibers spirally wound PU fibers (S) Conductive fabric inserted inside silicone rubber tube, and injecting silicone rubber	84 V, 5.8 μA	–	Energy harvesting

a plain-patterned fabric-based TENG was manufactured by interlacing the energy harvesting fiber presented in Figure 11j with commercial acrylic yarns.[33] By altering load applying methods and circuit connection modes, this fabric-based TENG could integrate the four operating modes of TENGs together. In addition, the nanostructured single energy harvesting fiber described in Figure 11d could also be woven into fabrics (Figure 13b).[207] By covering with a waterproof fabric on its surface, this fabric-based TENG could be used for all-weather conditions and had been applied as a footstep-driven large-scale power mat. In addition to weaving them together, single energy harvesting fibers can also be directly stitched into normal fabrics. As shown in Figure 13c, a power shirt as a wireless body temperature sensor was fabricated by stitching an energy harvesting fiber into a common knitted fabric.[220] The energy harvesting fiber was twisted from CNT fiber and PTFE coated CNT fiber. In addition to fabricating with single energy harvesting fibers or fabric bands, fabric-based TENGs can also be achieved with conductive or dielectric fibers through textile forming techniques.[221,222] Since no complex pre-processing is needed and the required materials are commercially available, it is more suitable for large-scale mechanized production. This type of fabric-based TENGs have been widely reported. As shown in Figure 13d, a machine-washable fabric-based
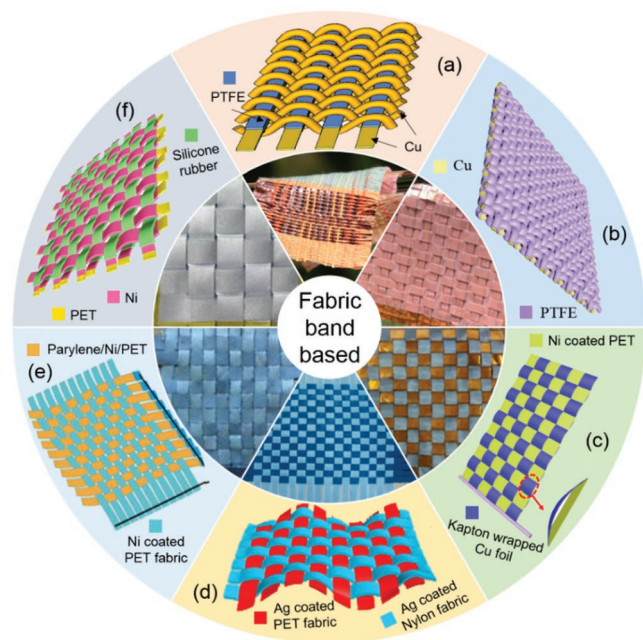
**ADVANCED
SCIENCE NEWS**
www.advancedsciencenews.com

**ADVANCED
MATERIALS**
www.advmat.de

Figure 12. Representative fabric band-based TENGs woven from narrow thin film tapes or cloth strips. a) A microcable structured power textile TENG fabricated by weaving Cu-coated PTFE stripes and Cu electrodes in a staggered way on an industrial weaving machine. Reproduced with permission.[214] Copyright 2016, Springer Nature. b) Washable textile-structured SE mode TENG woven by PTFE/Cu strips in a plain-woven pattern. Reproduced with permission.[215] Copyright 2018, Royal Society of Chemistry. c) A freestanding flag-type TENG for harvesting high-altitude wind energy developed by weaving Ni-coated PET strips with Kapton-sealed Cu belts. Reproduced with permission.[34] Copyright 2016, American Chemical Society. d) A FT mode woven structured TENG based on nylon/Ag fabrics and PET/Ag fabrics. Reproduced with permission.[216] Copyright 2016, American Chemical Society. e) A wearable TENG-cloth woven by Ni-coated PET fabric and that further covered by insulating parylene film. Reproduced with permission.[217] Copyright 2015, Wiley-VCH. f) A double-layer-stacked triboelectric textile designed by weaving Ni-coated PET warp yarns with silicone rubber covered Ni-coated PET weft yarns. Reproduced with permission.[219] Copyright 2017, Elsevier.

TENG was fabricated by weaving Cu coated PET fibers and PI-coated Cu/PET fibers into a plain pattern.[222] Its electrical generation depended on the relative contact and separation motion between the two kinds of fibers. This smart textile was sensitive to subtle human body motions and could work as a wearable respiratory monitor to record human respiratory rate and depth. Stretchability of the fabric-based TENGs with plain-weave organizational structure can also be achieved. As displayed in Figure 13e, a stretchable power textile was fabricated by interlacing an energy harvesting fiber and twisted double-plied conductive fibers into a plain-weave mode.[199] The continue energy harvesting fiber consisting of intrinsically elastic silicone rubber tubes and built-in helical-structured stainless-steel fibers was prepared by using melt spinning method. In addition to the relative contact–separation movement between fibers, the energy harvesting can also be realized between fibers and fabrics.[223,224] As illustrated in Figure 13f, a fabric-based TENG was fabricated by fixing the ends of parallel-arranged 1D conductive bundle yarns grown with ZnO NPs/NWs on the surface of 2D conductive fabric covered by nanostructured

PDMS.[224] Electrical output was generated by the relative contact–separation movement between the 1D fibers and the 2D fabric. In addition, conductive or dielectric fibers can first be woven into corresponding fabrics, and then electrical outputs are realized through the relative contact and separation motion between fabrics. For example, a fully stretchable knitted TENG constructed as a double-arc shaped structure was fabricated by sandwiching a Ag-coated conductive fabric between two Ag-coated PTFE fabrics (Figure 13g).[225] The looping structure and microporous structure endow the knitted TENG with good stretchability and large contact area, respectively. In addition to fabricating with knitted structure, woven structure is also used. As shown in Figure 13h, a fabric-based TENG was achieved between two kinds of fabrics, i.e., nylon-wrapped Ag fabric and PTFE wrapped Ag fabric, which were prepared by spirally winding nylon and PTFE fibers around Ag-coated conductive fibers by normal yarn winding machine, respectively.[226] From this section, it can be found that the fabric-based TENGs prepared from fibers have a variety of implementation forms. Moreover, it is more possible for fabric-based TENGs to achieve large-scale industrial production, due to commercially available materials and mature textile forming processes.

4.4.3. Fabric-Based TENGs with 3D Textile Forming Structures

2D textile forming structures are relatively simple, easy to prepare, and compatible with existing textile processing technology, making them popular in the design of smart textiles. However, due to the limitations of structural dimensions in the thickness direction, the power outputs of conventional 2D textile structures are still low. In order to further improve the output performance of power textiles, 3D textile structures have been gradually used. Instead of increasing transverse contact area or applying additional functional process, 3D textile structures increase the number of layers in the thickness direction, which can provide more contact and separation spaces. Among various 3D textile structures, 3D spacer knitting structure with inherent internal spaces and excellent resilience can provide enough contact and separation spaces. Therefore, it is widely adopted to design 3D fabric-based TENGs. For example, a new kind of 3D fabric-based TENG was fabricated with three types of fibers by a computerized knitting strategy.[227] As illustrated in **Figure 14**a, the top and bottom fabric layers were knitted from Ag-coated nylon fibers and PAN fibers, respectively. A third set of cotton fiber was alternatively knitted with a defined sequence to link the top and bottom fabric layers together as a structural integrity. The increased power output was attributed to the large hollow spaces between the top and bottom fabric layers. With truly wearable characteristics and versatile fashion designability, the 3D full fabric-based TENG was demonstrated as a smart carpet to harvest human walking energy. Instead of knitting functional fibers into 3D fabric-based TENGs, other 3D fabric-based TENG were achieved by imposing functional treatment on common 3D spacer knitted fabrics. For instance, a 3D spacer weft-knitted TENG was comprised of graphene coated nylon fibers as the upper surface, PTFE coated nylon fibers as the lower surface, and PET monofilament as the spacer layer (Figure 14b).[228,229] The PET fibers alternatively interlocked the
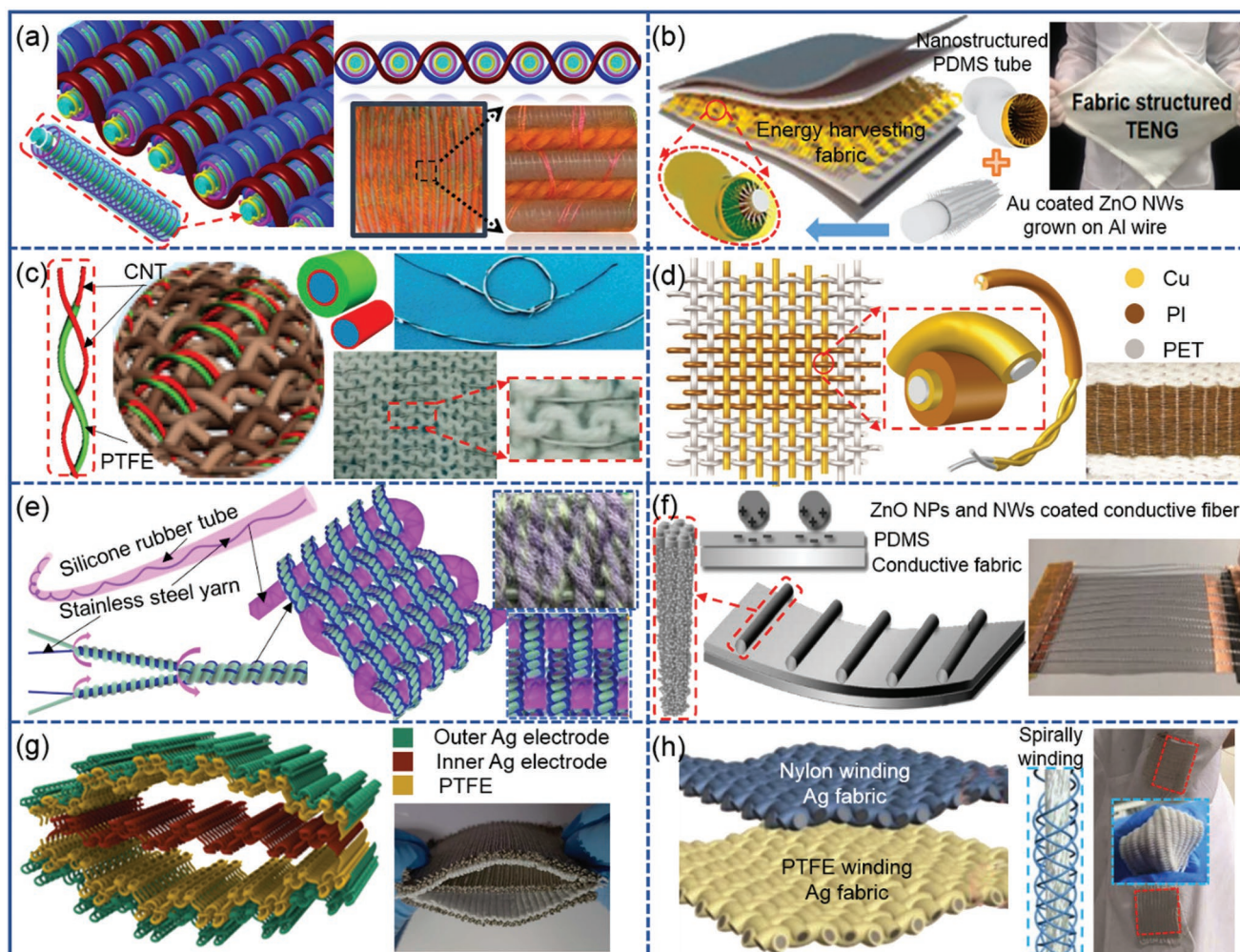
Figure 13. 2D fabric-based TENGs with fiber weaving structure. a) A large-area energy-harvesting fabrics by interlacing the versatile core–shell yarn with acrylic yarns into a plain-woven pattern. Reproduced with permission.[33] Copyright 2018, Wiley-VCH. b) A highly stretchable 2D fabric TENG woven from fibers, which is formed by inserting Au-coated Al wires into Al foil wrapped nanostructured PDMS tubes. Reproduced with permission.[207] Copyright 2015, American Chemical Society. c) Fiber-based TENG obtained by fabricating the energy harvesting yarn that is twisted the CNTs coated cotton yarn and that further coated by PTFE together into a common cloth system. Reproduced with permission.[36] Copyright 2014, American Chemical Society. d) A machine-washable textile consisting of 2-ply Cu-PET yarns and PI-Cu-PET yarns woven as warp and weft. Reproduced with permission.[222] Copyright 2016, Wiley-VCH. e) An energy textile woven with single-electrode triboelectric yarns and double-plied commercial yarns. The double-plied yarn is twisted from commercial stainless-steel yarn and water-resistant modified polyacrylonitrile yarn. Reproduced under the terms of the CC-BY Creative Commons Attribution 4.0 International License (http://creativecommons.org/licenses/by/4.0/).[199] Copyright 2019, The Authors, published by Springer Nature. f) A TENG constructed from nanostructured 1D conductive bundle yarns and 2D conductive fabric. Reproduced with permission.[224] Copyright 2016, Wiley-VCH. g) A double-arc shaped fully stretchable knitted-structural fabric TENG consisting of knitted PTFE and Ag fabrics on the top and bottom layers with a Ag electrode in the middle. Reproduced with permission.[225] Copyright 2017, American Chemical Society. h) A plain-patterned wearable TENG woven from compound yarns. The compound yarn with core–shell structure is formed by spirally winding PA6 and PTFE yarn on the Ag-plated filament via normal yarn winding machine, respectively. Reproduced with permission.[226] Copyright 2018, Wiley-VCH.

upper and lower fibers, offering good resilience for the whole fabric as well as providing enough separation spaces between them. The 3D fabric-based TENG was demonstrated to be able to in situ sense foot pressure during human walking. Similarly, another 3D fabric-based TENG was established based on a common 3D spacer knitted PET fabric. As shown in Figure 14c, its upper surface was coated with Ag as one electrode while lower surface was immersed in PDMS.[230] Aligned CNT sheets acting as the other electrode were further tightly stacked on the back of PDMS, the front of which was a large number of pyramidal structures with sizes of hundreds of micrometers to

millimeters. The middle PET fibers serving as pillars separated the upper and lower layers. In addition, 3D orthogonal woven structure is also adopted to design 3D fabric-based TENG. As exhibited in Figure 14d, a 3D orthogonal woven TENG was developed by using three-ply-twisted stainless-steel/polyester-blended fibers as the warp fibers, PDMS coated energy harvesting fibers as the weft fibers, and nonconductive cotton fibers as the binding Z-yarns in thickness direction.[37] Z-yarns combined the warp and weft layers by interlacing up and down along the warp direction over the weft yarns. In virtue of the 3D orthogonal woven TENG, a self-powered dancing blanket
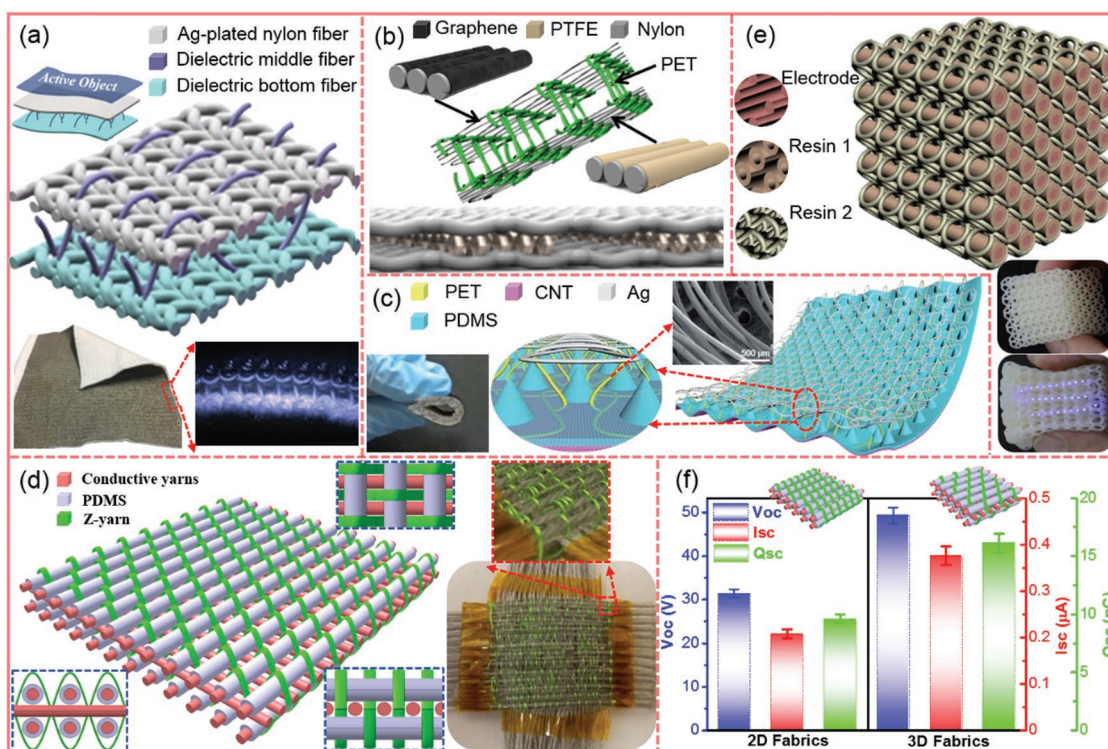
**ADVANCED
SCIENCE NEWS**

www.advancedsciencenews.com

**ADVANCED
MATERIALS**

www.advmat.de

Figure 14. 3D textile structure fabric-based TENGs. a) An all-textile TENG of 3D fabric structure with all conductive top layer, dielectric middle layer, and dielectric bottom layer. Reproduced with permission.[227] Copyright 2019, Elsevier. b) A 3D spacer fabric based TENG based on vertical contact triboelectrification between graphene and nylon with different tribo-polarities. Reproduced with permission.[228] Copyright 2016, Elsevier. c) A triboelectric textile with a 3D penetrated structure made of top Ag-coated fibers, middle PET spacer fibers, and bottom aligned CNT sheet. Reproduced with permission.[230] Copyright 2016, Royal Society of Chemistry. d) A 3D orthogonal woven TENG consisting of stainless-steel/PET blended warp yarn, PDMS-coated energy-harvesting weft yarn, and through-thickness binding yarn. Adapted with permission.[37] Copyright 2018, Wiley-VCH. e) A 3D ultraflexible TENG made by the 3D printing method. Reproduced with permission.[38] Copyright 2018, Elsevier. f) Comparison of electrical output performance between 2D and 3D fabric structures. Adapted with permission.[37] Copyright 2018, Wiley-VCH.

was demonstrated for fully harvesting human walking energy and simultaneously perceiving human motion signals. Recent popular 3D printing technology has also been used to design 3D fabric-based TENGs. As a case, a 3D ultraflexible TENG was printed with fiber-shaped composite resin parts and ionic hydrogel as the dielectrics and the electrodes, respectively (Figure 14e).[38] Based on its excellent flexibility and power output performance, self-powered SOS flickering distress signal systems and smart lighting shoes were successfully demonstrated. The electrical output performance between the 2D and 3D fabric-based TENGs are also compared. As presented in Figure 14f, the power outputs of 3D fabric structure are higher than those of 2D double-layer fabric structure.[37] There are more functional fibers incorporated in the 3D fabric system per unit area, providing more possibilities for the contact and separation motions between conductive and dielectric fibers. Due to the enlarged geometric space dimension, the electrical outputs of 3D fabric-based TENGs are increased.

4.4.4. Fabric-Based TENGs with Multilayer Fabric Stacking Structures

Compared with fabric-based TENGs obtained from conventional textile forming methods, it seems more convenient and efficient to obtain 2D fabric-based TENGs by directly stacking multilayer functional fabrics together. The simplest form of this structure only consists of a conductive fabric and a dielectric fabric.[231] In order to protect fabric electrode as well as prevent charges leakage, conductive fabric is usually sandwiched between two insulating fabrics. For example, an all-fabric-based TENG as a wearable keyboard was designed by placing a commercial Ni coated fabric between a top wool fabric cover and a bottom cotton fabric substrate.[102] Fabric substrates with dense structure and large specific area provide an excellent attachment platform for functional materials. For example, nanostructures are often imposed on the surface of fabrics to increase the effective contact area. As shown in **Figure 15**a, ZnO nanorods were grown on n Ag-coated common fabric, whose surface was further coated with PDMS.[39] By covering another Ag-coated fabric on its surface, a double-layer fabric stacking TENG with high power output performance and strong mechanical robustness was fabricated. A keyless vehicle entry system was demonstrated with the generating electrical signals of the fabric-based TENG without any help from external power source. Instead of growing nanorods or NWs on fabric substrate, nanoparticles or nanofibers can also be directly sprayed on the surface of fabrics. For instance, a highly flexible power fabric with satisfactory breathable, tailorable, and washable abilities was composed of a top PET fabric, a middle
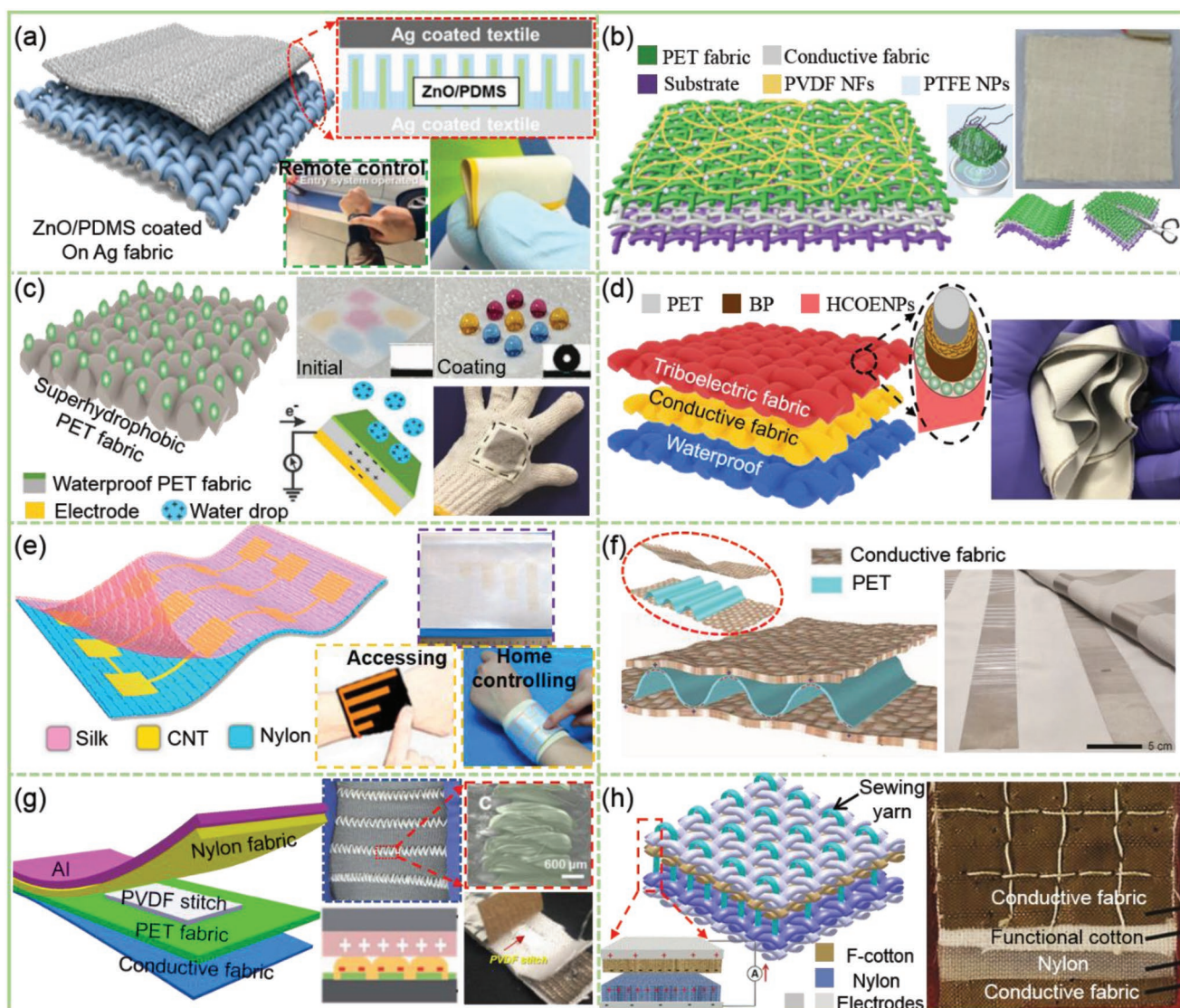
Figure 15. Fabric-based TENGs with multilayer fabric stacking pattern working in SE or CS mode. a) A fully flexible wearable TENG with Ag-coated fabric and PDMS nanopatterns based on ZnO nanorods on Ag-coated textile template as the tribomaterials. Reproduced with permission.[140] Copyright 2015, American Chemical Society. b) A highly flexible, breathable, tailorable, and washable power generation fabric designed by sandwiching conductive fabric between two PET fabrics. The PVDF NFs and PTFE NPs are adhered on the surface of top PET fabric. Reproduced with permission.[232] Copyright 2019, Elsevier. c) A wearable all-fabric-based TENG for water energy harvesting achieved by superhydrophobic coating. Reproduced with permission.[233] Copyright 2017, Wiley-VCH. d) A washable skin-touch-actuated textile-based TENG fabricated by sequentially stacking top dielectric fabric, middle conductive fabric, and bottom waterproof fabric. Reproduced under the terms of the Creative Commons Attribution 4.0 International License (http://creativecommons.org/licenses/by/4.0/).[234] Copyright 2018, The Authors, Published by Springer Nature. e) A screen-printed washable electronic textile with embedded electric circuits on normal fabrics. Reproduced with permission.[235] Copyright 2018, American Chemical Society. f) A large-scale and washable smart textile for self-powered sleep monitoring developed by sandwiching wavy-structured PET films between the top and bottom conductive fabrics. Reproduced with permission.[39] Copyright 2018, Wiley-VCH. g) A textile-pattern wearable triboelectric sensor fabricated by stitching PVDF fibers into fabric substrates with a sewing machine. Adapted with permission.[236] Copyright 2018, Royal Society of Chemistry. h) An all-textile TENG fabricated by assembling two different cloths of opposite surface charge characteristics in a face-to-face configuration. Adapted with permission.[237] Copyright 2016, Wiley-VCH.

conductive fabric, and a bottom fabric substrate (Figure 15b).[232] PVDF NFs and PTFE NPs were attached on the surface of the top PET fabric by electrospinning and electrospray methods, respectively. Functional nanomaterials can also be sprayed on the surface of fabric-based TENGs to achieve special properties, such as waterproof, antibacterial resistance, flame retardant, etc. For instance, a superhydrophobic fabric-based TENG for

water energy harvesting was developed by coating hydrophobic cellulose oleyl ester nanoparticles (HCOENPs) and Au electrode on the front and back surface of a common PET fabric, respectively (Figure 15c).[233] When water droplets fell off the waterproof TENG, their sliding energy would be converted into electricity. Another waterproof fabric-based TENG with the similar structure as above was constructed by sandwiching a

**ADVANCED
SCIENCE NEWS**
www.advancedsciencenews.com

**ADVANCED
MATERIALS**
www.advmat.de

conductive fabric between a top dielectric fabric and a bottom waterproof fabric (Figure 15d).[234] The top dielectric fabric was produced by coating black phosphorus encapsulated with HCOENPs on the surface of a knitted PET fabric. Screen-printing method is also commonly used to prepare conductive components on the surface of fabric substrates. As shown in Figure 15e, repellent CNTs/PU synthetic ink as electrode was printed on a nylon fabric and then covered with a top silk fabric.[235] The obtained washable fabric-based TENG was successfully applied in software accessing interfaces and wireless smart home control systems. In the design of fabric-based TENGs with multilayer fabric stacking, elastic dielectric films can be sandwiched between two conductive fabrics. As exhibited in Figure 15f, a pressure-sensitive smart textile for real-time sleep behavior monitoring was fabricated by sandwiching wavy-structured PET films between top and bottom conductive fabrics.[39] However, a tough problem arising in the TENGs with multilayer fabric stacking structure is that they are vulnerable to delamination failure, due to weak interfacial bonding ability between adjacent fabrics. In order to obtain strong bonding interfaces, stitching or sewing is usually adopted. In addition, with the advantages of pattern designability and high production efficiency, sewing machine stitching or embroidery techniques are suitable for the production of fabrics with sophisticated patterns. For instance, dry-jet wet spun PVDF fibers have been successfully stitched into fabrics with programmable textile patterns. As illustrated in Figure 15g, a pressure-sensitive triboelectric sensor for self-powered foot pressure mapping and pulse signal detecting was fabricated by stacking a Al covered nylon fabric on the surface of a PVDF stitched PET fabric.[236] Similarly, an all-fabric-based TENG was fabricated by sewing two different cloths with opposite surface charge characteristics in a face-to-face configuration (Figure 15h).[237] From the above introductions and analyses, it can be found that multilayer fabric stacking is a simple, convenient and efficient method to prepare fabric-based TENGs. Hierarchical structure of fibers and large surface area of fabrics provide an excellent adhesion carrier for functional nanomaterials. In addition, interfacial bonding between fabrics can also be improved by stitching/sewing method. However, the key issue to realize its practical application lies in its conformability with human body as well as current textile industry production.

4.4.5. Fabric-Based TENGs Working in In-Plane Sliding Mode

The fabric-based TENGs described in the above section are mainly operated in the vertical direction. But in some cases, horizontal friction motion is more likely to occur during human walking, such as between elbow and bilateral chest. In addition, the large surface area of fabric substrates and the absence of air gap make the in-plane sliding mode fabric-based TENGs more compatible with human cloth and movement behaviors. The simplest structure for in-plane sliding mode fabric-based TENGs is composed of two kinds of fabrics with different triboelectric polarities laterally sliding back and forth with each other. For example, a lateral-sliding mode fabric-based TENG was assembled with a PMMA coated conductive fabric and a PI-coated conductive fabric.[238] In the process of periodic rubbing process between the two fabrics, continuous alternating potential and current would be generated. In order to further improve output power and electromechanical energy conversion efficiency, fabric-based TENGs based on in-plane freestanding triboelectric-layer mode are proposed, which consist of interdigitated electrodes with grating structure. For example, an FT mode fabric-based TENG with interdigitated nylon and PET cloth strips was presented in **Figure 16**a.[239] Nylon and PET cloth strips attached with Cu foils were pasted on cotton fabrics. In addition to directly paste cloth strips, functional components can be deposited on fabric substrates via various physical or chemical techniques. As shown in Figure 16b, an FT mode fabric-based TENG was comprised of two kinds of fabrics, i.e., Ni deposited PET slider fabric and parylene covered Ni-deposited PET stator fabric.[32] The relative sliding between the two pairs of fabrics generated alternative electricity between two electrodes in the stator fabric. Nanostructures can be further applied on the surface of the FT mode fabric-based TENGs in order to improve the surface triboelectric charge density. As provided in Figure 16c, with the purpose of improving the electrical output performance of an FT mode fabric-based TENG, Au nanodot-pattern prepared by electro-beam sputtering method was deposited on the surface of a PU fabric.[240] Another FT-mode fabric-based TENG with the similar structure was exhibited in Figure 16d. It was made up of two kinds of carbon fabrics, one of which was coated alternately with PI and PU layer, while the other was covered with PDMS layer and Al foil in turn.[241] In order to harvest the swing energy of two arms during walking or running, the pair of fabrics was located on the sleeve and underneath the arm, respectively. Different from the above methods such as attaching, coating, depositing and sputtering, interdigitated fabric structure can be directly obtained from textile forming techniques, which not only maintains the integrity and aesthetic perception of fabrics, but also simplifies the whole preparation processes. As shown in Figure 16e, an FT mode fabric-based TENG with knitted structure was designed by knitting cotton fibers alternatively between two Ag-coated nylon fabrics at a fixed interval.[242] Its power generation was achieved by in-plane sliding with an upper PTFE fabric. The FT mode fabric-based TENG prepared with woven structure can also be realized between a pair of fabrics. As illustrated in Figure 16f, cotton fibers were adopted as warp fibers for both of the fabrics, while PTFE fibers and cotton fibers as weft fibers were alternately woven into the upper fabric, and carbon fibers and cotton fibers were woven as weft fibers for the lower fabric in turn.[243] The typical electrical output characteristics of in-plane FT mode fabric-based TENGs including V_{oc}, I_{sc}, and Q_{sc} at different velocities in one-way sliding cycle are presented in Figure 16g.[243] It is found that the V_{oc} and Q_{sc} curves present a triangular shape and that of I_{sc} is in rhomboidal. Furthermore, with the increase of sliding speed, the output signals first increase and then decrease. These phenomena can be attributed to the increasing, maximizing and decreasing trend of the effective contact area. The in-plane FT based fabric-based TENGs are especially fit for converting low-frequency human motion energy into high-frequency current outputs. The output performance of in-plane FT based fabric-based TENGs can be enhanced with small grating size and fast sliding speed.
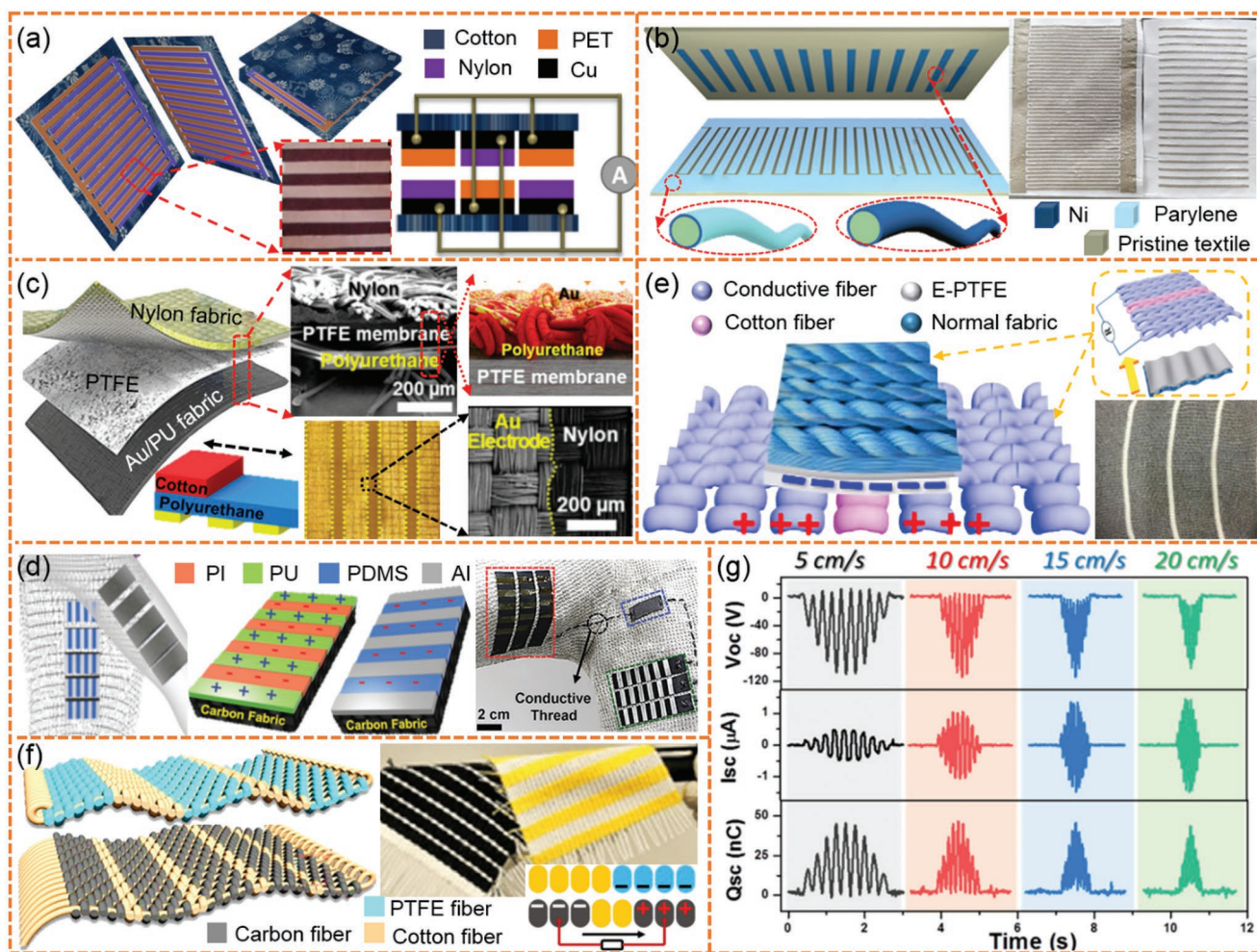
ADVANCED
SCIENCE NEWS
www.advancedsciencenews.com

ADVANCED
MATERIALS
www.advmat.de

Figure 16. Fabric-based TENGs working in in-plane freestanding triboelectric-layer based mode. a) A wearable FT mode TENG worked between nylon-Cu fabric and PET-Cu fabric. Reproduced with permission.[239] Copyright 2015, American Chemical Society. b) An interdigitated grating-structured and sliding-mode TENG fabric consisting of conformal Ni-coated PET slider fabric and parylene applied Ni-coated PET stator fabric. Reproduced with permission.[32] Copyright 2016, Wiley-VCH. c) A cost-effective textile-based flexible TENG with gold nanodot-patterned arrays designed by using in-plane sliding configuration. Reproduced with permission.[240] Copyright 2018, Elsevier. d) A FT mode fabric-based TENG worked between PI-PU interdigitated fabric and PDMS-Al alternatively patterned fabric. Reproduced with permission.[241] Copyright 2014, Wiley-VCH. e) A FT mode TENG that is formed between interdigitated knitted fabric and laminated composite fabric. Reproduced with permission.[242] Copyright 2019, Elsevier. f) A FT mode power TENG built by weaving cotton, carbon, and PTFE wires on the handloom. g) Typical electrical output characteristics of sliding-mode FT-based TENGs, mainly including V_{oc}, I_{sc}, and Q_{sc}. f,g) Reproduced with permission.[243] Copyright 2018, Elsevier.

4.4.6. Fabric-Based TENGs with Nanofiber Network or Textile-Related Membranous Structures

Different from the above fiber/fabric-based TENGs, some others are presented in the form of nanofibrous networks or textile-related membranes. Considering that textile components are involved and the characteristics of fabrics are exhibited in these TENGs, they are classified as fabric-based TENGs. At present, nanofiber webs or nonwoven membranes prepared via electrospinning method have been widely used to design textile-based TENGs.[40,244–248] The remarkable characteristics of electrospinning nanofibers, such as high specific surface area, inherently rough structure, and hierarchically porous structure, endow nanofiber-based TENGs with high electrical output and outstanding breathability. For instance, a multilayer

nanofiber-based TENG prepared by electrospinning was constructed between a pair of nanofibrous webs, one of which was cellulose acetate nanofibrous web, the other of which was polyethersulfone/carbon black/polystyrene composite nanofibrous web (**Figure 17**a).[246] It was found out that the composite three-layer nanofibrous structures exhibited a significantly higher electrical output performance compared with only single-layer structure. During the process of electrospinning, it is relatively simple and convenient to incorporate functional materials into polymer nanofibers. For example, MXene nanosheet has been integrated with polyvinyl alcohol (PVA) for electrospinning nanofibers to fabricate flexible TENGs. As provided in Figure 17b, a MXene-based all-electrospun TENG was designed with MXene/PVA electrospinning nanofiber film as an electronegative layer and silk fibroin as an electron donor, which shows
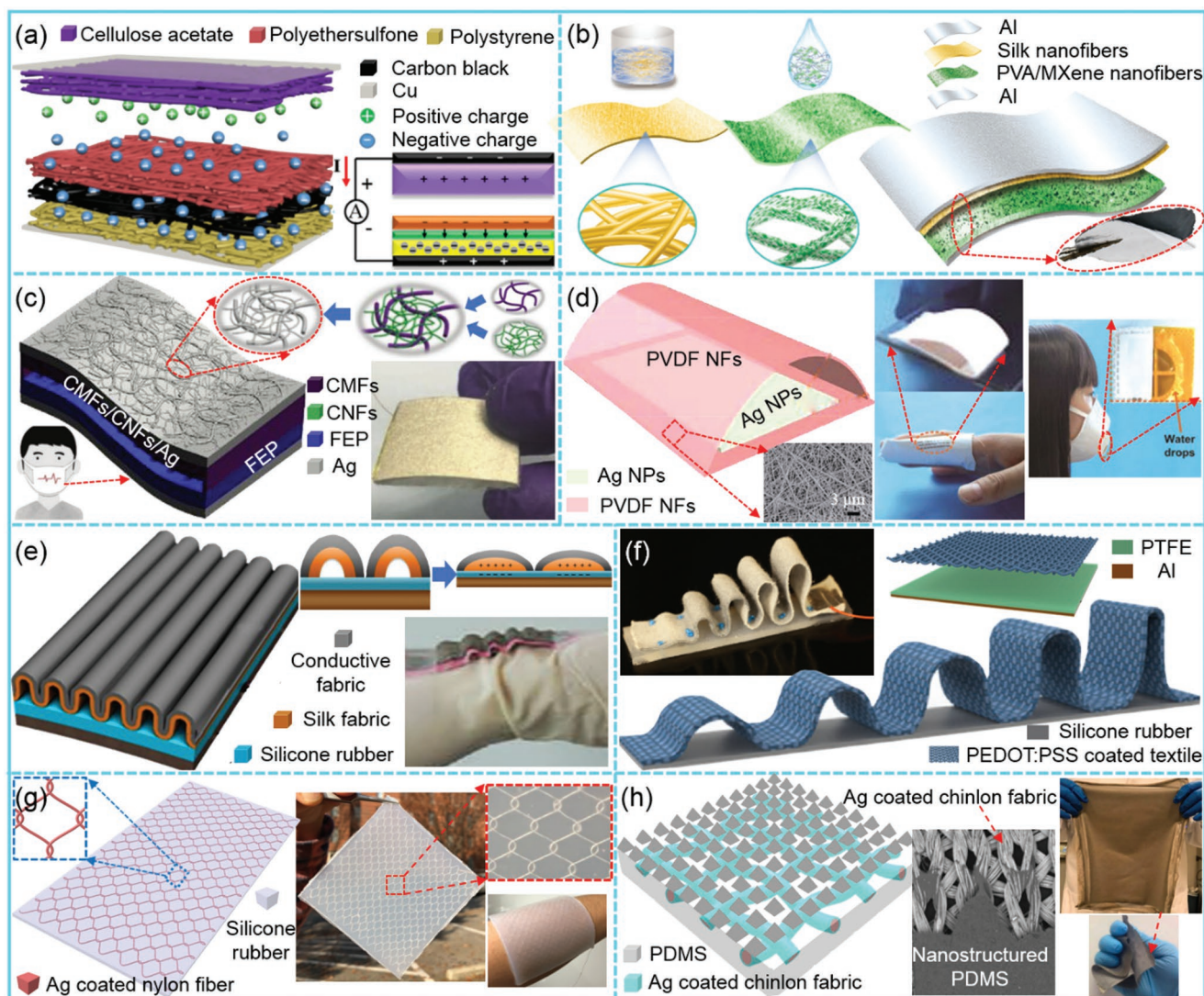
Figure 17. Textile-based TENGs fabricated with nanofiber network or textile-involved membranous structures. a) A multilayer nanofiber-based TENG constructed with cellulose acetate nanofiber as the upper layer and polyethersulfone/carbon black/polystyrene nanofibers as the lower layer. Reproduced with permission.[246] Copyright 2018, Elsevier. b) An all-electrospun TENG with MXene/PVA composite nanofibers and silk fibroin as a pair of triboelectric materials. Reproduced with permission.[249] Copyright 2019, Elsevier. c) A hierarchically nanocellulose fiber based TENG presented through developing 1D eco-friendly cellulose microfibers/nanofibers into 2D CMF/CNF/Ag hierarchical nanostructure. Reproduced with permission.[250] Copyright 2018, Wiley-VCH. d) A self-powered nanofiber-based triboelectric sensor with an arch structure for respiratory monitoring consisting of an electrospinning PVDF nanofiber film and a screen-printed Ag nanoparticle electrode. Reproduced with permission.[251] Copyright 2018, Tsinghua University Press and Springer-Verlag GmbH Germany, part of Springer Nature. e) A corrugated textile-based TENG consisting of undulatory silk conductive fabric on the top and silicone rubber covered conductive fabric on the bottom. Reproduced under the terms of the CC-BY Creative Commons Attribution 4.0 International License (http://creativecommons.org/licenses/by/4.0/).[252] Copyright 2017, The Authors, Published by Springer Nature. f) A height-varying multiarch TENG-based strain sensor achieved by fixing an arch-shaped PEDOT:PSS functionalized textile on silicone rubber elastomer. Reproduced with permission.[253] Copyright 2019, Elsevier. g) A stretchable yarn embedded TENG as electronic skin constructed by embedding conductive yarn networks into silicone rubber elastomer. Reproduced with permission.[35] Copyright 2018, Wiley-VCH. h) An ultraflexible, large-scale, and textile-based TENG by coating nanostructured PDMS film on a Ag-coated chinlon fabric. Adapted under the terms of the CC-BY 4.0 Creative Commons Attribution license (http://creativecommons.org/licenses/by/4.0/).[255] Copyright 2018, The Authors, Published by MDPI.

excellent stability and durability as well as extraordinary electrical output performance.[249] The porous nanostructures and large specific surface area of nanofiber-based TENG also render them with excellent particulate matter removal or absorptive capability. As exhibited in Figure 17c, a cellulose-based TENG for self-powered healthcare applications was presented through developing a 2D cellulose microfibers/nanofibers/silver (CMFs/CNFs/Ag) hierarchical nanostructured network.[250] The CMF skeleton provided a mesh-shaped framework for attaching the CNFs, which could not only enhance the triboelectrification effect, but also construct a desirable nanopore-on-micropore 2D hierarchical nanostructure for particulate matter removal. Enabled by its desirable porous nanostructure and unique electricity generation feature, the cellulose-based TENG was applicated

in removing $PM_{2.5}$, killing bacteria, and monitoring breathing status. Nanofiber-based TENGs with the similar functions can also be designed into other structures. As shown in Figure 17d, an arch-structural nanofiber-based triboelectric sensor was fabricated by screen printing Ag nanoparticles on an electrospinning PVDF nanofibrous web.[251] With the ability of breathability, low weight, and easy fabrication, the nanofiber-based TENG has been successfully demonstrated for healthcare monitoring, such as respiratory monitoring, finger motion detecting, and activity tracking. In addition to nanofiber reticular structures, textile-related membranous structures that combine textile materials with elastomeric polymers are also adopted, which can provide more designability and functionality for textile-based TENGs. For example, high stretchability of fabric-based TENGs can be achieved by fixing stretchable textile structures to rubber elastomers. As described in Figure 17e, a fabric-based TENG was assembled by stitching the upper corrugated structured fabrics composed of a silk cloth covered by a conductive woven fabric to the lower silicone rubber coated conductive knitted fabric.[252] Due to the upper corrugated structure as well as the inherent extensibility of silicone rubber and knitted structure, the fabric-based TENG was provided with excellent stretchability (≈120%). The corrugated structure can also be optimized to a height-varying multiarch structure for self-powered sensing applications. As presented in Figure 17f, a height-varying multiarch triboelectric strain sensor was developed by fixing an arch-shaped PEDOT:PSS coated fabric onto a silicone rubber substrate.[253] A variety of self-powered sensing applications of the TENG were demonstrated, including finger motion detecting, hand gesture capturing, robotic hand controlling, human activity monitoring, and gas concentration sensing. Considering that the external combination of textile materials and polymer membranes will lead to geometric complexity and large space occupancy, it seems more convenient and effective to embed conductive textile materials directly into elastomeric polymers. For example, a skin-inspired TENG was developed by embedding a planar and pattern designable conductive fiber network constructed from a three-ply-twisted Ag-coated nylon fiber into silicone rubber elastomer (Figure 17g).[35] Based on the merits of desired stretchability, good sensitivity, high detection precision, fast responsivity, and excellent mechanical stability, the skin-inspired TENG was successively demonstrated in wearable powering technology, physiological monitoring, intelligent prostheses, and human–machine interfaces. In addition to fiber network structure, stretchable conductive fabrics have also been used to design such kind of TENGs.[254,255] As demonstrated in Figure 17h, an ultraflexible fabric-based TENG was prepared by coating PDMS with microstructures on the surface of a Ag-coated chinlon fabric via a one-step doctor-blading technique.[255] Although the TENGs with textile-related membranous structure have the advantages of simple preparation method and high electrical output performance, their bad air permeability and poor skin affinity hinder their application in practical process. Furthermore, the polymer-encapsulated fabric-based TENGs are difficult to integrate with existing textile products.

The summary and comparison of the current fabric-based TENGs are listed in **Table 8**. Similar to PENGs, due to varied loading conditions and environmental factors, it is rather difficult or even impossible to distinguish good or bad between different fabric-based TENGs. However, in order to provide more intuitive and quantitative information for future researchers and product designers, they are still worth introducing here.

5. Textile-Based Piezoelectric and Triboelectric Hybrid Nanogenerator

Hybrid energy harvesters with the functions of simultaneously scavenging different kinds of energy, miniaturizing the size of device, and compensating for the respective shortcomings of each type are highly desirable for future wearable power sources, which have become a popular research topic.[256–259] Due to the collaboration of different mechanisms from individual components, the energy-harvesting capabilities are strengthened and the sensing of a variety of signals are enriched, which can meet the practical demand of wearable electronics. Since the PENG and TENG have matching impedance and similar structure features, and more importantly, both of them possess the capability to convert mechanical energy into electricity, it is very likely to combine them into one system so as to superimpose the electrical output from their distinct mechanisms. With appropriate structure designs and polarization direction modulations, the piezoelectric and triboelectric hybrid nanogenerators (PTHNGs) can combine the advantages of high piezoelectric output current and high triboelectric output voltage, which show promising application prospects in future wearable power sources.[260] Based on theoretical predictions, simulation analyses, and experimental measurements, the coupling mechanisms and superposition effects of PTHNGs have been extensively studied and reported.[261–263] It is found that the accordant direction of piezoelectric polarized charges and triboelectric induced charges would enhance power outputs, while their opposite direction would tremendously reduce electricity generation. According to the number of electrodes and combination ways of PENG and TENG, there are three different coupling modes of PTHNGs (**Figure 18**a), i.e., mode I in which PENG and TENG share a pair of electrodes,[264–272] mode II in which PENG and TENG share one common electrode,[273–275] and mode III in which PENG and TENG work independently.[276–282] Although each mode has its own characteristics, their electrical generation processes can be roughly divided into three steps, i.e., 1) TENG contacted and PENG pressed, 2) TENG contacted and PENG released, or 3) TENG separated and PENG released, according to the contact or separation state of triboelectric material and the compress or release state of piezoelectric material. Mode I can be further categorized based on whether the piezoelectric component and triboelectric material are the same, as displayed with red dotted boxes in Figure 18a. If the materials have both the piezoelectric and triboelectric effects, the simplest PTHNG with only three-layer structure can be developed. Compared with mode II, there is an additional insulating layer between PENG and TENG in mode III, which enables them to be structurally independent. Figure 18b demonstrates the simultaneous output voltage versus time curves of PENG and TENG in a single press-and-release process. It is found that the output voltage of TENG is a lot sharper than that of PENG, and there is a delay in the peaks

**ADVANCED
SCIENCE NEWS**

www.advancedsciencenews.com

**ADVANCED
MATERIALS**

www.advmat.de

Table 8. Summary and comparison of fabric-based TENGs.

Ref.	Modes	Electrodes	Triboelectric materials	Structures	Power outputs	Stretchability/durability	Washability	Main applications
[36]	CS	CNT	PTFE and CNT	Twisting	11 nA, 0.16 nC (5 Hz)	2.5%/5 h	–	Self-powered sensors
[192]	SE	Stainless-steel wire	Silicone rubber and skin	Sewing on fabric	200 V, 300 nC, 200 µA, 14 mW (1 MΩ)	100%	Washable	Biomedical sensing
[42]	SE	Stainless-steel wire	Silicone rubber and skin	2D knitting	150 V, 52 nC, 1.5 µA, 85 mW m^{-2} (3 Hz, 11 N, 100 MΩ)	100%/50 000 cycles	5 times	Energy harvesting
[194]	SE	Stainless-steel wire	Polymer fiber and cotton	2D wearing or knitting	75 V, 1.2 µA, 60 mW m^{-2} (200 MΩ)	5 h	120 times	Energy harvesting
[84]	SE	Liquid electrode	Silicone rubber and skin	2D wearing	130 V, 4 µA (2 Hz)	300%	–	Wearable electronics
[199]	SE	Stainless-steel wire	Silicone rubber and skin	2D weaving	19.8 V, 12.5 µW m^{-1} (0.5 Hz, 20 MΩ)	100%/2000 cycles	10 times	Energy harvesting
[236]	CS	Al foil	Nylon fabric and PVDF	Fabric stacking	2 V, 200 nA	Durable	50 times	Pulse signal monitoring
[39]	SE	Conductive fabric	Conductive fabric and PET	Fabric stacking	3 V, 15 nA	10 000 cycles	20 min	Sleeping monitoring
[214]	CS	Cu wire and cu foil	PTFE and Cu wire	2D weaving	6 V, 0.8 µA	Enough durability	Washable	Energy harvesting
[215]	SE	Cu foil strip	PTFE and skin	2D weaving	1050 V, 22 µA, 0.56 W m^{-2} (100 MΩ)	15%/12 h	30 min	Self-powered electronics
[216]	FT	Ag fabric	PET and nylon	2D weaving	90 V, 1 µA	–	Washable	Energy harvesting
[217]	CS	Ni-coated PET fabric	Parylene and Ni	2D weaving	50 V, 4 µA, 393.7 mW m^{-2}	–	–	Energy harvesting
[219]	FT	Ni-coated PET fabric	Silicone rubber and Ni	2D weaving	540 V, 140 µA, 0.89 mW m^{-2} (10 MΩ)	10 h	–	Energy harvesting
[222]	CS	Cu-coated PET fiber	PI and Cu	2D weaving	4.98 V, 15.5 mA m^{-2} (10 cm s^{-1})	1000 cycles	20 times	Respiratory monitoring
[225]	CS	Ag fabric	PTFE and Ag	2D knitting	23.5 V, 1.05 µA, 60 µW (3.3 Hz)	30%	–	Energy harvesting
[226]	CS	Ag-plated fiber	PA6 and PTFE	2D weaving	80 V, 4 µA, 11 mW m^{-2} (2 Hz, 10 MΩ)	1330 cycles	Washable	Wearable electronics
[227]	SE	Ag-coated fibers	Ag and PAN	3D full fabric	1768 mW m^{-2} (1200 N, 50 MΩ)	100 000 times	Washable	Energy harvesting
[228]	CS	Graphene	PTFE and nylon	3D spacer	3 V, 0.3 µA, 16 µW (0.6 MΩ)	–	–	Pressure sensing
[230]	CS	CNT and Ag	Ag and PDMS	3D penetrated	500 V, 20 µA, 153 mW m^{-2} (1 GΩ)	–	–	Energy harvesting
[37]	CS	Stainless-steel wire	Stainless-steel wire and PDMS	3D orthogonal	35 V, 18 nC, 263 mW m^{-2} (132 MΩ)	1500 cycles	10 times	Energy harvesting
[38]	SE	PAAM-LiCl	Composite resin and skin	3D printing	62 V, 26 mA m^{-3}, 0.65 mC m^{-3}, 11 W m^{-3}	1 month	–	Self-powered system
[246]	CS	Carbon black	Cellulose and polyethersulfone	Nanofiber stacking	115 V, 9 µA, 32 nC, 0.13 W m^{-2} (3 Hz, 30 MΩ)	6000 cycles	–	Energy harvesting
[237]	CS	Conductive fabric	Cotton and nylon	Fabric stacking	8 V, 1 µA cm^{-2}, 13 µW cm^{-2} (50 MΩ)	2 h	Washable	Energy harvesting
[234]	SE	Ag flake	Waterproof fabric and skin	Fabric stacking	880 V, 1.1 µA cm^{-2} (5 N, 4 Hz)	100%/600 stretch cycles	Washable	Energy harvesting
[233]	SE	Au foil	Water drop and waterproof fabric	Fabric stacking	15 V, 4 µA, 0.14 W m^{-2} (100 MΩ)	Stretchable and durable	Waterproof	Water energy harvesting
[232]	SE	Conductive fabric	PTFE NPs/PVDF NFs and skin	Fabric stacking	112.7 V, 1.98 µA, 80 mW m^{-2} (50 MΩ)	10 000 cycles	12 h	Wearable electronics
[235]	SE	CNT	Silk fabric and Skin	Fabric stacking	7 V, 180 nA (2 Hz)	2000 bending cycles	Washable	Touch/gesture sensor
[239]	FT	Cu strips	Nylon and PET fabric	Lateral sliding	2 kV, 0.2 mA	5400 cycles	Washable	Energy harvesting
[241]	FT	Carbon fabric	PI/PU and Al/PDMS	Lateral sliding	15 V, 130 nA (3 cm s^{-1})	Durable	–	Energy harvesting
[242]	FT	Ag-coated fabric	Interdigitated Ag fabric and PTFE	Lateral sliding	900 V, 19 µA	Stretchable/500 cycles	1 h	Energy harvesting
[243]	FT	Carbon fibers	Carbon fiber and PTFE fiber	Lateral sliding	118 V, 48 nC	Durable	Washable	Energy harvesting
[252]	CS	Ag plated fabric	Silk fabric and silicone rubber	Corrugated	28.13 V, 2.71 µA	120%	–	Self-powered system

Table 8. Continued.

Ref.	Modes	Electrodes	Triboelectric materials	Structures	Power outputs	Stretchability/ durability	Washability	Main applications
[35]	SE	Ag-coated nylon fiber	Skin and silicone rubber	Yarn embedded	160 V, 1.2 μA, 60 nC, 240 mW mm^{-2} (3 Hz)	100%/50000 cycles	Washable	Electronic skin
[255]	CS	Ag-coated fabric	Ag and PDMS	Fabric embedded	80 V, 8 μA, 0.2 mW cm^{-2} (20 MΩ)	Stretchable and durable	washable	Energy harvesting
[249]	CS	Al foil	Silk and PVA/MXnen	Nanofiber stacking	1087 mW m^{-2} (5 MΩ)	124 000 cycles	–	Self-powered devices
[250]	CS	Ag nanofibers	Cellulose nanofiber and FEP	Nanofiber stacking	22 V, 8 nC, 0.73 μA (5 Hz)	–	–	Healthcare monitoring
[251]	SE	Ag NPs	Ag NPs and PVDF	Arch-shaped	26 V, 250 nA, 0.12 mW (10 MΩ)	10 000 times	–	Respiratory monitoring
[253]	CS	PEDOT:PSS	PEDOT:PSS and silicone rubber	Multiarch	0.2 V (160% strain)	160%/4 h	Washable	Nanosensor
[102]	SE	Ni-coated fabric	Wool fabric and skin	Fabric stacking	13 V, 0.5 μA	10 000 cycles	Washable	Wearable keyboard
[245]	CS	Al foil	PVDF–AgNWs and nylon	Nanofiber stacking	240 V, 13 μA	60 min	–	Energy harvesting
[244]	CS	Cu foil	PVDF–HFP and PDMS	Nanofiber embedded	45 V, 0.9 W m^{-2} (700 kPa)	–	–	Pressure sensor
[248]	CS	Conductive fabric	Natural rubber and PVDF mat	Nanofiber stacking	1400 V, 0.78 mA, 21 mW (86 N)	50 000 cycles	Washable	Power source

in the second half cycle, which is due to the triboelectric charges are compensated faster than piezoelectric charges.[273,283] Furthermore, the activation states of TENG and PENG are out of sync, resulting in different phases of their alternative current (AC) signals. If PENG and TENG are directly connected in parallel mode, the total output power of PTHNG will be degraded to a certain extent due to the mutual cancellation between their electrical signals. In order to avoid the undesirable cancellation effect, a parallel circuit connection mode based on two full-wave bridge diodes circuits is designed for the circuit connection of PTHNGs (Figure 18c).

Considering the enormous enhancement effect of power output, PTHNGs have also gradually adopted to design wearable mechanical energy harvesting devices with textile structures. At present, the textile-based PTHNGs are fabricated basically based on the abovementioned three structural modes. Taking mode I as an example, an all-nanofiber-based PTHNG as a wearable gesture recognizer was prepared by electrospinning silk fibroin and PVDF nanofibers on conductive fabrics (Figure 18d).[40] Another similar all-nanofiber-based PTHNG as a power-generating insole was composed of PVDF nanofibers sandwiched between a pair of conductive fabrics (Figure 18e).[265] Both of them verified that the consistency direction of polarization charges and triboelectrification charges was particularly important for the PTHNG with high power output performance. A fabric-based PTHNG constructed with mode II was developed by stacking five-layer fabrics including three layers of fabric electrodes, an electrospinning PVDF/CNT/BaTiO$_3$ nonwoven fabric as the piezoelectric unit, and a PDMS/CNT/graphite composite film as the triboelectric unit, where the PENG and TENG shared one common fabric electrode (Figure 18f).[283] Compared with mode I and II, mode III with relatively independent piezoelectric and triboelectric structures is more convenient to design textile-based PTHNGs.

As exhibited in Figure 18g, a fiber-based PTHNG with core–shell structure was prepared by covering a TENG on the surface of a fiber-shaped PENG, in which the two NGs were separated by the middle nylon layer. In addition to single fibers, fabrics are also used to design this mode of PTHNG.[277] As shown in Figure 18h, a self-powered smart sock with piezoelectric and triboelectric hybrid mechanism for smart home applications was designed by integrating PEDOT:PSS-coated TENG fabric with PZT piezoelectric sensor, in which the PENG chip was embedded between two TENG fabrics.[284] Compared with single PENGs or TENGs, the power output performance of the abovementioned textile-based PTHNGs has been greatly improved. Although it will inevitably increase structural complexity, design cost and preparation difficulty, textile-based PTHNGs has taken a significant step toward a truly practical self-charging textile, which is still worthy of further research and large-scale promotion.

6. Conclusion and Perspectives

We have conducted a brief introduction of modern smart textiles as well as a comprehensive investigation and detailed discussion on current wearable textile-based nanogenerators. As textiles provide a large-area affiliated carrier and widespread service platform for the design and application of textile-related functional electronics, it is necessary to make a simple introduction and discussion on the current research status and future development trends of modern textiles as well as their new development forms, i.e., electronic textiles. In addition, in order to provide design guidance for smart textiles, the basic classification of textiles, commonly used conductive materials, and frequently adopted preparation methods are also summarized in detail. As a new mechanical energy harvesting and versatile
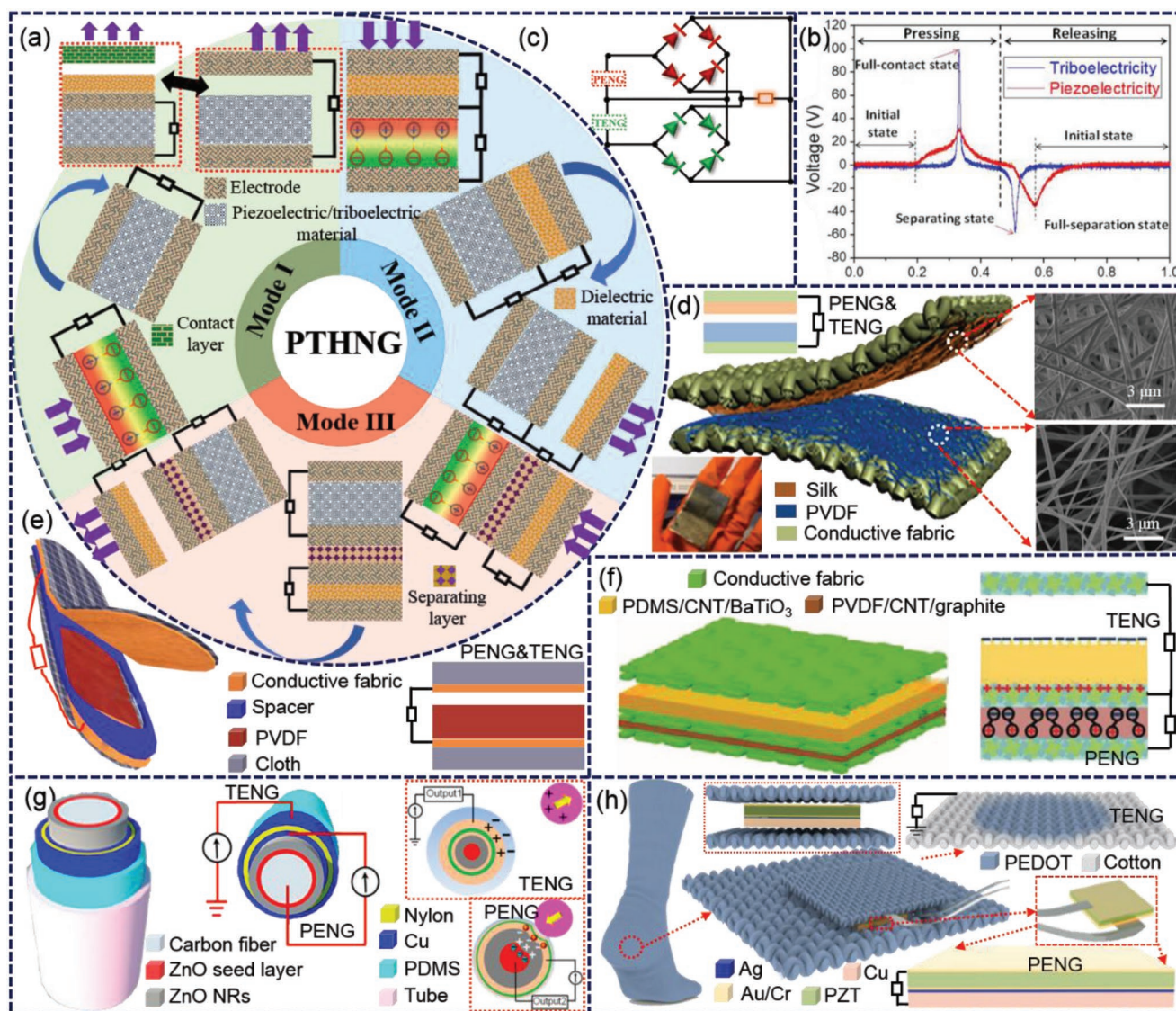
Figure 18. Fiber/fabric-based piezoelectric and triboelectric hybrid nanogenerators. a) Three typical configurations of PTHNG, i.e., mode I in which PENG and TENG share a pair of electrodes, mode II in which PENG and TENG share one common electrode, and mode III in which PENG and TENG work independently. b) Output voltage versus time curves of PENG and TENG, measured individually in a single press-and-release cycle. b) Reproduced under the terms of the Creative Commons Attribution 4.0 International License (http://creativecommons.org/licenses/by/4.0/).[273] Copyright 2015, Springer Nature. c) Concurrent connection circuit for PTHNG based on two full-wave bridge diodes circuits. d) An all-nanofiber-based PTHNG fabricated by electrospinning silk fibroin and PVDF nanofibers on conductive fabrics. d) Reproduced with permission.[40] Copyright 2018, Elsevier. e) An all-nanofiber-based PTHNG as an energy-harvesting insole composed of electrospinning piezoelectric PVDF nanofibers sandwiched between a pair of conductive fabrics. Reproduced with permission.[265] Copyright 2015, Elsevier. f) A highly flexible and large-area fabric-based PTHNG for mechanical energy harvesting. Reproduced with permission.[283] Copyright 2018, Wiley-VCH. g) A fiber-based PTHNG for energy harvesting and as a self-powered pressure sensor. Reproduced with permission.[277] Copyright 2014, American Chemical Society. h) A self-powered and self-functional cotton sock using piezoelectric and triboelectric hybrid mechanism for healthcare and sports monitoring. Reproduced with permission.[284] Copyright 2019, American Chemical Society.

self-powered sensing technology, NGs have shown strong vitality and enormous advantage which have great application prospects in various fields of future society. NGs are mainly divided into two categories, i.e., PENGs and TENGs, in term of compositional structures and working mechanisms. General speaking, power outputs of PENGs are much less than those of TENGs, while PENGs are better than TENGs with respect to working stability. Textile-based NGs in the form of fibers

and fabrics are born in the combination of modern textiles and NG technology. In order to make an overall grasp about textile-based NGs, the basic knowledge and current research situation of fiber/fabric-based PENGs and TENGs are also presented and discussed here, which mainly include basic concepts, material selection systems, structure characteristics, working modes and corresponding mechanisms, and respective application occasions. It is found that piezoceramics and piezopolymers are two

ADVANCED
SCIENCE NEWS
www.advancedsciencenews.com

ADVANCED
MATERIALS
www.advmat.de

main categories of piezoelectric materials, while triboelectric series are the main selection standard for TENGs. Electrical output properties of PENGs mainly depend on the polarization charge of piezoelectric materials, while these of TENGs rely on the induced potential difference between the two paired tribo-materials. Metal–insulator–metal is the typical structural type as well as basic design principle of PENGs. The ubiquitous tri-boelectric effect endows TENGs with more design possibilities and diversified structure choices. Based on structural characteristics and fabrication techniques, both of textile-based PENGs and TENGs can be classified as single fiber-shaped type, fabric-based type with textile forming and multilayer stacking structures. Particularly, in term of the final forming dimension of fabric-based NGs, the textile forming structure can be further categorized into 2D and 3D. According to the preparation method of fabric-based NGs, the multilayer stacking structures can be divided into 2D fabric, nanofiber network, and textile-related membrane stacking. For each classified structure, a large number of recent research works have been overviewed and corresponding discussions are also given.

It is well known that the applications of textile-based NGs are ubiquitous and endless. However, there are two representative aspects, i.e., wearable electronics and artificial intelligence that are particularly noteworthy, from which we can see the future prospects of textile-based NGs. The potential applications of textile-based NGs based on the two aspects are also introduced as follows:

1) *Wearable Electronics*: Wearable electronics are electronic devices constantly worn by a person as unobstructively as clothing to provide intelligent assistance for human life such as communicating, interacting, monitoring and sensing.[285–289] Thus, it is necessary to endow wearable electronics with electric conductive and signal transmission functions. Textile-based NGs with two main functions of wearable power supplying and self-powered sensing just cater to the sustainable development needs of future wearable electronics. On the one hand, textile-based NGs can effectively harvest human motion energy in a continuous, convenient and environmentally friendly way, thus providing a feasible supply power path for wearable electronics. For example, textile-based NGs worn on human body will be able to power up electronic watches, mobile phone, tablet PC, laptop PC, and even more. On the other hand, electrical signals generating from textile-based NGs can also be regarded as important observed indicators for the variations of human body or environment. In such case, textile-based NGs are transformed to active self-powered sensors, which can realize a variety of functional applications without additional power supply, such as motion tracking, health monitoring, pressure pixel array, and human–machine interactive. It is firmly believed that textile-based NGs will be bound to shine brightly in future wearable electronics.

2) *Artificial Intelligence*: AI is the simulation of human intelligence process by machines, aiming at creating a technology that allows computers and machines to function in an intelligent manner such as planning, learning, reasoning, motioning, manipulating, problem solving, knowledge representation, language programming, and so on.[290–295] AI has become an essential part of the information society which is revolutionizing and reshaping our physical and spiritual world. The development and application of textile-based NGs will certainly contribute to the advancement of AI, which will provide feasible implementation approaches and versatile communication channels for AI. In principle, textile-based NGs can be applied in almost every field related to AI such as healthcare, garment, education, military, manufacture, finance, communication, business, sport, transportation, etc. Herein, some representative application occasions in terms of these fields are presented in **Figure 19**. For example, identity recognition based on unique human physiological characteristics, such as face, voice, odor, fingerprint, and heartbeat, has been adopted in many fields. In order to enhance the authentical, interactive, exercise and competitive effects, somatosensory and 3D visualized functions are gradually incorporated into modern games. Bionics is a novel engineering design technology based on the imitation of natural biological characteristics. In term of human body, several kinds of bionomic systems have already been developed, such as electronic skin, intelligent prosthesis, and soft robotic. Although some satisfactory results have been achieved about AI, it is still in its infancy and many difficulties need to be overcome. However, there is no doubt that the application of AI in all fields is an inevitable trend. In future, it can be forecasted that textile-based NGs will become an important part of AI.

Although great progress related to textile-based NGs has been achieved in terms of theoretical research and multifaceted application demonstrations, there is still a huge gap between research and practical commercial applications. Herein, potential difficulties and challenges for the widespread commercial applications of textile-based NGs are also analyzed and discussed from the perspectives of wearability, stability, fabrication, power output, evaluation standard, and target market. As shown in **Figure 20**, each factor contains several aspects and interacts with each other.

1) *Working Stability*: The service life of wearable textile-based NGs depends on their long-term working and complex environmental stability. In practical use, there are many factors that threaten their stabilities and even their lives. For example, functional nanomaterials such as conductive, dielectric, piezoelectric or triboelectric components, or special nanostructures such as nanowire, nanorod, and nanofiber, are often incorporated into textile systems to enhance their working performance. However, after complex, repetitive and intense external mechanical loads or chemical treatments, the electrical outputs of NGs will be dramatically reduced or completely vanished with the weakening or disappearance of nanostructures. In addition, the operation of NGs sensitively depends on external environmental conditions, such as temperature, humidity, water, gas, absorption, and radiation. It turns out that temperature has a negative effect on the electrical output performance of NGs.[296] Piezoelectric materials will lose their permanent electric dipoles above their Curie or melting temperature.[297] The operation temperature of TENGs is also limited owing to electron thermion emission.[188,298] Piezoelectric output increases with the increase of oxygen concentrations, because more
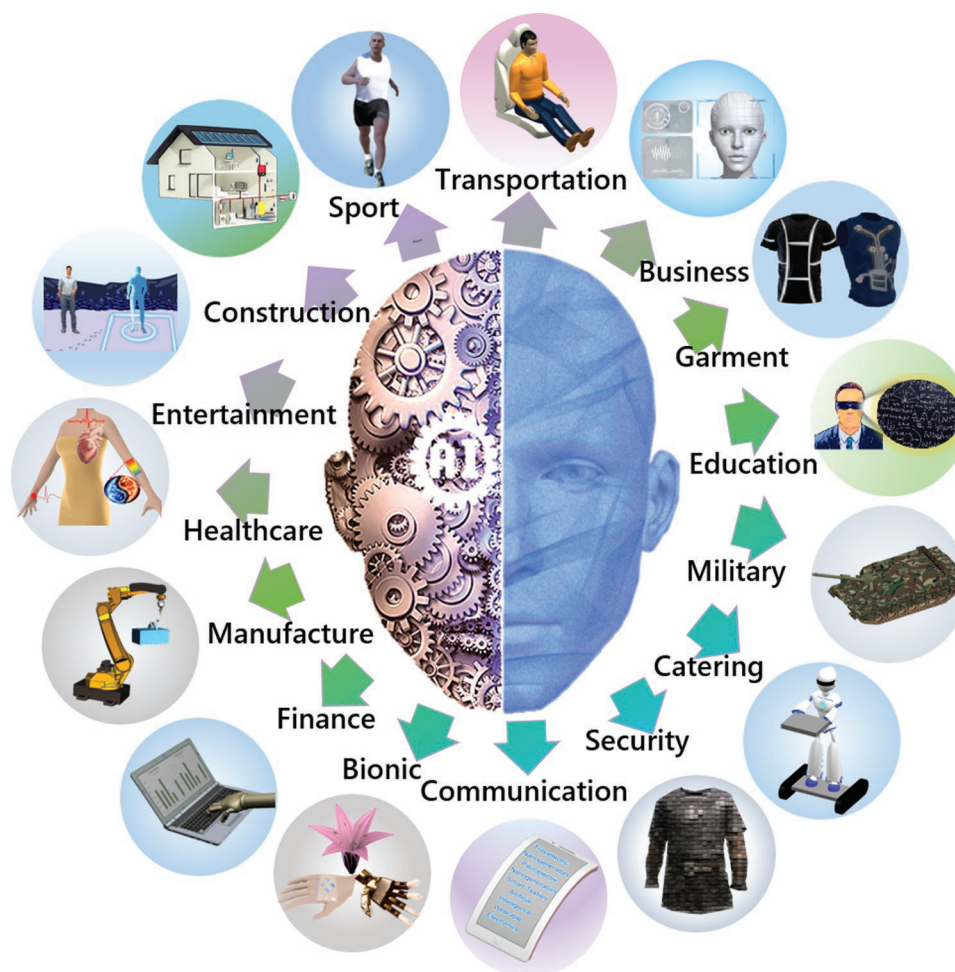
ADVANCED
SCIENCE NEWS
www.advancedsciencenews.com

ADVANCED
MATERIALS
www.advmat.de

Figure 19. Promising application fields of NGs in artificial intelligence (AI). For example, home-furnishing decoration in construction; self-driving in transportation; physiological signal monitoring in healthcare; individualized learning in education; real-time positioning and tracking for the military; automatic production in manufacture; food delivery in catering; automatic analysis and transaction in finance; face recognition in business; wireless video calls in communication; somatosensory games in entertainment; action guidance and adjustment in sport; body protection in security; luminous, conductive or thermally regulating cloth for garments; and versatile bionic systems including electronic skin, intelligent protheses, and soft robotics.

absorbed oxygen mitigates the surface free-carrier screening effect.[299] UV radiations will desorb oxygen molecules and thus suppress piezoelectric output.[300] Water intrusion or high humidity normally degrades the performance of NGs. In frequent use, contaminants will inevitably be absorbed on the surface of NGs, which will reduce electrical outputs due to weakened charge transfer.[42,301] It should be noted that these environmental factors are not fatal to NGs because electrical output performance can be recovered when the environmental condition is removed. In future, the stability of NGs is no longer a key issue since most of them are used at one time.

2) *Various Wearability*: Since textile-based NGs are mainly for wearable purposes, they must be qualified with various wearability that common fabrics possess, including flexibility, stretchability, breathability, comfortability, washability, tailorability, biocompatibility, aesthetics, desired mechanical properties, etc. Complex mechanical deformations caused by human motions require textile-based NGs to possess desired flexibility/stretchability and considerable mechanical

strength. Unfortunately, most of the current fiber-shaped conductive materials are either too hard or too soft. For example, most flexible polymers are prone to fracture under intense mechanical loadings, while metal wire/foil are too rigid to textile-based NGs. As an important factor of comfortability, breathability that is mainly involved with the permeability of air, moisture, water, heat and light plays a role in managing and regulating the balance of temperature and humidity in human microenvironment. To make textile-based NGs have good breathability, space between fibers is necessary, which acts as flow channels/bridges between human skin and outer environment. Moreover, static air trapped with the space between fibers is benefit for warmth retention of textile-based NGs. In addition to the heat-moisture comforts, tactile comforts such as prickle sensation, fabric weight, static electricity, and cold stimulation is also important for wearability, which are often associated with biocompatibility. As textile-based NGs are often in contact with human skin, the selected materials for them must be nontoxic, safe and highly biocompatible. Harmful conductive materials (e.g., carbon
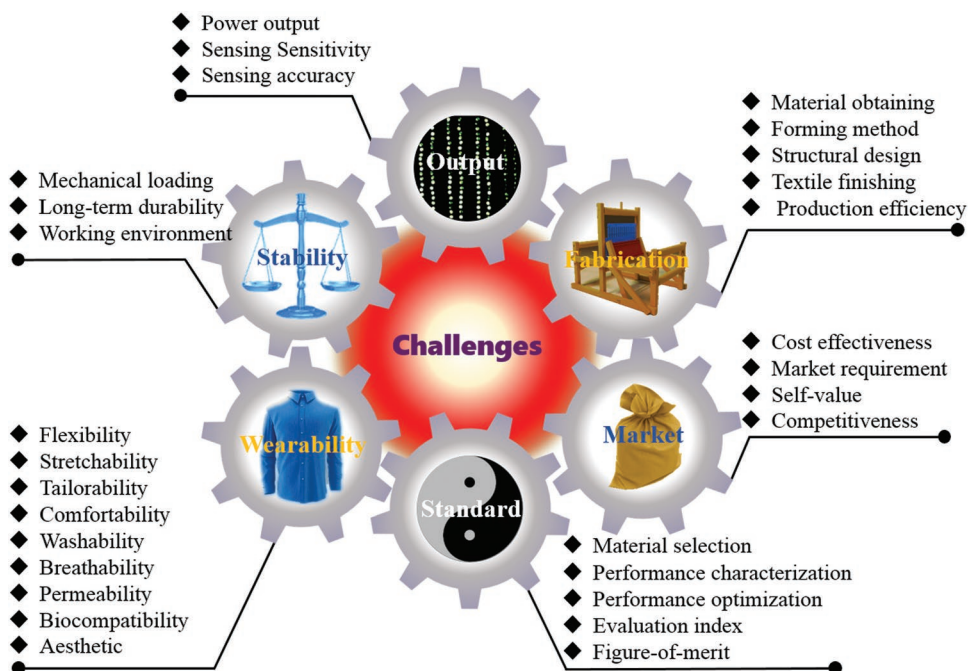
**ADVANCED
SCIENCE NEWS**

www.advancedsciencenews.com

**ADVANCED
MATERIALS**

www.advmat.de

Figure 20. Potential difficulties and challenges that impede the large-scale industrial fabrication and commercial application of textile-based NGs.

fillers and hazardous metals) and chemical reagents should be avoided as far as possible in the process of fabrication. Due to soft texture and thin thickness, most of textile-based NGs have good tailorability. However, the tricky problem for the tailored textile-based NGs is circuit connection. Machine washability is particularly important for textile-based NGs because it involves whether they can be used many times. Recently, it has received more and more attentions in the design and application of textile-based NGs. To prevent functional materials from being washed away or damaged, the common way is to encapsulate with waterproof materials or cover directly with hydrophobic/repellent materials. However, these additional protective materials are bound to increase overall weight and weaving difficulty. For fabric-based NGs with multilayer fabrics stacking, nanofiber network, or textile related membranous structures, their breathability and comfortability are poor. Furthermore, in practical use, they are usually attached to or decorated on common fabrics, which not only results in the loss of aesthetics, but also greatly restricts normal human activities. Therefore, textile-based NGs fabricated from individual functional fibers are more suitable for wearable use in a wide range.

3) *Industrial Fabrication*: Large-scale industrialized production of textile-based NGs is one of basic premises for their wide commercial applications. However, it is disappointing to note that most of the textile-based NGs reported above are manually fabricated. Although several efforts and attempts have been made to promote their rapid preparation, there are still many difficulties and challenges ahead that remain to be overcome. From the perspective of materials, due to curved surface structure, high aspect ratio, and limited covering area of fibers, it is rather difficult for functional materials to cover on their surface. Even if these materials are initially successfully added to fibers, they are still vulnerable to damage in use

due to weak interfacial bonding between functional materials and textile substrates. The cracking/delamination of surface insulation layer and the rupture of fibers may easily lead to the occurrence of open-circuit and short-circuit failures of textile-based NGs. From the point of view of structure design, it is difficult to find a textile structure with both rapid preparation capability and excellent wearability. On the one hand, although fabric-based NGs with multilayer stacking structures have the advantages of rapid prototyping, large contact area, and high output efficiency, poor wearability make them difficult to become the mainstream of future wearable NGs. On the other hand, in spite of good wearability, most functional fibers are incompatible with current mature textile manufacturing process. For instance, fibers containing piezoelectric or triboelectric materials usually have diameters larger than the maximum yarn crossing caliber of modern looms. The chemical treated fibers exhibit brittle and hard textures, which are liable to break under large loom tension. In addition, special structural designs are also required for textile-based PENGs and TENGs, which increases the complexity and cost of preparation.

4) *Electrical Output*: Low output power and poor sensing capability of textile-based NGs make them difficult to effectively use. On the one hand, power outputs of textile-based NGs are far less than the actual demand of most wearable electronics. At present, there are several approaches to improve the energy conversion efficiency of textile-based NGs, such as increasing effective contact area, improving softness, establishing nanostructured contact interface, and using hybrid energy harvesters.[302] However, none of them is feasible without increasing the difficulty of fabrication. As a mature textile forming method, 3D fabrics can effectively increase the number of fiber layers in the thickness direction, which have been proved to be an effective method to increase power outputs

Table 9. Comparison the sensing accuracy of PENGs and TENGs with commercial devices.

Applications	PENGs	TENGs	Ref.
Wide-range pressure sensor	Well matched	–	[303]
Wind-velocity detection	Similar performance while with lower working limit	–	[304]
Impact acceleration sensor	–	Fewer clutters and better than commercial	[305]
Blood pressure detection	–	Slight discrepancy (about 0.87–3.65%)	[306]
Heart-rate monitoring	–	More accurate than commercial	[307]
Accelerometer	–	Better than commercial	[308]
Motion sensor	–	Multifunctional	[171]
Driving status monitoring	–	Similar output performance	[309]
Wind speed sensor	–	Favorable correlation	[310]
Vibration sensor	–	Basic consistent	[210]

with a smaller contact area. On the other hand, the electrical signals of textile-based NGs are easily disturbed by surrounding environments. Although sensor-oriented NGs have been extensively studied, few works have compared its sensing accuracy with commercial devices. In the early development stage of NGs, the sensing accuracy of NGs is often neglected since most researchers are committed to achieving sensing ability instead of improving it. With the rapid development of NGs and their expanding application fields, sensing accuracy will gradually become an unavoidable problem in the process of their commercialization. Fortunately, the sensing capability of textile-based NGs can be improved through structural design, systematic circuit management, and custom personalized user interface. As listed in **Table 9**, the sensing accuracies of several optimized NGs are similar to or even better than those of commercial devices.[171,210,303–310] Therefore, it is firmly believed that the power output of future NGs will be greatly enhanced and improved.

5) *Evaluation Standard*: There is an incredible fact behind the vigorous development of NGs that the electrical output performance of different NGs are unable to compare. Although there are some common indicators to characterize the electrical output performance of NGs, including open-circuit voltage, short-circuit current, short-circuit charge transfer, energy conversion efficiency, charging capacity, sensing sensitivity, and response time, it is quite difficult or almost impossible to compare power outputs among different NGs due to inconsistent test conditions such as working environment, contact area, applied load, material modification, electrode connection mode, operating mode, etc. Current disordered and confusing research status of NGs cannot provide correct guidance for future researchers and product designers. It is hoped that systematic research systems and standardized evaluation criteria will be developed in the near future, which mainly cover material selection, performance characterization, performance optimization, evaluation index, and figure of merit.

6) *Target Market*: Even if the above five aspects can be well solved, the wide commercial applications of textile-based NGs are still influenced by market factors. In the future market of wearable electronic and artificial intelligence, whether textile-based NGs can stand out among various energy equipment still depends on their cost efficiency, market demand, and

self-value. In order to improve the market competitiveness of textile-based NG, we must always focus on improving its performance, reducing its production cost, and enhancing its production efficiency.

Although these unresolved issues and tough challenges have seriously hindered the development process of wearable fiber/fabric-based NGs, their vigorous development and widespread application are an irresistible trend of our times. It is firmly believed that many major issues of the current textile-based NGs will be well solved with the progress of science and technology. In a word, textile-based NGs have great possibilities to become the mainstream of future daily wearing textiles.

Conflict of Interest

The authors declare no conflict of interest.

[1] V. Plumwood, *Environmental Culture: The Ecological Crisis of Reason*, Routledge, New York **2005**.

[2] Z. L. Wang, *Nano Energy* **2018**, *54*, 477.

[3] J. Mokyr, *Storia dell'economia Mondiale*, Laterza Publishing, Rome, Italy **1998**, p. 219.

**ADVANCED
SCIENCE NEWS**

www.advancedsciencenews.com

**ADVANCED
MATERIALS**

www.advmat.de

[4] S. Günes, H. Neugebauer, N. S. Sariciftci, *Chem. Rev.* **2007**, *107*, 1324.

[5] F. C. Krebs, *Sol. Energy Mater. Sol. Cells* **2009**, *93*, 394.

[6] S. B. Riffat, X. Ma, *Appl. Therm. Eng.* **2003**, *23*, 913.

[7] D. Champier, *Energy Convers. Manage.* **2017**, *140*, 167.

[8] A. Heller, *Phys. Chem. Chem. Phys.* **2004**, *6*, 209.

[9] R. A. Bullen, T. Arnot, J. Lakeman, F. Walsh, *Biosens. Bioelectron.* **2006**, *21*, 2015.

[10] Z. L. Wang, *Mater. Today* **2017**, *20*, 74.

[11] Z. L. Wang, J. Song, *Science* **2006**, *312*, 242.

[12] F.-R. Fan, Z.-Q. Tian, Z. L. Wang, *Nano Energy* **2012**, *1*, 328.

[13] Y. Yang, W. Guo, K. C. Pradel, G. Zhu, Y. Zhou, Y. Zhang, Y. Hu, L. Lin, Z. L. Wang, *Nano Lett.* **2012**, *12*, 2833.

[14] Z. L. Wang, G. Zhu, Y. Yang, S. Wang, C. Pan, *Mater. Today* **2012**, *15*, 532.

[15] W. Zeng, L. Shu, Q. Li, S. Chen, F. Wang, X. M. Tao, *Adv. Mater.* **2014**, *26*, 5310.

[16] M. Syduzzaman, S. U. Patwary, K. Farhana, S. Ahmed, *J. Text. Sci. Eng.* **2015**, *5*, 100081.

[17] S. Park, S. Jayaraman, *MRS Bull.* **2003**, *28*, 585.

[18] M. Stoppa, A. Chiolerio, *Sensors* **2014**, *14*, 11957.

[19] L. M. Castano, A. B. Flatau, *Smart Mater. Struct.* **2014**, *23*, 053001.

[20] J. S. Heo, J. Eom, Y. H. Kim, S. K. Park, *Small* **2018**, *14*, 1703034.

[21] K. Cherenack, L. van Pieterson, *J. Appl. Phys.* **2012**, *112*, 091301.

[22] A. Lund, N. M. van der Velden, N.-K. Persson, M. M. Hamedi, C. Müller, *Mater. Sci. Eng., R* **2018**, *126*, 1.

[23] M. Liu, X. Pu, C. Jiang, T. Liu, X. Huang, L. Chen, C. Du, J. Sun, W. Hu, Z. L. Wang, *Adv. Mater.* **2017**, *29*, 1703700.

[24] J. Ge, L. Sun, F. R. Zhang, Y. Zhang, L. A. Shi, H. Y. Zhao, H. W. Zhu, H. L. Jiang, S. H. Yu, *Adv. Mater.* **2016**, *28*, 722.

[25] X. Pu, H. Guo, Q. Tang, J. Chen, L. Feng, G. Liu, X. Wang, Y. Xi, C. Hu, Z. L. Wang, *Nano Energy* **2018**, *54*, 453.

[26] S. K. Ghosh, D. Mandal, *Nano Energy* **2018**, *53*, 245.

[27] S. Siddiqui, H. B. Lee, D.-I. Kim, L. T. Duy, A. Hanif, N.-E. Lee, *Adv. Energy Mater.* **2018**, *8*, 1701520.

[28] W. Zeng, X.-M. Tao, S. Chen, S. Shang, H. L. W. Chan, S. H. Choy, *Energy Environ. Sci.* **2013**, *6*, 2631.

[29] N. Soin, T. H. Shah, S. C. Anand, J. Geng, W. Pornwannachai, P. Mandal, D. Reid, S. Sharma, R. L. Hadimani, D. V. Bayramol, E. Siores, *Energy Environ. Sci.* **2014**, *7*, 1670.

[30] Z. Zhang, Y. Chen, J. Guo, *Phys. E* **2019**, *105*, 212.

[31] Y. Chen, Z. Liu, D. Zhu, S. Handschuh-Wang, S. Liang, J. Yang, T. Kong, X. Zhou, Y. Liu, X. Zhou, *Mater. Horiz.* **2017**, *4*, 591.

[32] X. Pu, W. Song, M. Liu, C. Sun, C. Du, C. Jiang, X. Huang, D. Zou, W. Hu, Z. L. Wang, *Adv. Energy Mater.* **2016**, *6*, 1601048.

[33] K. Dong, J. Deng, W. Ding, A. C. Wang, P. Wang, C. Cheng, Y.-C. Wang, L. Jin, B. Gu, B. Sun, Z. L. Wang, *Adv. Energy Mater.* **2018**, *8*, 1801114.

[34] Z. Zhao, X. Pu, C. Du, L. Li, C. Jiang, W. Hu, Z. L. Wang, *ACS Nano* **2016**, *10*, 1780.

[35] K. Dong, Z. Wu, J. Deng, A. C. Wang, H. Zou, C. Chen, D. Hu, B. Gu, B. Sun, Z. L. Wang, *Adv. Mater.* **2018**, *30*, 1804944.

[36] J. Zhong, Y. Zhang, Q. Zhong, Q. Hu, B. Hu, Z. L. Wang, J. Zhou, *ACS Nano* **2014**, *8*, 6273.

[37] K. Dong, J. Deng, Y. Zi, Y. C. Wang, C. Xu, H. Zou, W. Ding, Y. Dai, B. Gu, B. Sun, Z. L. Wang, *Adv. Mater.* **2017**, *29*, 1702648.

[38] B. Chen, W. Tang, T. Jiang, L. Zhu, X. Chen, C. He, L. Xu, H. Guo, P. Lin, D. Li, J. Shao, Z. L. Wang, *Nano Energy* **2018**, *45*, 380.

[39] Z. Lin, J. Yang, X. Li, Y. Wu, W. Wei, J. Liu, J. Chen, J. Yang, *Adv. Funct. Mater.* **2018**, *28*, 1704112.

[40] Y. Guo, X.-S. Zhang, Y. Wang, W. Gong, Q. Zhang, H. Wang, J. Brugger, *Nano Energy* **2018**, *48*, 152.

[41] M. W. Han, S. H. Ahn, *Adv. Mater.* **2017**, *29*, 1700244.

[42] K. Dong, Y. C. Wang, J. Deng, Y. Dai, S. L. Zhang, H. Zou, B. Gu, B. Sun, Z. L. Wang, *ACS Nano* **2017**, *11*, 9490.

[43] R. Fangueiro, F. Soutinho, *Fibrous and Composite Materials for Civil Engineering Applications*, Woodhead Publishing, Cambridge **2011**, p. 62.

[44] A. Pourmohammadi, *Joining Textiles*, Woodhead Publishing, Cambridge **2013**, p. 565.

[45] S. S. Badawi, *Ph.D. Thesis*, Technical University of Dresden, Dresden, Germany **2007**.

[46] M. Karahan, S. V. Lomov, A. E. Bogdanovich, D. Mungalov, I. Verpoest, *Composites, Part A* **2010**, *41*, 1301.

[47] S. Z. Sheng, S. van Hoa, *J. Thermoplast. Compos. Mater.* **2003**, *16*, 45.

[48] K. Dong, K. Liu, L. Pan, B. Gu, B. Sun, *Compos. Struct.* **2016**, *154*, 319.

[49] P. Tan, L. Tong, G. P. Steven, *Composites, Part A* **1999**, *30*, 637.

[50] P. G. Unal, *3D Woven Fabrics*, IntechOpen Access Publisher, London, UK **2012**.

[51] W. Renkens, Y. Kyosev, *Text. Res. J.* **2011**, *81*, 437.

[52] K. Kim, M. Jung, S. Jeon, J. Bae, *Smart Mater. Struct.* **2019**, *28*, 065019.

[53] S. Adanur, T. Liao, *Composites, Part B* **1998**, *29*, 787.

[54] K. Dong, J. Zhang, L. Jin, B. Gu, B. Sun, *Compos. Struct.* **2016**, *143*, 9.

[55] N. Khokar, *J. Text. Inst.* **2002**, *93*, 52.

[56] Z. Cao, R. Wang, T. He, F. Xu, J. Sun, *ACS Appl. Mater. Interfaces* **2018**, *10*, 14087.

[57] R. Jalili, J. M. Razal, P. C. Innis, G. G. Wallace, *Adv. Funct. Mater.* **2011**, *21*, 3363.

[58] C. Y. Wang, V. Mottaghitalab, C. O. Too, G. M. Spinks, G. G. Wallace, *J. Power Sources* **2007**, *163*, 1105.

[59] Y. Chen, B. Zhang, G. Liu, X. Zhuang, E. T. Kang, *Chem. Soc. Rev.* **2012**, *41*, 4688.

[60] J. Foroughi, G. M. Spinks, S. R. Ghorbani, M. E. Kozlov, F. Safaei, G. Peleckis, G. G. Wallace, R. H. Baughman, *Nanoscale* **2012**, *4*, 940.

[61] P. Lee, J. Ham, J. Lee, S. Hong, S. Han, Y. D. Suh, S. E. Lee, J. Yeo, S. S. Lee, D. Lee, S. H. Ko, *Adv. Funct. Mater.* **2014**, *24*, 5671.

[62] A. Mirabedini, J. Foroughi, G. G. Wallace, *RSC Adv.* **2016**, *6*, 44687.

[63] T. D. Ngo, A. Kashani, G. Imbalzano, K. T. Q. Nguyen, D. Hui, *Composites, Part B* **2018**, *143*, 172.

[64] S. Ye, A. R. Rathmell, Z. Chen, I. E. Stewart, B. J. Wiley, *Adv. Mater.* **2014**, *26*, 6670.

[65] T. Sannicolo, M. Lagrange, A. Cabos, C. Celle, J. P. Simonato, D. Bellet, *Small* **2016**, *12*, 6052.

[66] A. R. Rathmell, S. M. Bergin, Y. L. Hua, Z. Y. Li, B. J. Wiley, *Adv. Mater.* **2010**, *22*, 3558.

[67] B. Wu, A. Heidelberg, J. J. Boland, *Nat. Mater.* **2005**, *4*, 525.

[68] F. Xu, Y. Zhu, *Adv. Mater.* **2012**, *24*, 5117.

[69] A. G. N. Sofiah, M. Samykano, K. Kadirgama, R. V. Mohan, N. A. C. Lah, *Appl. Mater. Today* **2018**, *11*, 320.

[70] M. H. Naveen, N. G. Gurudatt, Y.-B. Shim, *Appl. Mater. Today* **2017**, *9*, 419.

[71] T. Nezakati, A. Seifalian, A. Tan, A. M. Seifalian, *Chem. Rev.* **2018**, *118*, 6766.

[72] H. J. Lee, Z. X. Jin, A. N. Aleshin, J. Y. Lee, M. J. Goh, K. Akagi, Y. S. Kim, D. W. Kim, Y. W. Park, *J. Am. Chem. Soc.* **2004**, *126*, 16722.

[73] J. Huang, S. Virji, B. H. Weiller, R. B. Kaner, *J. Am. Chem. Soc.* **2003**, *125*, 314.

[74] T. S. Kang, S. W. Lee, J. Joo, J. Y. Lee, *Synth. Met.* **2005**, *153*, 61.

[75] X. Li, C. Li, J. Chen, C. Li, C. Sun, *J. Chromatogr. A* **2008**, *1198–1199*, 7.

[76] W. Baik, W. Luan, R. H. Zhao, S. Koo, K.-S. Kim, *Synth. Met.* **2009**, *159*, 1244.

[77] S. Seyedin, S. Moradi, C. Singh, J. M. Razal, *Appl. Mater. Today* **2018**, *11*, 255.

[78] L. V. Kayser, D. J. Lipomi, *Adv. Mater.* **2019**, *31*, 1806133.

[79] D. Kumar, R. Sharma, *Eur. Polym. J.* **1998**, *34*, 1053.

[80] L. Wen, F. Li, H. M. Cheng, *Adv. Mater.* **2016**, *28*, 4306.

**ADVANCED
SCIENCE NEWS**

www.advancedsciencenews.com

**ADVANCED
MATERIALS**

www.advmat.de

[81] J. Du, S. Pei, L. Ma, H. M. Cheng, *Adv. Mater.* **2014**, *26*, 1958.

[82] M. D. Dickey, R. C. Chiechi, R. J. Larsen, E. A. Weiss, D. A. Weitz, G. M. Whitesides, *Adv. Funct. Mater.* **2008**, *18*, 1097.

[83] S. Q. Liu, D. D. Qu, S. D. McDonald, K. Nogita, *Solid State Phenomena*, Vol. 273, Trans Tech Publications, Zurich, Switzerland **2018**, p. 3.

[84] Y. Yang, N. Sun, Z. Wen, P. Cheng, H. Zheng, H. Shao, Y. Xia, C. Chen, H. Lan, X. Xie, C. Zhou, J. Zhong, X. Sun, S. T. Lee, *ACS Nano* **2018**, *12*, 2027.

[85] X. Wang, R. Guo, J. Liu, *Adv. Mater. Technol.* **2018**, *4*, 1800549.

[86] G. Bo, L. Ren, X. Xu, Y. Du, S. Dou, *Adv. Phys.: X* **2018**, *3*, 1446359.

[87] S. Liu, K. Sweatman, S. McDonald, K. Nogita, *Materials* **2018**, *11*, 1384.

[88] S. Zhao, J. Li, D. Cao, G. Zhang, J. Li, K. Li, Y. Yang, W. Wang, Y. Jin, R. Sun, C. P. Wong, *ACS Appl. Mater. Interfaces* **2017**, *9*, 12147.

[89] H. Lee, H. Kim, M. S. Cho, J. Choi, Y. Lee, *Electrochim. Acta* **2011**, *56*, 7460.

[90] J. Sun, Y. Huang, C. Fu, Z. Wang, Y. Huang, M. Zhu, C. Zhi, H. Hu, *Nano Energy* **2016**, *27*, 230.

[91] T. Tokuno, M. Nogi, J. Jiu, K. Suganuma, *Nanoscale Res. Lett.* **2012**, *7*, 281.

[92] Y. Xu Y. Wang, J. Liang, Y. Huang, Y. Ma, X. Wan, Y. Chen, *Nano Res.* **2009**, *2*, 343.

[93] Z. Liu, K. Parvez, R. Li, R. Dong, X. Feng, K. Mullen, *Adv. Mater.* **2015**, *27*, 669.

[94] R. Sainz, A. M. Benito, M. T. Martínez, J. F. Galindo, J. Sotres, A. M. Baró, B. Corraze, O. Chauvet, W. K. Maser, *Adv. Mater.* **2005**, *17*, 278.

[95] H. Zengin, W. Zhou, J. Jin, R. Czerw, D. Smith Jr., L. Echegoyen, D. L. Carroll, S. H. Foulger, J. Ballato, *Adv. Mater.* **2002**, *14*, 1480.

[96] K. Wang, Q. Meng, Y. Zhang, Z. Wei, M. Miao, *Adv. Mater.* **2013**, *25*, 1494.

[97] J. Eom, J.-S. Heo, M. Kim, J. H. Lee, S. K. Park, Y.-H. Kim, *RSC Adv.* **2017**, *7*, 53373.

[98] X. Fan, N. Wang, F. Yan, J. Wang, W. Song, Z. Ge, *Adv. Mater. Technol.* **2018**, *3*, 1800030.

[99] Z. Lu, J. Foroughi, C. Wang, H. Long, G. G. Wallace, *Adv. Energy Mater.* **2018**, *8*, 1702047.

[100] S. Pyo, J. Choi, J. Kim, *Adv. Electron. Mater.* **2019**, *5*, 1800737.

[101] Y. Zhu, L. Li, C. Zhang, G. Casillas, Z. Sun, Z. Yan, G. Ruan, Z. Peng, A. R. Raji, C. Kittrell, R. H. Hauge, J. M. Tour, *Nat. Commun.* **2012**, *3*, 1225.

[102] S.-B. Jeon, S.-J. Park, W.-G. Kim, I.-W. Tcho, I.-K. Jin, J.-K. Han, D. Kim, Y.-K. Choi, *Nano Energy* **2018**, *53*, 596.

[103] W. Wu, *Nanoscale* **2017**, *9*, 7342.

[104] M. Gao, L. Li, Y. Song, *J. Mater. Chem. C* **2017**, *5*, 2971.

[105] B. Kumar, S.-W. Kim, *J. Mater. Chem.* **2011**, *21*, 18946.

[106] H. Liu, J. Zhong, C. Lee, S.-W. Lee, L. Lin, *Appl. Phys. Rev.* **2018**, *5*, 041306.

[107] S. Waqar, L. Wang, S. John, *Electronic Textiles*, Woodhead Publishing, Cambridge **2015**, p. 173.

[108] A. C. Wang, C. Wu, D. Pisignano, Z. L. Wang, L. Persano, *J. Appl. Polym. Sci.* **2018**, *135*, 45674.

[109] B. A. Newman, P. Chen, K. D. Pae, J. I. Scheinbeim, *J. Appl. Phys.* **1980**, *51*, 5161.

[110] D. Matsouka, S. Vassiliadis, D. V. Bayramol, *Mater. Res. Express* **2018**, *5*, 065508.

[111] J. Fang, H. Niu, H. Wang, X. Wang, T. Lin, *Energy Environ. Sci.* **2013**, *6*, 2196.

[112] D. Mandal, S. Yoon, K. J. Kim, *Macromol. Rapid Commun.* **2011**, *32*, 831.

[113] M. B. Kechiche, F. Bauer, O. Harzallah, J. Y. Drean, *Sens. Actuators, A* **2013**, *204*, 122.

[114] C.-C. Hong, S.-Y. Huang, J. Shieh, S.-H. Chen, *Macromolecules* **2012**, *45*, 1580.

[115] S. K. Karan, R. Bera, S. Paria, A. K. Das, S. Maiti, A. Maitra, B. B. Khatua, *Adv. Energy Mater.* **2016**, *6*, 1601016.

[116] X. Lu, H. Qu, M. Skorobogatiy, *ACS Nano* **2017**, *11*, 2103.

[117] A. J. Lovinger, *Science* **1983**, *220*, 1115.

[118] L. F. Brown, *IEEE Trans. Ultrason. Ferroelectr. Freq. Control* **2000**, *47*, 1377.

[119] J. Yan, M. Liu, Y. G. Jeong, W. Kang, L. Li, Y. Zhao, N. Deng, B. Cheng, G. Yang, *Nano Energy* **2018**, *56*, 662.

[120] M. Kim, Y. Wu, E. Kan, J. Fan, *Polymers* **2018**, *10*, 745.

[121] G. Wang, Y. Deng, Y. Xiang, L. Guo, *Adv. Funct. Mater.* **2008**, *18*, 2584.

[122] K.-Y. Shin, J. S. Lee, J. Jang, *Nano Energy* **2016**, *22*, 95.

[123] H. H. Singh, N. Khare, *Nano Energy* **2018**, *51*, 216.

[124] P. Fakhri, B. Amini, R. Bagherzadeh, M. Kashfi, M. Latifi, N. Yavari, S. A. Kani, L. Kong, *RSC Adv.* **2019**, *9*, 10117.

[125] V. Cauda, G. Canavese, S. Stassi, *J. Appl. Polym. Sci.* **2015**, *132*, 41667.

[126] Y. Qin, X. Wang, Z. L. Wang, *Nature* **2008**, *451*, 809.

[127] Z. Li, Z. L. Wang, *Adv. Mater.* **2011**, *23*, 84.

[128] Y. Du, C. Fu, Y. Gao, L. Liu, Y. Liu, L. Xing, F. Zhao, *RSC Adv.* **2017**, *7*, 21452.

[129] L. Zhang, S. Bai, C. Su, Y. Zheng, Y. Qin, C. Xu, Z. L. Wang, *Adv. Funct. Mater.* **2015**, *25*, 5794.

[130] Q. Liao, Z. Zhang, X. Zhang, M. Mohr, Y. Zhang, H.-J. Fecht, *Nano Res.* **2014**, *7*, 917.

[131] M. Choi, G. Murillo, S. Hwang, J. W. Kim, J. H. Jung, C.-Y. Chen, M. Lee, *Nano Energy* **2017**, *33*, 462.

[132] H. Gao, P. T. Minh, H. Wang, S. Minko, J. Locklin, T. Nguyen, S. Sharma, *Smart Mater. Struct.* **2018**, *27*, 095018.

[133] M. Lee, C. Y. Chen, S. Wang, S. N. Cha, Y. J. Park, J. M. Kim, L. J. Chou, Z. L. Wang, *Adv. Mater.* **2012**, *24*, 1759.

[134] S. Egusa, Z. Wang, N. Chocat, Z. M. Ruff, A. M. Stolyarov, D. Shemuly, F. Sorin, P. T. Rakich, J. D. Joannopoulos, Y. Fink, *Nat. Mater.* **2010**, *9*, 643.

[135] R. L. Hadimani, D. V. Bayramol, N. Sion, T. Shah, L. Qian, S. Shi, E. Siores, *Smart Mater. Struct.* **2013**, *22*, 075017.

[136] A. Lund, K. Rundqvist, E. Nilsson, L. Yu, B. Hagström, C. Müller, *npj Flexible Electron.* **2018**, *2*, 9.

[137] E. Nilsson, A. Lund, C. Jonasson, C. Johansson, B. Hagström, *Sens. Actuators, A* **2013**, *201*, 477.

[138] H. J. Sim, C. Choi, C. J. Lee, Y. T. Kim, G. M. Spinks, M. D. Lima, R. H. Baughman, S. J. Kim, *Adv. Eng. Mater.* **2015**, *17*, 1270.

[139] M. Kim, K.-S. Yun, *Micromachines* **2017**, *8*, 115.

[140] M. Baniasadi, J. Huang, Z. Xu, S. Moreno, X. Yang, J. Chang, M. A. Quevedo-Lopez, M. Naraghi, M. Minary-Jolandan, *ACS Appl. Mater. Interfaces* **2015**, *7*, 5358.

[141] Y. B. Lee, J. K. Han, S. Noothongkaew, S. K. Kim, W. Song, S. Myung, S. S. Lee, J. Lim, S. D. Bu, K. S. An, *Adv. Mater.* **2017**, *29*, 1604500.

[142] F. Mokhtari, J. Foroughi, T. Zheng, Z. X. Cheng, G. M. Spinks, *J. Mater. Chem. A* **2019**, *7*, 8245.

[143] Y. Zhou, J. He, H. Wang, K. Qi, N. Nan, X. You, W. Shao, L. Wang, B. Ding, S. Cui, *Sci. Rep.* **2017**, *7*, 12949.

[144] S. Bai, L. Zhang, Q. Xu, Y. Zheng, Y. Qin, Z. L. Wang, *Nano Energy* **2013**, *2*, 749.

[145] M. Zhang, T. Gao, J. Wang, J. Liao, Y. Qiu, Q. Yang, H. Xue, Z. Shi, Y. Zhao, Z. Xiong, L. Chen, *Nano Energy* **2015**, *13*, 298.

[146] S. Song, K.-S. Yun, *Smart Mater. Struct.* **2015**, *24*, 045008.

[147] Y. Ahn, S. Song, K.-S. Yun, *Smart Mater. Struct.* **2015**, *24*, 075002.

[148] A. Talbourdet, F. Rault, G. Lemort, C. Cochrane, E. Devaux, C. Campagne, *Smart Mater. Struct.* **2018**, *27*, 075010.

[149] H. Kim, S. M. Kim, H. Son, H. Kim, B. Park, J. Ku, J. I. Sohn, K. Im, J. E. Jang, J.-J. Park, O. Kim, S. Cha, Y. J. Park, *Energy Environ. Sci.* **2012**, *5*, 8932.

[150] A. Khan, M. Ali Abbasi, M. Hussain, Z. Hussain Ibupoto, J. Wissting, O. Nur, M. Willander, *Appl. Phys. Lett.* **2012**, *101*, 193506.

[151] A. Khan, M. Hussain, O. Nur, M. Willander, *J. Phys. D: Appl. Phys.* **2014**, *47*, 345102.

[152] A. Khan, M. A. Abbasi, J. Wissting, O. Nur, M. Willander, *Phys. Status Solidi RRL* **2013**, *7*, 980.

[153] M. Riaz, J. Song, O. Nur, Z. L. Wang, M. Willander, *Adv. Funct. Mater.* **2011**, *21*, 628.

[154] Z. H. Liu, C. T. Pan, L. W. Lin, J. C. Huang, Z. Y. Ou, *Smart Mater. Struct.* **2014**, *23*, 025003.

[155] Y. K. Fuh, H. C. Ho, B. S. Wang, S. C. Li, *Nanotechnology* **2016**, *27*, 435403.

[156] M.-H. You, X.-X. Wang, X. Yan, J. Zhang, W.-Z. Song, M. Yu, Z.-Y. Fan, S. Ramakrishna, Y.-Z. Long, *J. Mater. Chem. A* **2018**, *6*, 3500.

[157] K. Maity, D. Mandal, *ACS Appl. Mater. Interfaces* **2018**, *10*, 18257.

[158] M. S. Sorayani Bafqi, R. Bagherzadeh, M. Latifi, *J. Polym. Res.* **2015**, *22*, 130.

[159] X. Chen, S. Xu, N. Yao, Y. Shi, *Nano Lett.* **2010**, *10*, 2133.

[160] W. Wu, S. Bai, M. Yuan, Y. Qin, Z. L. Wang, T. Jing, *ACS Nano* **2012**, *6*, 6231.

[161] J. Yuh, J. C. Nino, W. M. Sigmund, *Mater. Lett.* **2005**, *59*, 3645.

[162] B. Bajaj, S. Hong, S. M. Jo, S. Lee, H. J. Kim, *RSC Adv.* **2016**, *6*, 64441.

[163] L. L. Zhong Lin Wang, J. Chen, S. Niu, Y. Zi, *Triboelectric Nanogenerators*, Springer International Publishing, Berlin **2016**.

[164] Z. L. Wang, *ACS Nano* **2013**, *7*, 9533.

[165] Z. L. Wang, *Faraday Discuss.* **2014**, *176*, 447.

[166] Z. L. Wang, J. Chen, L. Lin, *Energy Environ. Sci.* **2015**, *8*, 2250.

[167] P. Wang, L. Pan, J. Wang, M. Xu, G. Dai, H. Zou, K. Dong, Z. L. Wang, *ACS Nano* **2018**, *12*, 9433.

[168] R. Liu, X. Kuang, J. Deng, Y. C. Wang, A. C. Wang, W. Ding, Y. C. Lai, J. Chen, P. Wang, Z. Lin, *Adv. Mater.* **2018**, *30*, 1705195.

[169] Z. Wen, Y. Yang, N. Sun, G. Li, Y. Liu, C. Chen, J. Shi, L. Xie, H. Jiang, D. Bao, *Adv. Funct. Mater.* **2018**, *28*, 1803684.

[170] P. Wang, R. Liu, W. Ding, P. Zhang, L. Pan, G. Dai, H. Zou, K. Dong, C. Xu, Z. L. Wang, *Adv. Funct. Mater.* **2018**, *28*, 1705808.

[171] Z. Wu, W. Ding, Y. Dai, K. Dong, C. Wu, L. Zhang, Z. Lin, J. Cheng, Z. L. Wang, *ACS Nano* **2018**, *12*, 5726.

[172] Y. Zi, H. Guo, Z. Wen, M.-H. Yeh, C. Hu, Z. L. Wang, *ACS Nano* **2016**, *10*, 4797.

[173] J. Chen, Z. L. Wang, *Joule* **2017**, *1*, 480.

[174] J. Chen, G. Zhu, W. Yang, Q. Jing, P. Bai, Y. Yang, T. C. Hou, Z. L. Wang, *Adv. Mater.* **2013**, *25*, 6094.

[175] M. Xu, P. Wang, Y. C. Wang, S. L. Zhang, A. C. Wang, C. Zhang, Z. Wang, X. Pan, Z. L. Wang, *Adv. Energy Mater.* **2018**, *8*, 1702432.

[176] B. Chen, Y. Yang, Z. L. Wang, *Adv. Energy Mater.* **2018**, *8*, 1702649.

[177] Y. Xie, S. Wang, L. Lin, Q. Jing, Z.-H. Lin, S. Niu, Z. Wu, Z. L. Wang, *ACS Nano* **2013**, *7*, 7119.

[178] L. Zhang, B. Zhang, J. Chen, L. Jin, W. Deng, J. Tang, H. Zhang, H. Pan, M. Zhu, W. Yang, *Adv. Mater.* **2016**, *28*, 1650.

[179] B. D. Chen, W. Tang, C. He, C. R. Deng, L. J. Yang, L. P. Zhu, J. Chen, J. J. Shao, L. Liu, Z. L. Wang, *Mater. Today* **2018**, *21*, 88.

[180] M. Xu, T. Zhao, C. Wang, S. L. Zhang, Z. Li, X. Pan, Z. L. Wang, *ACS Nano* **2019**, *13*, 1932.

[181] Z. L. Wang, T. Jiang, L. Xu, *Nano Energy* **2017**, *39*, 9.

[182] C. C. Gillispie, *Scribner*, Charles Coulston Gillispie, New York **1976**, p. 352.

[183] C. H. Park, J. K. Park, H. S. Jeon, B. C. Chun, *J. Electrost.* **2008**, *66*, 578.

[184] B. W. Lee, D. E. Orr, The Triboelectric Series, https://www.alphalabinc.com/triboelectric-series (accessed: March 2019).

[185] H. Zou, Y. Zhang, L. Guo, P. Wang, X. He, G. Dai, H. Zheng, C. Chen, A. C. Wang, C. Xu, Z. L. Wang, *Nat. Commun.* **2019**, *10*, 1427.

[186] B. Zhang, J. Lei, D. Qi, Z. Liu, Y. Wang, G. Xiao, J. Wu, W. Zhang, F. Huo, X. Chen, *Adv. Funct. Mater.* **2018**, *28*, 1801683.

[187] X. Tao, *Acc. Chem. Res.* **2019**, *52*, 307.

[188] C. Xu, Y. Zi, A. C. Wang, H. Zou, Y. Dai, X. He, P. Wang, Y. C. Wang, P. Feng, D. Li, Z. L. Wang, *Adv. Mater.* **2018**, *30*, 1706790.

[189] C. Xu, A. C. Wang, H. Zou, B. Zhang, C. Zhang, Y. Zi, L. Pan, P. Wang, P. Feng, Z. Lin, Z. L. Wang, *Adv. Mater.* **2018**, *30*, 1803968.

[190] C. Xu, B. Zhang, A. C. Wang, H. Zou, G. Liu, W. Ding, C. Wu, M. Ma, P. Feng, Z. Lin, Z. L. Wang, *ACS Nano* **2019**, *13*, 2034.

[191] S. Lin, L. Xu, C. Xu, X. Chen, A. C. Wang, B. Zhang, P. Lin, Y. Yang, H. Zhao, Z. L. Wang, *Adv. Mater.* **2019**, *31*, 1808197.

[192] Y.-C. Lai, J. Deng, S. L. Zhang, S. Niu, H. Guo, Z. L. Wang, *Adv. Funct. Mater.* **2017**, *27*, 1604462.

[193] M. Liu, Z. Cong, X. Pu, W. Guo, T. Liu, M. Li, Y. Zhang, W. Hu, Z. L. Wang, *Adv. Funct. Mater.* **2019**, 1806298.

[194] A. Yu, X. Pu, R. Wen, M. Liu, T. Zhou, K. Zhang, Y. Zhang, J. Zhai, W. Hu, Z. L. Wang, *ACS Nano* **2017**, *11*, 12764.

[195] M. Zhang, M. Zhao, M. Jian, C. Wang, A. Yu, Z. Yin, X. Liang, H. Wang, K. Xia, X. Liang, J. Zhai, Y. Zhang, *Matter* **2019**, *1*, 1.

[196] J. Park, A. Y. Choi, C. J. Lee, D. Kim, Y. T. Kim, *RSC Adv.* **2017**, *7*, 54829.

[197] Y. Yang, L. Xie, Z. Wen, C. Chen, X. Chen, A. Wei, P. Cheng, X. Xie, X. Sun, *ACS Appl. Mater. Interfaces* **2018**, *10*, 42356.

[198] J. Park, D. Kim, A. Y. Choi, Y. T. Kim, *APL Mater.* **2018**, *6*, 101106.

[199] W. Gong, C. Hou, J. Zhou, Y. Guo, W. Zhang, Y. Li, Q. Zhang, H. Wang, *Nat. Commun.* **2019**, *10*, 868.

[200] L. Xie, X. Chen, Z. Wen, Y. Yang, J. Shi, C. Chen, M. Peng, Y. Liu, X. Sun, *Nano-Micro Lett.* **2019**, *11*, 39.

[201] Z. Lin, Q. He, Y. Xiao, T. Zhu, J. Yang, C. Sun, Z. Zhou, H. Zhang, Z. Shen, J. Yang, Z. L. Wang, *Adv. Mater. Technol.* **2018**, *3*, 1800144.

[202] J. Zhong, Q. Zhong, Q. Hu, N. Wu, W. Li, B. Wang, B. Hu, J. Zhou, *Adv. Funct. Mater.* **2015**, *25*, 1798.

[203] S. H. Kim, C. S. Haines, N. Li, K. J. Kim, T. J. Mun, C. Choi, J. Di, Y. J. Oh, J. P. Oviedo, J. Bykova, *Science* **2017**, *357*, 773.

[204] X. He, Y. Zi, H. Guo, H. Zheng, Y. Xi, C. Wu, J. Wang, W. Zhang, C. Lu, Z. L. Wang, *Adv. Funct. Mater.* **2017**, *27*, 1604378.

[205] W. Gong, C. Hou, Y. Guo, J. Zhou, J. Mu, Y. Li, Q. Zhang, H. Wang, *Nano Energy* **2017**, *39*, 673.

[206] Y. Cheng, X. Lu, K. Hoe Chan, R. Wang, Z. Cao, J. Sun, G. Wei Ho, *Nano Energy* **2017**, *41*, 511.

[207] K. N. Kim, J. Chun, J. W. Kim, K. Y. Lee, J.-U. Park, S.-W. Kim, Z. L. Wang, J. M. Baik, *ACS Nano* **2015**, *9*, 6394.

[208] H. J. Sim, C. Choi, S. H. Kim, K. M. Kim, C. J. Lee, Y. T. Kim, X. Lepro, R. H. Baughman, S. J. Kim, *Sci. Rep.* **2016**, *6*, 35153.

[209] X. Yu, J. Pan, J. Zhang, H. Sun, S. He, L. Qiu, H. Lou, X. Sun, H. Peng, *J. Mater. Chem. A* **2017**, *5*, 6032.

[210] Z. Tian, J. He, X. Chen, T. Wen, C. Zhai, Z. Zhang, J. Cho, X. Chou, C. Xue, *RSC Adv.* **2018**, *8*, 2950.

[211] J. Wang, S. Li, F. Yi, Y. Zi, J. Lin, X. Wang, Y. Xu, Z. L. Wang, *Nat. Commun.* **2016**, *7*, 12744.

[212] T. Zhao, J. Li, H. Zeng, Y. Fu, H. He, L. Xing, Y. Zhang, X. Xue, *Nanotechnology* **2018**, *29*, 405504.

[213] D. Kim, J. Park, Y. T. Kim, *ACS Appl. Energy Mater.* **2019**, *2*, 1357.

[214] J. Chen, Y. Huang, N. Zhang, H. Zou, R. Liu, C. Tao, X. Fan, Z. L. Wang, *Nat. Energy* **2016**, *1*, 16138.

[215] C. Ning, L. Tian, X. Zhao, S. Xiang, Y. Tang, E. Liang, Y. Mao, *J. Mater. Chem. A* **2018**, *6*, 19143.

[216] T. Zhou, C. Zhang, C. B. Han, F. R. Fan, W. Tang, Z. L. Wang, *ACS Appl. Mater. Interfaces* **2014**, *6*, 14695.

[217] X. Pu, L. Li, H. Song, C. Du, Z. Zhao, C. Jiang, G. Cao, W. Hu, Z. L. Wang, *Adv. Mater.* **2015**, *27*, 2472.

[218] X. Pu, L. Li, M. Liu, C. Jiang, C. Du, Z. Zhao, W. Hu, Z. L. Wang, *Adv. Mater.* **2016**, *28*, 98.

**ADVANCED
SCIENCE NEWS**

www.advancedsciencenews.com

**ADVANCED
MATERIALS**

www.advmat.de

[219] Z. Tian, J. He, X. Chen, Z. Zhang, T. Wen, C. Zhai, J. Han, J. Mu, X. Hou, X. Chou, C. Xue, *Nano Energy* **2017**, *39*, 562.

[220] H. Liu, Q. Li, S. Zhang, R. Yin, X. Liu, Y. He, K. Dai, C. Shan, J. Guo, C. Liu, C. Shen, X. Wang, N. Wang, Z. Wang, R. Wei, Z. Guo, *J. Mater. Chem. C* **2018**, *6*, 12121.

[221] Z. Wen, M.-H. Yeh, H. Guo, J. Wang, Y. Zi, W. Xu, J. Deng, L. Zhu, X. Wang, C. Hu, *Sci. Adv.* **2016**, *2*, e1600097.

[222] Z. Zhao, C. Yan, Z. Liu, X. Fu, L. M. Peng, Y. Hu, Z. Zheng, *Adv. Mater.* **2016**, *28*, 10267.

[223] J. Wang, X. Li, Y. Zi, S. Wang, Z. Li, L. Zheng, F. Yi, S. Li, Z. L. Wang, *Adv. Mater.* **2015**, *27*, 4830.

[224] W. B. Ko, D. S. Choi, C. H. Lee, J. Y. Yang, G. S. Yoon, J. P. Hong, *Adv. Mater.* **2017**, *29*, 1704434.

[225] S. S. Kwak, H. Kim, W. Seung, J. Kim, R. Hinchet, S. W. Kim, *ACS Nano* **2017**, *11*, 10733.

[226] H. Li, S. Zhao, X. Du, J. Wang, R. Cao, Y. Xing, C. Li, *Adv. Mater. Technol.* **2018**, *3*, 1800065.

[227] J. Gong, B. Xu, X. Guan, Y. Chen, S. Li, J. Feng, *Nano Energy* **2019**, *58*, 365.

[228] M. Zhu, Y. Huang, W. S. Ng, J. Liu, Z. Wang, Z. Wang, H. Hu, C. Zhi, *Nano Energy* **2016**, *27*, 439.

[229] Z. Wang, Z. Ruan, W. S. Ng, H. Li, Z. Tang, Z. Liu, Y. Wang, H. Hu, C. Zhi, *Small Methods* **2018**, *2*, 1800150.

[230] L. Liu, J. Pan, P. Chen, J. Zhang, X. Yu, X. Ding, B. Wang, X. Sun, H. Peng, *J. Mater. Chem. A* **2016**, *4*, 6077.

[231] Y. Song, J. Zhang, H. Guo, X. Chen, Z. Su, H. Chen, X. Cheng, H. Zhang, *Appl. Phys. Lett.* **2017**, *111*, 073901.

[232] Q. Qiu, M. Zhu, Z. Li, K. Qiu, X. Liu, J. Yu, B. Ding, *Nano Energy* **2019**, *58*, 750.

[233] J. Xiong, M.-F. Lin, J. Wang, S. L. Gaw, K. Parida, P. S. Lee, *Adv. Energy Mater.* **2017**, *7*, 1701243.

[234] J. Xiong, P. Cui, X. Chen, J. Wang, K. Parida, M. F. Lin, P. S. Lee, *Nat. Commun.* **2018**, *9*, 4280.

[235] R. Cao, X. Pu, X. Du, W. Yang, J. Wang, H. Guo, S. Zhao, Z. Yuan, C. Zhang, C. Li, Z. L. Wang, *ACS Nano* **2018**, *12*, 5190.

[236] Y.-E. Shin, J.-E. Lee, Y. Park, S.-H. Hwang, H. G. Chae, H. Ko, *J. Mater. Chem. A* **2018**, *6*, 22879.

[237] L. Zhang, Y. Yu, G. P. Eyer, G. Suo, L. A. Kozik, M. Fairbanks, X. Wang, T. L. Andrew, *Adv. Mater. Technol.* **2016**, *1*, 1600147.

[238] C. Wu, T. W. Kim, F. Li, T. Guo, *ACS Nano* **2016**, *10*, 6449.

[239] N. Cui, J. Liu, L. Gu, S. Bai, X. Chen, Y. Qin, *ACS Appl. Mater. Interfaces* **2015**, *7*, 18225.

[240] T. Kim, S. Jeon, S. Lone, S. J. Doh, D.-M. Shin, H. K. Kim, Y.-H. Hwang, S. W. Hong, *Nano Energy* **2018**, *54*, 209.

[241] S. Jung, J. Lee, T. Hyeon, M. Lee, D. H. Kim, *Adv. Mater.* **2014**, *26*, 6329.

[242] T. Huang, J. Zhang, B. Yu, H. Yu, H. Long, H. Wang, Q. Zhang, M. Zhu, *Nano Energy* **2019**, *58*, 375.

[243] J. Chen, H. Guo, X. Pu, X. Wang, Y. Xi, C. Hu, *Nano Energy* **2018**, *50*, 536.

[244] M.-F. Lin, J. Xiong, J. Wang, K. Parida, P. S. Lee, *Nano Energy* **2018**, *44*, 248.

[245] S. Cheon, H. Kang, H. Kim, Y. Son, J. Y. Lee, H. J. Shin, S. W. Kim, J. H. Cho, *Adv. Funct. Mater.* **2018**, *28*, 1703778.

[246] Z. Li, M. Zhu, Q. Qiu, J. Yu, B. Ding, *Nano Energy* **2018**, *53*, 726.

[247] J.-H. Zhang, Y. Li, J. Du, X. Hao, H. Huang, *J. Mater. Chem. A* **2019**, *7*, 11724.

[248] J.-H. Zhang, Y. Li, J. Du, X. Hao, Q. Wang, *Nano Energy* **2019**, *61*, 486.

[249] C. Jiang, C. Wu, X. Li, Y. Yao, L. Lan, F. Zhao, Z. Ye, Y. Ying, J. Ping, *Nano Energy* **2019**, *59*, 268.

[250] X. He, H. Zou, Z. Geng, X. Wang, W. Ding, F. Hu, Y. Zi, C. Xu, S. L. Zhang, H. Yu, M. Xu, W. Zhang, C. Lu, Z. L. Wang, *Adv. Funct. Mater.* **2018**, *28*, 1805540.

[251] R. Cao, J. Wang, S. Zhao, W. Yang, Z. Yuan, Y. Yin, X. Du, N.-W. Li, X. Zhang, X. Li, Z. L. Wang, C. Li, *Nano Res.* **2018**, *11*, 3771.

[252] A. Y. Choi, C. J. Lee, J. Park, D. Kim, Y. T. Kim, *Sci. Rep.* **2017**, *7*, 45583.

[253] T. He, Q. Shi, H. Wang, F. Wen, T. Chen, J. Ouyang, C. Lee, *Nano Energy* **2019**, *57*, 338.

[254] D. Choi, S. Yang, C. Lee, W. Kim, J. Kim, J. Hong, *ACS Appl. Mater. Interfaces* **2018**, *10*, 33221.

[255] J. Song, L. Gao, X. Tao, L. Li, *Materials* **2018**, *11*, 2120.

[256] H. Ryu, H. J. Yoon, S. W. Kim, *Adv. Mater.* **2019**, 1802898.

[257] A. A. Khan, A. Mahmud, D. Ban, *IEEE Trans. Nanotechnol.* **2019**, *18*, 21.

[258] L. Liu, W. Tang, C. Deng, B. Chen, K. Han, W. Zhong, Z. L. Wang, *Nano Res.* **2018**, *11*, 3972.

[259] S. Maiti, S. K. Karan, J. K. Kim, B. B. Khatua, *Adv. Energy Mater.* **2019**, *9*, 1803027.

[260] K. Y. Lee, M. K. Gupta, S.-W. Kim, *Nano Energy* **2015**, *14*, 139.

[261] M. Han, X. Chen, B. Yu, H. Zhang, *Adv. Electron. Mater.* **2015**, *1*, 1500187.

[262] S. Chen, X. Tao, W. Zeng, B. Yang, S. Shang, *Adv. Energy Mater.* **2017**, *7*, 1601569.

[263] X. Chen, M. Han, H. Chen, X. Cheng, Y. Song, Z. Su, Y. Jiang, H. Zhang, *Nanoscale* **2017**, *9*, 1263.

[264] B. Shi, Q. Zheng, W. Jiang, L. Yan, X. Wang, H. Liu, Y. Yao, Z. Li, Z. L. Wang, *Adv. Mater.* **2016**, *28*, 846.

[265] T. Huang, C. Wang, H. Yu, H. Wang, Q. Zhang, M. Zhu, *Nano Energy* **2015**, *14*, 226.

[266] H. Li, L. Su, S. Kuang, Y. Fan, Y. Wu, Z. L. Wang, G. Zhu, *Nano Res.* **2017**, *10*, 785.

[267] G. Suo, Y. Yu, Z. Zhang, S. Wang, P. Zhao, J. Li, X. Wang, *ACS Appl. Mater. Interfaces* **2016**, *8*, 34335.

[268] X. Yang, W. A. Daoud, *Adv. Funct. Mater.* **2016**, *26*, 8194.

[269] A. R. Chowdhury, A. M. Abdullah, I. Hussain, J. Lopez, D. Cantu, S. K. Gupta, Y. Mao, S. Danti, M. J. Uddin, *Nano Energy* **2019**, *61*, 327.

[270] K. Shi, X. Huang, B. Sun, Z. Wu, J. He, P. Jiang, *Nano Energy* **2019**, *57*, 450.

[271] S. Wang, Z. L. Wang, Y. Yang, *Adv. Mater.* **2016**, *28*, 2881.

[272] D. H. Kim, B. Dudem, J. S. Yu, *ACS Sustainable Chem. Eng.* **2018**, *6*, 8525.

[273] W.-S. Jung, M.-G. Kang, H. G. Moon, S.-H. Baek, S.-J. Yoon, Z.-L. Wang, S.-W. Kim, C.-Y. Kang, *Sci. Rep.* **2015**, *5*, 9309.

[274] M. Han, X.-S. Zhang, B. Meng, W. Liu, W. Tang, X. Sun, W. Wang, H. Zhang, *ACS Nano* **2013**, *7*, 8554.

[275] X. Wang, B. Yang, J. Liu, Y. Zhu, C. Yang, Q. He, *Sci. Rep.* **2016**, *6*, 36409.

[276] X. Chen, Y. Song, Z. Su, H. Chen, X. Cheng, J. Zhang, M. Han, H. Zhang, *Nano Energy* **2017**, *38*, 43.

[277] X. Li, Z.-H. Lin, G. Cheng, X. Wen, Y. Liu, S. Niu, Z. L. Wang, *ACS Nano* **2014**, *8*, 10674.

[278] J. Zhu, X. Hou, X. Niu, X. Guo, J. Zhang, J. He, T. Guo, X. Chou, C. Xue, W. Zhang, *Sens. Actuators, A* **2017**, *263*, 317.

[279] Y. Zi, L. Lin, J. Wang, S. Wang, J. Chen, X. Fan, P. K. Yang, F. Yi, Z. L. Wang, *Adv. Mater.* **2015**, *27*, 2340.

[280] C. Zhao, Q. Zhang, W. Zhang, X. Du, Y. Zhang, S. Gong, K. Ren, Q. Sun, Z. L. Wang, *Nano Energy* **2019**, *57*, 440.

[281] G. Wei, Y. Bi, X. Li, D. Xu, W. Xu, L.-J. Yang, Y. Qin, H. Guo, X. Zhao, X. Chen, *Nano Energy* **2018**, *54*, 10.

[282] C. Chen, C. Tsai, M. Xu, C. Wu, C. Huang, T. Lee, Y. Fuh, *eXPRESS Polym. Lett.* **2019**, *13*, 533.

[283] J. Song, B. Yang, W. Zeng, Z. Peng, S. Lin, J. Li, X. Tao, *Adv. Mater. Technol.* **2018**, *3*, 1800016.

[284] M. Zhu, Q. Shi, T. He, Z. Yi, Y. Ma, B. Yang, T. Chen, C. Lee, *ACS Nano* **2019**, *13*, 1940.

**ADVANCED
SCIENCE NEWS**

www.advancedsciencenews.com

**ADVANCED
MATERIALS**

www.advmat.de

[285] X. Tao, *Wearable Electronics and Photonics*, Elsevier, Amsterdam, The Netherlands **2005**.

[286] S. C. Mukhopadhyay, *IEEE Sens. J.* **2014**, *15*, 1321.

[287] E. Gibney, *Nature* **2015**, *528*, 26.

[288] Y. Liu, M. Pharr, G. A. Salvatore, *ACS Nano* **2017**, *11*, 9614.

[289] W. Wu, *Sci. Technol. Adv. Mater.* **2019**, *20*, 187.

[290] Z. Ghahramani, *Nature* **2015**, *521*, 452.

[291] J. V. Abellan-Nebot, F. R. Subirón, *Int. J. Adv. Manuf. Technol.* **2010**, *47*, 237.

[292] K. Kumar, G. S. M. Thakur, *Int. J. Inf. Sci. Comput.* **2012**, *6*, 57.

[293] V. Dunjko, H. J. Briegel, *Rep. Prog. Phys.* **2018**, *81*, 074001.

[294] M. Koch, *Cell* **2018**, *173*, 531.

[295] F. Jiang, Y. Jiang, H. Zhi, Y. Dong, H. Li, S. Ma, Y. Wang, Q. Dong, H. Shen, Y. Wang, *Stroke. Vasc. Neurol.* **2017**, *2*, 230.

[296] V. Nguyen, R. Zhu, R. Yang, *Nano Energy* **2015**, *14*, 49.

[297] Y. Hu, B. D. Klein, Y. Su, S. Niu, Y. Liu, Z. L. Wang, *Nano Lett.* **2013**, *13*, 5026.

[298] C. X. Lu, C. B. Han, G. Q. Gu, J. Chen, Z. W. Yang, T. Jiang, C. He, Z. L. Wang, *Adv. Eng. Mater.* **2017**, *19*, 1700275.

[299] X. Xue, Y. Nie, B. He, L. Xing, Y. Zhang, Z. L. Wang, *Nanotechnology* **2013**, *24*, 225501.

[300] S. Dhara, P. Giri, *Nanoscale Res. Lett.* **2011**, *6*, 504.

[301] Y. Lee, S. H. Cha, Y.-W. Kim, D. Choi, J.-Y. Sun, *Nat. Commun.* **2018**, *9*, 1804.

[302] C. Wu, A. C. Wang, W. Ding, H. Guo, Z. L. Wang, *Adv. Energy Mater.* **2019**, *9*, 1802906.

[303] W. Li, J. Duan, J. Zhong, N. Wu, S. Lin, Z. Xu, S. Chen, Y. Pan, L. Huang, B. Hu, *ACS Appl. Mater. Interfaces* **2018**, *10*, 29675.

[304] R. Zhang, L. Lin, Q. Jing, W. Wu, Y. Zhang, Z. Jiao, L. Yan, R. P. Han, Z. L. Wang, *Energy Environ. Sci.* **2012**, *5*, 8528.

[305] K. Dai, X. Wang, F. Yi, C. Jiang, R. Li, Z. You, *Nano Energy* **2018**, *45*, 84.

[306] K. Meng, J. Chen, X. Li, Y. Wu, W. Fan, Z. Zhou, Q. He, X. Wang, X. Fan, Y. Zhang, *Adv. Funct. Mater.* **2019**, *29*, 1806388.

[307] Z. Lin, J. Chen, X. Li, Z. Zhou, K. Meng, W. Wei, J. Yang, Z. L. Wang, *ACS Nano* **2017**, *11*, 8830.

[308] H. Yu, X. He, W. Ding, Y. Hu, D. Yang, S. Lu, C. Wu, H. Zou, R. Liu, C. Lu, *Adv. Energy Mater.* **2017**, *7*, 1700565.

[309] Y. Feng, X. Huang, S. Liu, W. Guo, Y. Li, H. Wu, *Nano Energy* **2019**, *62*, 197.

[310] J. Wang, W. Ding, L. Pan, C. Wu, H. Yu, L. Yang, R. Liao, Z. L. Wang, *ACS Nano* **2018**, *12*, 3954.